

**AN ACTIVE LANDFILL DESIGN FOR INDEFINITE WASTE STORAGE**

by

Emmett Davidson Gillispie, II

thesis submitted to the Faculty of the  
Virginia Polytechnic Institute and State University  
in partial fulfillment of the requirements for the degree of  
Master of Science  
in  
Civil Engineering

APPROVED:

---

Dr. Oner Yuçel

---

Dr. James Wiggert

---

Dr. G. W. Swift

July 1986

Blacksburg, Virginia

# AN ACTIVE LANDFILL DESIGN FOR INDEFINITE WASTE STORAGE

by

Emmett Davidson Gillispie, II

Dr. Oner Yucel

Civil Engineering

(ABSTRACT)

The design characteristics of an active waste disposal capsule placed within a saturated groundwater environment is investigated, with the objective of developing a methodology to determine environmentally, technically and economically feasible conditions for its operation. In operation, conditions are created and maintained within and surrounding a containment cell to insure that a potential for convective inflow exists everywhere across an encapsulating barrier which tends to counter the potential for outward dispersion through the barrier. A computer algorithm based on the finite element method has been developed in the *BASIC* language to aid in the hydraulic analysis. Essentially, it provides a numerical solution to potential flow through porous media for two dimensional anisotropic solution domains of various materials. Data generated from this algorithm for cases of varying geometric material and boundary properties are used to verify and quantify assumed relationships involving critical design parameters which have been developed through dimensional analysis and physical reasoning. An expression describing the concentration profiles developed across the barrier is obtained by solving the one-dimensional convection-dispersion equation for steady conditions within and bounding the capsule barrier. Applying this result to an identified critical point allows conservative barrier design criteria to be developed so that operation of the active capsule results in only negligibly small amounts of contamination escaping through the barrier to the environment. By introducing cost coefficients which are descriptive of various aspects of construction, operation and maintenance of the active capsule, a total cost function is formulated from which, when minimized with respect to various design variables, optimizing criteria are developed. Finally, a predictor-corrector optimization program which incorporates the results of this study is developed and used to investigate an illustrative problem.

## ACKNOWLEDGEMENTS

The essence of this work cannot be attributed to me alone. From the beginning, the research seemed to have followed a path projected from previous results, thus leading to a natural end. I am very fortunate, and feel blessed, in having had the opportunity to conduct research on a topic of such importance in today's world.

For this opportunity, I acknowledge, with great appreciation, the Virginia Center for Coal and Energy Research, and especially its director Dr. Walter Hibbard. I can only hope that I have proved worthy of the quiet confidence that he has exhibited in my abilities. Dr. Oner Yucel, also of the Center, has been a guiding influence throughout, returning me to the "right track" as I have swayed while still allowing me a great deal of freedom in my attempt to follow the path suggested by the research. For the understanding he has shown and the insights he has given me, I am deeply grateful. The Center personnel have all contributed by creating an enjoyable work environment, one that I hate to leave. They are not so many that they cannot be named individually. Thanks specifically to Barbara and Turgay, to Mr. Jones and Ray Chisholm, to Ted and Dr. Randolph, and to Amanda and Deanna. I would also like to thank Dr. Wiggert, especially for his diligent reading and helpful editing, and Dr. Swift, especially for his aid in chasing down the cause of a particular numerical inconsistency. Finally, George Wills was helpful in the preparation of certain illustrations.

My family has been a tremendous source of support in this endeavor. My father, with his stern conviction and endless insight, is an example of great strength and perception to which we all would do well to strive. My mother, with her unconditional dedication to family, provides for us all a stable center. I love them both dearly. For all things there is a purpose, and Martha Jo has, perhaps more than any of us, fulfilled hers. It is to her and to all those of her innocence that I dedicate this work.

# TABLE OF CONTENTS

|  |           |
|--|-----------|
| <b>Introduction</b> .....                                | <b>1</b>  |
| 1.1 Critique of Passive Systems .....                    | 1         |
| 1.2 Characteristics of the Active Design .....           | 2         |
| 1.3 Qualitative Justification .....                      | 4         |
| 1.4 Objectives of the Study .....                        | 6         |
| <br>   |           |
| <b>Summary</b> .....                                     | <b>8</b>  |
| 2.1 Notation .....                                       | 8         |
| 2.2 Results of Investigations .....                      | 9         |
| 2.2.1 Potential-Flow Characteristic Relationships .....  | 9         |
| 2.2.2 Concentration Profiles Within The Barrier .....    | 11        |
| 2.2.3 Economic Optimization of the Capsule .....         | 11        |
| 2.3 Conclusions .....                                    | 12        |
| <br>   |           |
| <b>Potential-Flow Characteristic Relationships</b> ..... | <b>14</b> |
| 3.1 Notation .....                                       | 14        |
| 3.2 Development of Functional Relationships .....        | 15        |
| 3.2.1 One Dimensional Simplification .....               | 16        |
| <br>   |           |
| <b>Table of Contents</b>                                 | <b>v</b>  |

|         |  |           |
|---------|--|-----------|
| 3.2.2   | Two Dimensional Capsule Representation           | 19        |
| 3.2.2.1 | Capsule Description                              | 19        |
| 3.2.2.2 | Dimensional Analysis                             | 21        |
| 3.2.2.3 | Derivation of Functionals                        | 22        |
| 3.2.2.4 | Physical Significance                            | 28        |
| 3.3     | Numerical Analysis of Capsule Hydraulics         | 29        |
| 3.3.1   | Finite-Element Analysis of Steady Potential Flow | 29        |
| 3.3.2   | The Computational Algorithm                      | 31        |
| 3.3.3   | Accuracy of Solution                             | 35        |
| 3.3.4   | Example Output                                   | 43        |
| 3.3.5   | Capsule Characteristic Curve                     | 43        |
| 3.3.6   | Ranges of Validity                               | 53        |
| 3.3.7   | Correction Factors for Non-Standard Conditions   | 55        |
| 3.3.7.1 | Anisotropic Conditions                           | 55        |
| 3.3.7.2 | Partially Penetrating Outlet Drains              | 58        |
|         | <b>Concentration Profiles within the Barrier</b> | <b>60</b> |
| 4.1     | Notation   | 61        |
| 4.2     | Problem Identification                           | 61        |
| 4.3     | Analytical solution                              | 63        |
| 4.4     | Physical Significance                            | 67        |
|         | <b>Economic Optimization of the Capsule</b>      | <b>71</b> |
| 5.1     | Notation   | 72        |
| 5.2     | The Specific Cost Function                       | 73        |
| 5.2.1   | Initial Capital Costs                            | 73        |
| 5.2.2   | Annual Operating and Maintenance Costs           | 76        |
| 5.2.3   | Combined Cost Function                           | 78        |

|         |   |            |
|---------|---|------------|
| 5.3     | Optimum Capsule Design Criteria                               | 80         |
| 5.3.1   | Optimum Capsule Length  | 82         |
| 5.3.1.1 | Physical Significance   | 83         |
| 5.3.1.2 | Verification of Minimizing Conditions                         | 84         |
| 5.3.2   | Optimum Barrier Thickness                                     | 86         |
| 5.3.2.1 | Physical Significance   | 89         |
| 5.3.3   | Optimum Containment Region Permeability                       | 89         |
| 5.3.3.1 | Physical Significance   | 91         |
| 5.3.4   | Optimum Drain Penetration                                     | 92         |
| 5.4     | Evaluation of the Optimum Capsule Design                      | 93         |
| 5.4.1   | Outline of the Optimization Methodology                       | 93         |
| 5.4.2   | Illustrative Problem  | 94         |
|         | <b>Finite-Element Program Listing</b>                         | <b>97</b>  |
|         | <b>Sample Auxiliary Program Listings</b>                      | <b>100</b> |
|         | <b>Example Intermediate Results of the Solution Algorithm</b> | <b>113</b> |
|         | <b>Data For Anisotropic Conditions</b>                        | <b>119</b> |
|         | <b>Data For Partially Penetrating Drains</b>                  | <b>121</b> |
|         | <b>Optimization Program Listing and Example Output</b>        | <b>123</b> |
|         | <b>References</b>   | <b>128</b> |
|         | <b>Vita</b>   | <b>131</b> |

## LIST OF ILLUSTRATIONS

|   |    |
|---|----|
| Figure 1. The Active Landfill Design Concept .....                    | 3  |
| Figure 2. Conditions for One Dimensional Flow .....                   | 17 |
| Figure 3. The Containment Capsule .....                               | 20 |
| Figure 4. Schematic of Data Generation Methodology .....              | 32 |
| Figure 5. Quarter Capsule Solution Domain .....                       | 46 |
| Figure 6. Half Capsule Solution Domain .....                          | 49 |
| Figure 7. Containment Capsule Characteristic Curves .....             | 52 |
| Figure 8. Anisotropic Conditions .....                                | 57 |
| Figure 9. Partially Penetrating Drains .....                          | 59 |
| Figure 10. The Barrier Problem .....                                  | 62 |
| Figure 11. Barrier Performance Curves .....                           | 70 |
| Figure 12. Optimum Capsule Length Relative To Barrier Thickness ..... | 85 |
| Figure 13. Optimum Barrier Thickness .....                            | 90 |



## LIST OF TABLES

|  |    |
|--|----|
| Table 1. Characteristic Parameters of the Capsule .....                              | 10 |
| Table 2. Results of Dimensional Analysis .....                                       | 23 |
| Table 3. Characteristic Parameters of the Capsule .....                              | 27 |
| Table 4. Values of the Standard Design Variables .....                               | 37 |
| Table 5. Finite-Element Mesh Refinement .....  | 38 |
| Table 6. Other Accuracy Considerations .....   | 42 |
| Table 7. Quarter-Capsule Solution Domain: Nodal Potentials .....                     | 44 |
| Table 8. Quarter-Capsule Solution Domain: Elemental Velocities .....                 | 45 |
| Table 9. Half-Capsule Solution Domain: Nodal Potentials .....                        | 47 |
| Table 10. Half-Capsule Solution Domain: Elemental Velocities .....                   | 48 |
| Table 11. Data For Standard Potential-Flow Characteristic Curves .....               | 51 |
| Table 12. Valid Ranges of the Dimensionless Numbers .....                            | 54 |
| Table 13. Characteristic Barrier Design Parameters .....                             | 68 |
| Table 14. Components of the Initial Capital Cost Coefficients .....                  | 75 |
| Table 15. Components of the Annual Operating and Maintenance Cost Coefficients ..... | 77 |
| Table 16. Numerical Test of Minimizing Conditions .....                              | 87 |

# CHAPTER 1

## INTRODUCTION

Landfill systems currently seem to be based exclusively on passive designs which assume minimal long-term contamination and therefore make no provisions for active operation beyond the useful life of the facility [20] [24]. Contrary to design assumptions, they seem to have resulted in both actual, as well as potential, long-term and extensive environmental damage [20] [8] [28] [13]. This study investigates the possibility of reducing the environmental degradation caused by such passive landfill systems by adding provisions for long-term, active operation to the landfill design. References and examples are based primarily on the disposal of uranium mill tailings but the results herein are directly applicable to a wide range of wastes which pose long-term environmental threats.

### 1.1 CRITIQUE OF PASSIVE SYSTEMS

Landfill disposal of waste material within ambient groundwater regions is not unheard of in the literature [18] [9], but is generally avoided [20]. Considering that passive designs may hinder but can never eliminate the potential for contaminant migration, and that saturated porous media has migration promoting characteristics on these passively contained wastes [16], this tendency to maintain waste disposal areas above the groundwater table is understandable. However, key to the

active landfill concept is to use the predictable, manipulable characteristics of a saturated disposal region to reverse the potential for contaminant migration. Thus, a landfill design is proposed which effectively creates an active containment environment as opposed to the hindered migration offered by passive systems.

The concept of reversing potential has been applied as a corrective measure after failure of landfill systems have caused groundwater contamination [22]. Continuous pumping in the vicinity of the contamination creates a cone of depression in the groundwater table. This lower potential halts or even may reverse the outward migration of contaminants. This study investigates the feasibility of using the same technique to continuously lower the potential within the cell, but with finesse, to eliminate the possibility of contaminant migration from the source.

## 1.2 CHARACTERISTICS OF THE ACTIVE DESIGN

Consider a containment capsule represented in two dimensions by a rectangular permeable containment region, saturated with a certain level of resident concentration, and bounded above and below by relatively impermeable barriers which separate it from ambient groundwater conditions. Further, assume the end boundaries of the capsule to be drained outlets in which constant below ambient potential heads are imposed. These conditions create a potential for convective inflow from the ambient regions above and below, through the barriers and containment region, to the drained outlets.

Figure 1 illustrates how a series of these containment capsules might be combined in order to represent the proposed active landfill design in two dimensions. Notice that the drained outlets are represented by parallel drains running normal to the plane of the sketch. Wells screened into these drains may be pumped to create constant below-ambient potentials at the ends of the containment region. Under these constant imposed potentials and assuming constant ambient potential outside the capsule, steady state or equilibrium conditions will eventually develop under which flow through the capsule will be constant. It is under these equilibrium conditions that various relations

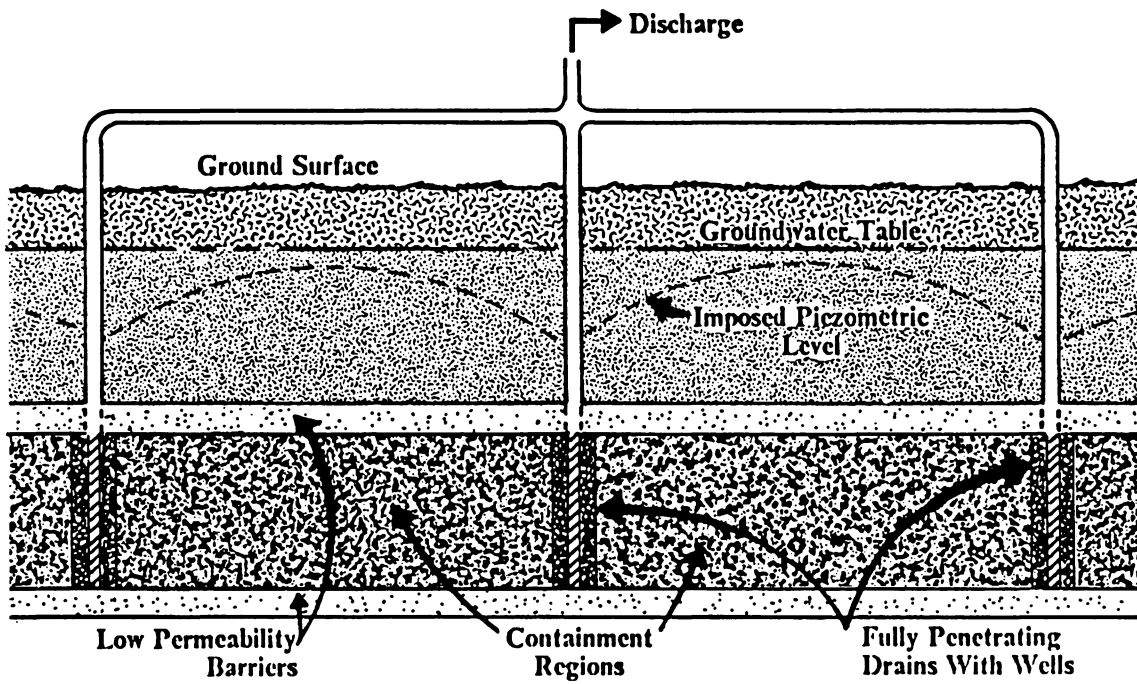


**Figure 1. The Active Landfill Design Concept:** A series of containment capsules placed within a saturated, constant potential, groundwater environment.

describing operational characteristics of the active capsule are developed. The practical application of this posed problem is immediately seen upon realizing that the dispersive migration potential of the resident concentration held between the barriers is inhibited, and possibly effectively eliminated, by the inward convective potential across the barriers.

This study focuses on operational characteristics of an active capsule based on the design features illustrated in Figure 1. The parallel drains, in addition to providing lower potential within the capsule, allow the capsule to be represented in just two dimensions. However, alternative designs, each with its own operational characteristics, are conceivable. For example, a drainage grid, or even no drains per se but lower potential provided by a network of pumping wells within the encapsulation, are possible construction scenarios. The capsule resulting from either would require a three-dimensional solution domain to be defined. A single pumping well at the center of a roughly circular encapsulation would suggest a two-dimensional, radially symmetric capsule design. Potential-flow relationships for these capsule scenarios could just as well have been studied and their long-term operational characteristics developed.

This study concentrates on long-term landfill disposal. The active concept may also conceivably be used in disposal pond design for short-term storage required by hazardous waste handling facilities. Again, operational characteristics can be developed for such designs having specific features similar to what has been done herein.

### 1.3 QUALITATIVE JUSTIFICATION

Environmental degradation resulting from improper disposal of wastes is a classic example of an economic externality where those bearing costs (users of the environment) are different from those reaping benefits (disposers). *Passive landfill* systems [24], those which are designed to require no institutional constraints beyond useful life and closure period, have often been chosen as the most economical means to dispose of (or more descriptively, *to indefinitely store*) hazardous wastes. Their economic attractiveness, however, has usually been based upon the assumption that they,

designed under what might be called *walk-away-technology*, provide permanent separation of hazardous wastes from the environment. The cost of environmental contamination resulting from unanticipated leakage has often been treated as economically external in nature and has, consequently, been grossly underestimated or totally disregarded [12]. Unfortunately, such leakages, perhaps due to the lack of long-term maintenance and monitoring requirements, have occurred quite frequently and gone undetected for long periods of time. Thus, the long term external cost, whether realized in cleanup costs or felt as a lost environmental resource, is often astronomical. Only after decades of landfill disposal of hazardous wastes has it become apparent that insecure passive systems have not effectively dealt with the external cost so often associated with landfill disposal. On the contrary, these systems, by hiding the problem in the short-term, have effectively compounded the identified externality so that the cost bearers, in addition to being different people, are also of a different generation. Unfortunately, the phrase *out-of-sight, out-of-mind* all too well describes landfill practices where such walk-away-technology has been implored.

Recognizing that passive landfill designs, though effective in eliminating the external pollution cost in the short term, have not resolved the long term pollution problem posed by disposal of hazardous waste, the *active landfill* design is proposed. This system is a long term operational undertaking which actively creates and maintains a *containment environment* according to some defined minimum allowable contamination migration criterion. Monitoring will indicate required adjustments of operational characteristics to insure compliance with this criterion. Provision for maintenance is also necessary for long term effectiveness.

Obviously, the long term institutional constraints inherent in the active landfill design will dramatically increase the cost of hazardous waste disposal. This increased cost is necessary to eliminate the external cost of environmental contamination by internalizing, through institutional constraints, the cost required to *prevent* such contamination. These costs will then be more equitably born by those deriving benefits from the wastes, namely the disposers and the generators, and ultimately the consumers of products of which the wastes are by-products. The true cost of landfill disposal must include the cost required to insure that environmental contamination does not occur as a consequence of that disposal.

A secondary effect of the increased cost of safer landfill designs will be a reduction in the categories of wastes feasible to landfill. Just as innovative recycling or otherwise more final disposal alternatives became feasible with requirements that hazardous waste disposers use the passive designs incorporating minimum safety features, the further addition of operating, monitoring and maintenance cost to landfill systems should similarly shift the economic handling of certain categories of hazardous waste away from the indefinite storage landfill option. The resulting reduction in the volume of wastes to be landfilled is obviously a great advantage [21] [23]. For those categories of hazardous wastes still deemed more feasible to handle using the herein described designs, optimally safe indefinite storage is provided through continuous monitoring and adjustments of operational characteristics and through maintenance as required.

#### **1.4 OBJECTIVES OF THE STUDY**

The primary objective of the study is to develop a means through which the potential effectiveness of an active landfill design might be assessed. Although based on a rather specific capsule design, it is intended to be an example of the methodology for developing a descriptive solution to designs involving the active containment concept rather than a rigid solution to any particular design. Such a methodology would involve the three steps used in this study.

1. Investigation of operational characteristics of the design including describing the flow and potential fields and identifying critical design features.
2. Investigation of the potential for contaminant migration at the critical design point and establishment of a minimum allowable contaminant migration criterion.
3. Economic optimization through development of a cost function relating capital, operating and maintenance costs to design features and operational characteristics.

An attempt to maintain a broad perspective of the problem has been made, keeping in mind the ultimate goal of providing a means to estimate the technical and economic feasibility. At various points throughout the development, further investigation would be warranted under a more detailed study of any particular design and suggestions for possible further analysis have occasionally been made. However, considering that the present study is preliminary, such detail would seem to detract from the overview nature or comprehensiveness intended. Thus, in the interest of completing all three phases of the investigation within the context of this work, some details, or possible offshoot or parallel investigations, have been left to other studies.



## CHAPTER 2

### SUMMARY

#### 2.1 NOTATION

|            |   |  |
|------------|---|--|
| $C(s)$     | = | Steady state variation of concentration across the barrier [-] |
| $C_0$      | = | Ambient or background level of contaminant concentration [-]   |
| $\Delta C$ | = | Total change in concentration across the barrier [-]           |
| $d$        | = | Dispersivity of the barrier material [L]                       |
| $f_c$      | = | Correction factor either anisotropy or partial penetration [-] |
| $f_h$      | = | Fraction of added material in the cell half depth [-]          |
| $f_p$      | = | Degree of partial penetration [-]                              |
| $f_q$      | = | Factor to obtain gross capsule discharge from net [-]          |
| $H$        | = | Half thickness of cell in the capsule design [L]               |
| $K$        | = | Darcy's permeability coefficient of the barrier material [L/T] |
| $K_t$      | = | Darcy horizontal permeability of the cell [L/T]                |
| $L$        | = | Half spacing of parallel drains in the capsule design [L]      |
| $q_s$      | = | Net specific discharge [1/T]                                   |
| $r$        | = | Present worth factor for an annual series [T]                  |

- s = Spatial coordinate across the barrier [L]
- T = Thickness of the barrier [L]
- $\alpha_1 - \alpha_4$  = Capital cost coefficients of capsule components [\$/L<sup>3</sup>]
- $\alpha_5 - \alpha_6$  = Capital cost coefficients linked to discharge [\$/L<sup>3</sup>]
- $\beta_1 - \beta_4$  = Annual cost coefficients linked to discharge [\$/L<sup>3</sup>]
- $\beta_5$  = Annual cost coefficient of capsule maintenance [\$/T L<sup>3</sup>]
- $\Delta\Phi_{\max}$  = Potential difference between ambient conditions and the drain [L]
- $\Delta\Phi_{\min}$  = Potential difference across the barrier at the critical location [L]
- $\eta_1 - \eta_4$  = Parameters describing potential flow through the capsule [-]
- $\gamma$  = Grouped cost coefficient linked to discharge [\$/L<sup>3</sup>]
- $\mu_1 - \mu_3$  = Parameters describing dispersion across the barrier [-]

## 2.2 RESULTS OF INVESTIGATIONS

### 2.2.1 Potential-Flow Characteristic Relationships

The four physically significant potential flow parameters that are described and defined in Table 1a have been identified and found to describe operational characteristics of the capsule. They relate capsule design features, which define the geometry and the material properties of the capsule, to critical potential values. These potentials are in turn related to a flow parameter from which the capsule discharge may be determined. The following two relationships have been obtained:

$$\eta_2 = f_c (-0.67 \eta_1^2 + 1.69 \eta_1 - 0.03) \quad (2.1)$$

$$\eta_4 = \eta_3 \quad \text{for} \quad 0.2 < \eta_1 < 1 \quad (2.2)$$

**Table 1. Characteristic Parameters of the Capsule**

(a) Potential Flow Parameters

| <i>Parameter</i> | <i>Definition</i>                                     | <i>Description or Significance</i> |
|------------------|---|------------------------------------|
| $\eta_1$         | $\left[1 + \frac{K L^2}{K_1 T H}\right]^{-1}$         | Capsule Design Parameter           |
| $\eta_2$         | $\frac{\Delta\Phi_{\min}}{\Delta\Phi_{\max}}$         | Potential Parameter                |
| $\eta_3$         | $\frac{2 \Delta\Phi_{\min} + \Delta\Phi_{\max}}{3 T}$ | Barrier Gradient Parameter         |
| $\eta_4$         | $\frac{q_s H}{K}$                                     | Flow Parameter                     |

(b) Barrier Design Parameters

| <i>Parameter</i> | <i>Definition</i>             | <i>Description or Significance</i> |
|------------------|-------------------------------|------------------------------------|
| $\mu_1$          | $s/T$                         | Relative Penetration               |
| $\mu_2$          | $\frac{C(s) - C_0}{\Delta C}$ | Relative Concentration             |
| $\mu_3$          | $T/d$                         | Barrier Properties Parameter       |

where  $f_c$  is the combined correction factor which allows capsule designs with anisotropic conditions and partially penetrating drains to be related to a standard curve developed under isotropic, fully penetrating capsule conditions.

Numerical values of  $f_c$  have been obtained and plotted as a function of both degree of anisotropy and of partial penetration. It has also been noted that in both cases, values of  $f_c$  are sensitive to the capsule aspect ratio ( $H/L$ ) and the design parameter  $\eta_1$ .

### **2.2.2 Concentration Profiles Within The Barrier**

Dispersion has been investigated at the critical design point of the capsule resulting in an analytical description of the equilibrium concentration profiles across the barrier at this point. The following equation has been found to describe these profiles:

$$\mu_2 = \frac{e^{\mu_3 \mu_1} - 1}{e^{\mu_3} - 1} \quad (2.3)$$

where an additional three physically significant parameters  $\mu_1$ ,  $\mu_2$ , and  $\mu_3$ , which are related to contaminant migration through porous media, have been described and defined as in Table 1b. This description of the concentration profiles developed across the barrier may be used to establish a conservative, minimum migration criterion.

### **2.2.3 Economic Optimization of the Capsule**

The final step, development of the specific cost function from which optimizing trends can be identified, has resulted in the following expression:

$$C_s = \alpha_1 \frac{T}{H} + \alpha_2 + \alpha_3 \frac{W f_p}{L} + \alpha_4 f_h + \gamma \frac{r K \Delta \Phi_{\min}}{3 T H} \left[ 2 + \frac{1}{\eta_2} \right] + \beta_5 r \quad (2.4)$$

where the term  $\gamma$  has been defined as follows:

$$\gamma = \frac{\alpha_5 f_q + \alpha_6}{r} + \beta_1 f_q + \beta_2 + \beta_3 f_q + \beta_4 \quad (2.5)$$

This cost function was minimized with respect to each of the eight design variables that it contains. The results are four optimizing trends involving the design variables H, W, K, and  $\Delta\Phi_{\min}$ , three optimizing relationships involving L, T, and  $K_1$ , and an optimizing tendency that has been identified with regard to  $f_p$ . The optimizing trend identified for  $\Delta\Phi_{\min}$  coupled with a minimum migration criterion developed from the profiles described by Eq (2.3) must be taken together so that negligible migration occurs through the barrier. This and the other seven optimizing criteria have been incorporated in a predictor-corrector subroutine capable of finding the one optimum solution which minimizes the specific cost of Eq (2.4).

## 2.3 CONCLUSIONS

For existing landfill systems leaking into the surrounding groundwater, a recognized method by which outward migration of contamination can be slowed or reversed is through the creation of a cone of depression (lowering potential head) surrounding the contamination source. However, the cost of this remedial action involving continuous, long term pumping can be quite large. The active system proposed works on the same concept of creating and maintaining a lower potential surrounding the contamination source. The main difference is that *optimum* conditions are designed into this system which, when maintained, *prevent* leakage.

The ultimate objective of this study has been to provide an indication of the actual cost of safe, long-term landfill disposal of waste material. This actual cost includes long-term assurances that no external costs will develop as a result of leakage into the groundwater. Thus, the externality identified in Chapter 1 is internalized through the requirement of continuous operating and maintenance. Certainly the cost will be greater than that of the corresponding passive landfill disposal system which considers only the capital construction costs of the disposal system; however, it is

anticipated to fall far short of the astronomical external costs so often associated with such passive systems. Conceivably, the additional cost of active containment, in excess of the passive design option, might make other more permanent disposal alternatives more feasible than the landfill option altogether. It is suggested that this cost be used when comparing the feasibility of alternatives to landfill disposal systems.

# CHAPTER 3

## POTENTIAL-FLOW CHARACTERISTIC RELATIONSHIPS

### 3.1 NOTATION

- $f_a$  = Degree of anisotropy within the cell [-]
- $f_c$  = Correction factor either anisotropy or partial penetration [-]
- $f_h$  = Fraction of added material in the cell half depth [-]
- $f_p$  = Degree of partial penetration [-]
- $H$  = Half thickness of cell in the capsule design [L]
- $K$  = Darcy permeability of the barrier [L/T]
- $K_a$  = Darcy permeability of the added cell material [L/T]
- $K_b$  = Darcy permeability of the base disposal material [L/T]
- $K_1$  = Darcy horizontal permeability of the cell [L/T]
- $K_2$  = Darcy vertical permeability of the cell [L/T]
- $L$  = Half spacing of parallel drains in the capsule design [L]
- $L'$  = Linear distance through the cell from barrier to drain (1-D configuration only) [L]
- $q$  = Net discharge per linear foot through the quarter-capsule [L<sup>2</sup>/T]

- $q_s$  = Net specific discharge [L/T]  
 $t_a$  = Thickness of the added layers in the cell [L]  
 $t_b$  = Thickness of the base layers in the cell [L]  
 $T$  = Thickness of the barrier [L]  
 $v$  = Darcy's average velocity (1-D configuration only) [L/T]  
 $\Delta\Phi_{\max}$  = Potential difference between ambient conditions and the drain,  $\Phi_2 - \Phi_0$  [L]  
 $\Delta\Phi_{\min}$  = Potential difference across the barrier at the critical location,  $\Phi_1 - \Phi_0$  [L]  
 $\eta_1$  = Capsule design parameter [-]  
 $\eta_2$  = Potential parameter [-]  
 $\eta_3$  = Barrier gradient parameter [-]  
 $\eta_4$  = Flow parameter [-]  
 $\Phi_0$  = Ambient potential outside the barrier [L]  
 $\Phi_1$  = Potential at the critical point along barrier/cell interface [L]  
 $\Phi_2$  = Imposed potential within the drain [L]  
 $\bar{\Phi}$  = Representative (average) potential along the barrier/cell interface [L]  
 $\Phi(x)$  = Variation of potential as a function of the distance along the barrier/cell interface [L]

## 3.2 DEVELOPMENT OF FUNCTIONAL RELATIONSHIPS

This section identifies variables descriptive of geometric, material, and potential conditions of the active capsule and develops characteristic relationships between them. This development results from physical reasoning, dimensional analysis, and analogy to a simplified one dimensional situation. The resulting *functionals* are quantified with data generated through a numerical algorithm developed to describe potential flow through the capsule under various geometric, material, and boundary condition scenarios. The algorithm is based upon the finite-element method used to solve potential flow through anisotropic porous media comprised of various materials. It also



consists of input data generator programs and output data analysis programs for ease of interpreting the results for the specific capsule design.

A one dimensional potential flow representation through a domain of two adjacent materials of different permeabilities is first investigated. Solution over a domain having these characteristics is perhaps an over-simplification of the active capsule, and also possibly of little practical interest in itself. However, an analytical solution for these conditions is easily obtained and can be used to indicate the form of the more complex, as well as more practical, two dimensional situation.

### 3.2.1 One Dimensional Simplification

One dimensional steady flow from an ambient region, through two adjacent materials of different permeabilities (e.g., corresponding to barrier and cell), to a drained outlet is investigated. Figure 2 illustrates this one dimensional flow configuration resulting from the difference between the ambient potential  $\Phi_0$  along the left boundary, and the lower imposed potential  $\Phi_2$  at a drain along the right boundary. Darcy's law is used to establish the potential flow relationship both within the barrier and within the cell. This law [2] [3] [7] states that, in general, the average flow velocity  $v$  in the direction  $l$  is negatively proportional to the potential gradient in that direction. Taking  $k$  to be this negative proportionality constant, it is written:

$$v = k \frac{\partial}{\partial l} [\Phi]. \quad (3.1)$$

Since dispersion effects are not considered in the immediate analysis, the averaging of the velocity resulting from direct application of this law presents no problem in developing the relationships at hand. The potential gradient is assumed to be constant for homogeneous, porous materials under equilibrium conditions and is represented by a constant hydraulic gradient (i.e.  $\Delta\Phi/\Delta L$ , the change in potential relative to change in position) through each material. Referring again to Figure 2 and substituting directly into Darcy's law, two expressions, one describing flow through the cell, the other describing flow through the barrier, are obtained, respectively:

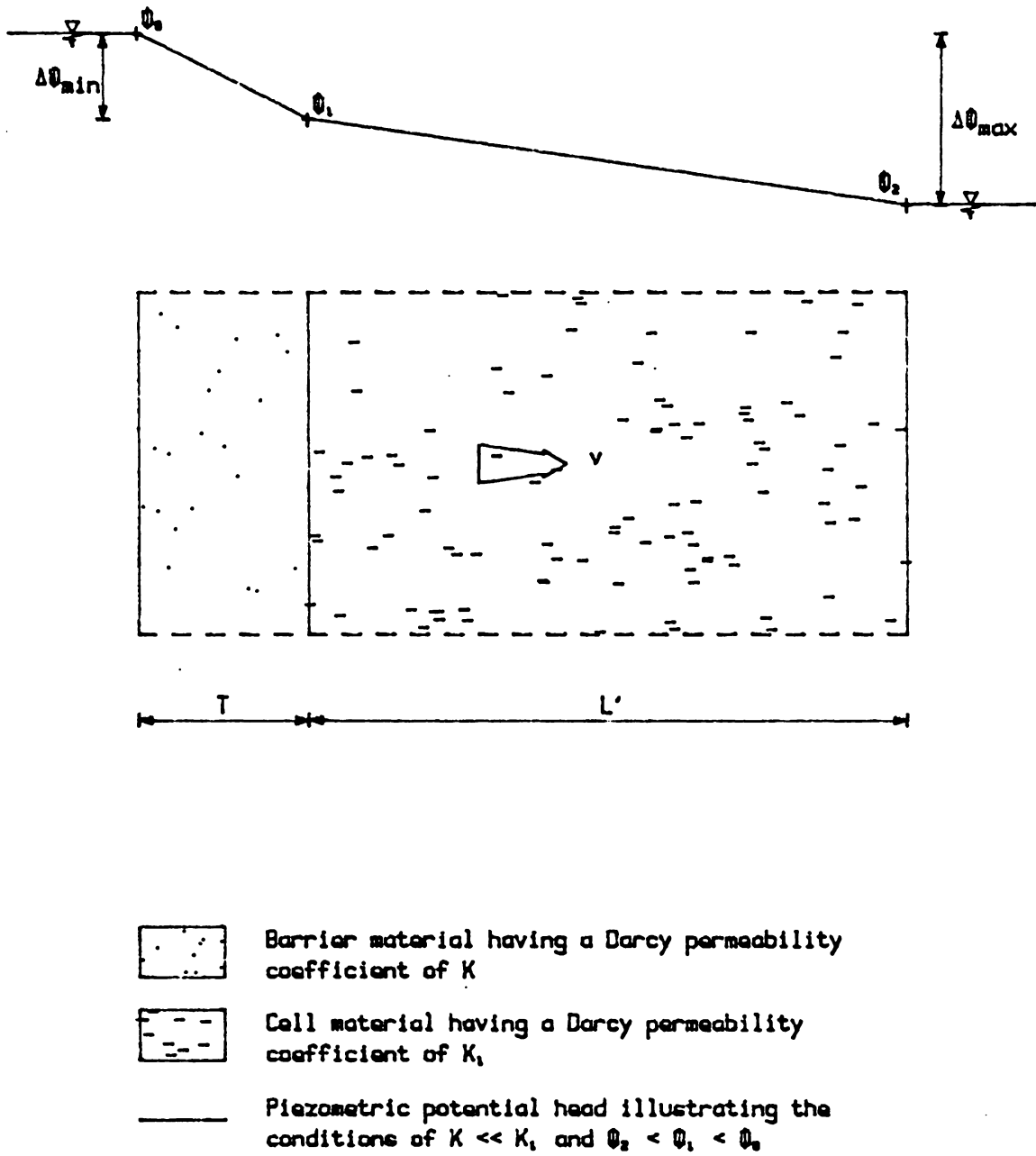


Figure 2. Conditions for One Dimensional Flow

$$v = K_1 \frac{\Phi_2 - \Phi_1}{L'} \quad (3.2)$$

$$v = K \frac{\Phi_1 - \Phi_0}{T} \quad (3.3)$$

Elimination of  $v$  by combining Eqs (3.1) and (3.2) effectively imposes the necessary condition of continuity between barrier and cell. Thus:

$$K_1 \frac{\Phi_2 - \Phi_1}{L'} = K \frac{\Phi_1 - \Phi_0}{T} \quad (3.4)$$

Through simple algebraic manipulations, noting the definitions of potential variables as illustrated in Figure 2 and indicated in the notation, a non-dimensionalized equation describing the relationship between potential variables and geometric and material design variables is obtained, as follows:

$$\frac{\Delta\Phi_{\min}}{\Delta\Phi_{\max}} = \left[ 1 + \frac{K L'}{K_1 T} \right]^{-1} \quad (3.5)$$

Finally, rewriting Eq (3.3) to include the definition of  $\Delta\Phi_{\min} = \Phi_1 - \Phi_0$  per the notation, a non-dimensionalized form of Darcy's law is obtained which describes a relationship between flow through the barrier and potential gradient across the barrier.

$$\frac{v}{K} = \frac{\Delta\Phi_{\min}}{T} \quad (3.6)$$

Eq (3.5) may be used to predict the resulting potential difference across the barrier  $\Delta\Phi_{\min}$  upon imposing the total difference in potential  $\Delta\Phi_{\max}$  at the drain for known values of the design variables  $K$ ,  $K_1$ ,  $L'$  and  $T$ . The significance of this relationship is apparent upon realizing that the value of  $\Delta\Phi_{\min}$  is critical in the investigation of the dispersion across the barrier. Eq (3.6) evaluates the flow velocity, constant for both barrier and cell, from this critical potential difference. These two equations which describe potential and flow respectively, represent a complete solution to the one dimensional problem as presented. Thus, two pairs of physically significant dimensionless param-

eters have been identified in Eqs (3.5) and (3.6). The first describes the primary relationship between a *design parameter* and a *potential parameter* and the second describes a secondary relationship between a *barrier gradient parameter* and a *flow parameter*. Through physical reasoning, dimensional analysis, and comparison to this one-dimensional analytical solution, four analogous parameters have been identified which characterize a two-dimensional capsule descriptive of the active landfill design illustrated in Figure 1 on page 3.

### **3.2.2 Two Dimensional Capsule Representation**

#### **3.2.2.1 Capsule Description**

Figure 3 gives details of conditions within and surrounding the containment capsule which result in convective inflow through the barrier and cell. The symmetrical nature of the two dimensional containment capsule is immediately apparent and advantage is taken of it. Lines of symmetry, as illustrated and described on the figure, correspond to lines across which there is no flow. They divide the idealized capsule into four regions, all having completely similar characteristics. The solution of any one quarter thus effectively describes the whole capsule, and, for that matter, the entire active landfill encapsulation, which consists of any number of such capsules as illustrated in Figure 1 on page 3. The ability to evaluate the performance of the entire landfill system based on the performance of individual capsules, and even quarter-capsules, is obviously a great advantage from the computational standpoint.

Of practical interest is the minimum value of the potential difference across the barrier,  $\Delta\Phi_{\min}$ , which results from the operation of the capsule as illustrated in Figure 3. Notice that  $\Delta\Phi_{\min}$  occurs at a point midway between the parallel drains and thus defines the location of the critical point shown on the figure. It is at this point that a minimum allowable migration criterion should be met. For all other points along the barrier, the greater potential difference across the barrier makes the migration retarding convective inflow greater, and thus, the outward migration

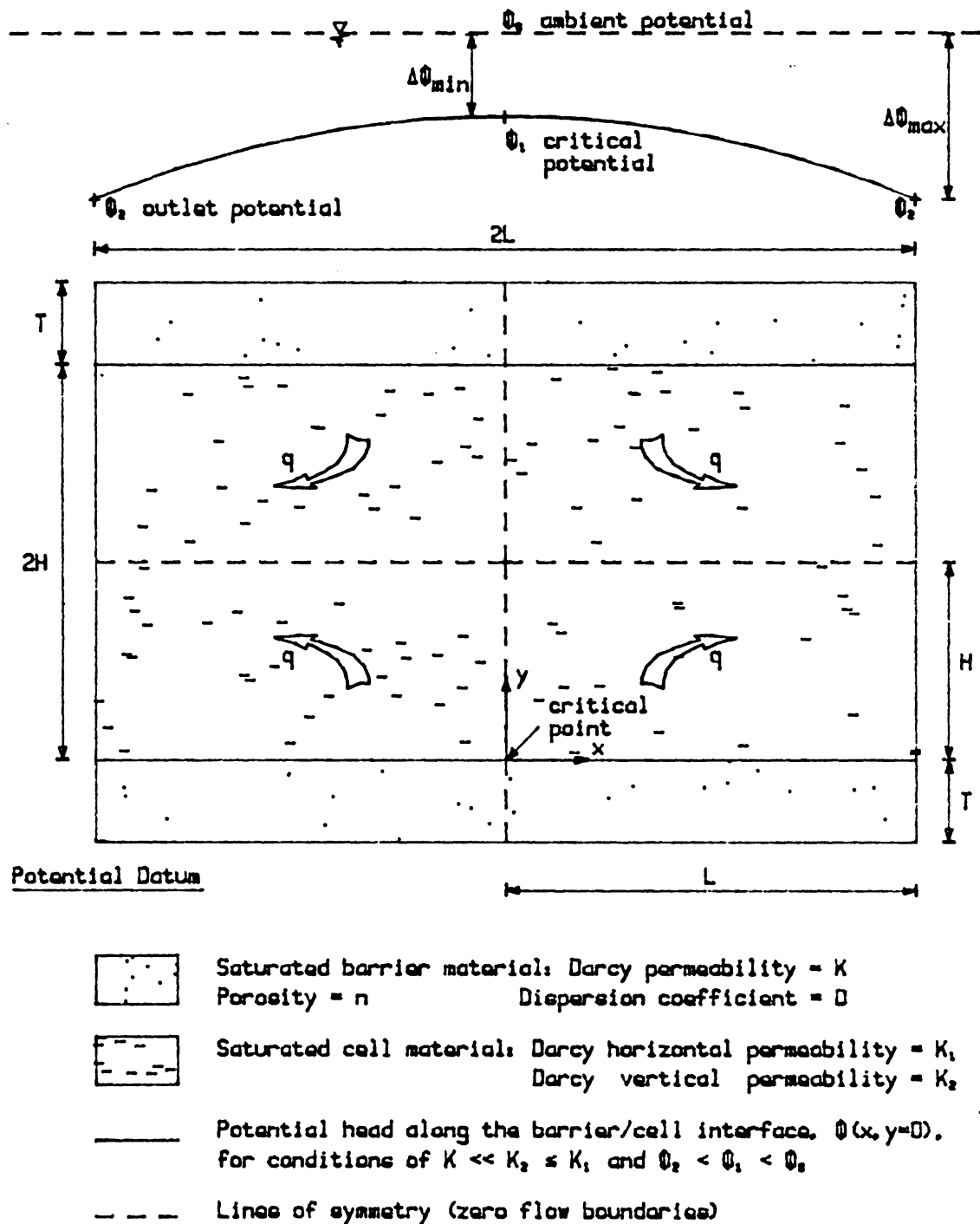


Figure 3. The Containment Capsule: Definition sketch.

potential lesser. The migration characteristics at the critical point is investigated in Chapter 4 to supplement this analysis of the containment capsule, but the primary interest at present is the determination of the potential within the defined quarter solution domain, and particularly, that value corresponding to the critical point,  $\Delta\Phi_{\min}$ .

Of secondary interest is the value of  $q$ , the flow or discharge per linear foot through the capsule, since to reduce this flow will obviously be an important constraint in the cost effectiveness of the operation of active landfill designs. The specific discharge of the capsule, defined as  $q_s = \frac{q}{HL}$ , has dimensions of reciprocal time, and can be visualized as the inverse of the time required to fill a volume equivalent to that of the containment cell at a flow rate  $q$ . This variable has the same value whether referenced to the quarter-capsule solution domain area, the full-capsule area, or any multiple of the full-capsule area, thus its value is directly comparable between various solutions regardless of the geometry of those solutions.

The solution domain for the active capsule must be at least two dimensional so that an adequate description of the potential and flow conditions of the capsule under practical circumstances is provided. Under these conditions, curvilinear flow paths within the possibly anisotropic cell (and the barrier to a lesser degree) result, for which no directly applicable analytical description has yet been found. Therefore, functional forms of the primary and secondary relationships describing potential and flow are sought by analogous derivation to the one dimensional case. But first, a dimensional analysis is performed for the purpose of identifying dimensionless groups upon which the cell's potential characteristics are dependent, and to aid in the later identification of valid ranges.

### 3.2.2.2 Dimensional Analysis

The six variables of Eq (3.5) are required to describe the primary relationship for the simplified one-dimensional case illustrated in Figure 2 on page 17. In comparison to the practical two-dimensional situation illustrated in Figure 3, each of the six variables can be associated with a variable of like name and definition, with the noted exception of the difference in definitions of  $L'$  and  $L$  (see the notation). The added degree of freedom of a two-dimensional solution domain

makes necessary the addition of the geometric variable  $H$  which describes the half depth of the cell. Thus, seven variables are assumed to be involved in the primary relation between potential and design characteristics of the capsule.

|                     |   |   |
|---------------------|---|---|
| $H$                 | = | Half thickness of cell [L]                      |
| $K$                 | = | Darcy permeability of the barrier [L/T]         |
| $K_1$               | = | Darcy horizontal permeability of the cell [L/T] |
| $L$                 | = | Half spacing of parallel drains [L]             |
| $T$                 | = | Thickness of the barrier [L]                    |
| $\Delta\Phi_{\max}$ | = | Maximum potential difference across barrier [L] |
| $\Delta\Phi_{\min}$ | = | Minimum potential difference across barrier [L] |

According to Buckingham's  $\pi$ -Theorem [15] the seven primary variables involving only the two dimensions of length [L] and time [T] can be grouped by selecting two of the variables as repeating variables so that five dimensionless numbers ( $\pi$ 's) result, each corresponding to one of the remaining non-repeating variables. By choosing  $K$  and  $H$  as the two repeating variables, the dimensionless groups of Table 2 have been formed. Each  $\pi$  has fundamental physical significance in describing capsule characteristics as indicated in the table.

The following derivations result in relationships between parameters formed of these  $\pi$ 's. These relationships are quantified using data generated under varying values of these  $\pi$ 's. Further derivations using these relationships, specifically those in the economic analysis of Chapter 5, are subject to the ranges of the  $\pi$ 's for which they were developed.

### 3.2.2.3 Derivation of Functionals

Following an analogous derivation to the one-dimensional case, Darcy's Law and the requirements of continuity between barrier and cell are used to describe significant flow and potential relationships for the capsule conditions. Under two dimensional flow conditions, the lengths and widths of the flow paths between points of interest now curvilinear and are therefore represented by characteristic geometric lengths. Thus, proportional relationships are assumed rather than

**Table 2. Results of Dimensional Analysis**

| <i>Dimensionless Number</i> | <i>Variable Grouping</i>      | <i>Significance</i>                    |
|-----------------------------|-------------------------------|--|
| $\pi_1$                     | $\frac{K_1}{K}$               | Permeability ratio                     |
| $\pi_2$                     | $\frac{H}{L}$                 | Aspect ratio                           |
| $\pi_3$                     | $\frac{T}{H}$                 | Relative barrier thickness             |
| $\pi_4$                     | $\frac{\Delta\Phi_{\max}}{H}$ | Relative outlet potential difference   |
| $\pi_5$                     | $\frac{\Delta\Phi_{\min}}{H}$ | Relative critical potential difference |



equalities as in the one dimensional case. For the purpose of this derivation, equalities are assumed through the use of proportionality constants.

$\bar{\Phi}$  is introduced, for now, as an arbitrarily defined variable which represents, in some sense, an average value of potential head along the barrier/cell interface. Being analogous to  $\Phi_1$  defined for the one dimensional solution, its value will depend not only on the characteristics of the cell but of the barrier as well. Using this representative value of potential at the barrier/cell interface and assuming the *form* of one dimensional Darcy flow to approximate the curvilinear features of the two dimensional solution domain, two relationships result. The first one is obtained by applying Darcy's Law through the cell:

$$q = C_1 \left[ \frac{\Phi_2 - \bar{\Phi}}{L} K_1 H \right] \quad (3.7)$$

where  $C_1$  is assumed to account for uncertainties involved in defining  $\bar{\Phi}$  as well as for using the cell dimensions  $L$  and  $H$  as characterizing curvilinear length and width of flow path respectively. Next, Darcy's Law is applied across the barrier, now using the barrier dimensions  $T$  and  $L$  as flow path characteristic length and width, respectively:

$$q = C_2 \left[ \frac{\bar{\Phi} - \Phi_0}{T} K L \right] \quad (3.8)$$

Elimination of  $q$  by combining Eqs (3.7) and (8) effectively imposes continuity between barrier and cell, yielding:

$$\frac{\Phi_2 - \bar{\Phi}}{L} K_1 H = C_3 \left[ \frac{\bar{\Phi} - \Phi_0}{T} K L \right] \quad (3.9)$$

Upon rearranging, the following non-dimensional expression is obtained.

$$\frac{\Phi_2 - \Phi_0}{\bar{\Phi} - \Phi_0} = C_4 \left[ 1 + \frac{K L^2}{K_1 T H} \right] \quad (3.10)$$

The specific discharge,  $q_s$ , (or flow per protected volume--a physically more significant variable in describing the containment capsule performance as previously indicated) is used to replace  $q$  in Eq (3.8), and after rearranging, this equation yields:

$$\frac{q_s H}{K} = C_5 \left[ \frac{\bar{\Phi} - \Phi_0}{T} \right] \quad (3.11)$$

Eqs (3.10) and (3.11) can be further quantified by explicitly defining  $\bar{\Phi}$  as some function of the more meaningful variables  $\Phi_1$  and  $\Phi_2$ . Assuming the average potential value along the barrier/cell interface as this representative potential, and by referring to Figure 3 on page 20,  $\bar{\Phi}$  may be defined as follows:

$$\bar{\Phi} = \frac{1}{L} \int_0^L \Phi(x) dx \quad (3.12)$$

To evaluate this integral, a function for  $\Phi(x)$  is assumed. Obviously,  $\Phi(0) = \Phi_1$  and  $\Phi(L) = \Phi_0$  are two boundary conditions that must be met. Also, the zero flow boundary which exists along the left edge of the quarter solution domain due to symmetry provides a third boundary condition. That is,  $\frac{\partial}{\partial x}[\Phi(x=0) = 0]$ . With three boundary conditions to satisfy, a second degree polynomial (or parabolic approximation) seems to be the natural choice to represent  $\bar{\Phi}$ . A linear approximation is impossible due to the zero flow boundary condition along the left edge of the domain and a third order is not reasonable because there is no physical reason for the existence of an inflection point on the *surface of depression*. Thus, the relationship describing potential along the barrier is approximated as a parabola.

$$\Phi(x) \cong A x^2 + B x + C \quad (3.13)$$

A, B, and C are coefficients of the parabola and can be determined through application of the boundary conditions to yield:

$$\Phi(x) \cong \frac{\Phi_2 - \Phi_1}{L^2} x^2 + \Phi_1 \quad (3.14)$$

Finally using the results of Eq (3.14) in Eq (3.12) and carrying out the required integration, the representative value (having now been defined as the average value) along the barrier/cell interface, is defined in terms of  $\Phi_1$  and  $\Phi_2$  as follows:

$$\bar{\Phi} \cong \frac{2\Phi_1 + \Phi_2}{3}. \quad (3.15)$$

This result is used to modify Eq (3.10). Upon simplification, noting definitions of  $\Delta\Phi_{\min}$  and  $\Delta\Phi_{\max}$  per the notation at the beginning of the chapter and referring again to Figure 3 on page 20:

$$\frac{\Delta\Phi_{\min}}{\Delta\Phi_{\max}} = C_6 \left[ \frac{1.5}{1 + \frac{KL^2}{K_1 TH}} - 0.5 \right] \quad (3.16)$$

The translation term (-0.5) and the scale factor (1.5) above are combined with proportionality constants to obtain the following primary relationship describing capsule characteristics:

$$\frac{\Delta\Phi_{\min}}{\Delta\Phi_{\max}} = C_7 \left[ \left[ 1 + \frac{KL^2}{K_1 TH} \right]^{-1} \right] + C_8 \quad (3.17)$$

Similarly modifying Eq (3.11), making use of the results of Eq (3.15) and the definitions of  $\Delta\Phi_{\min}$  and  $\Delta\Phi_{\max}$ , a secondary relationship is produced:

$$q_s \frac{H}{K} = C_9 \left[ \frac{2\Delta\Phi_{\min} + \Delta\Phi_{\max}}{3T} \right] \quad (3.18)$$

In order to simplify the interpretation of a parameter defined and evaluated subsequently, the scale factor (1/3) of this expression is retained.

**Table 3. Characteristic Parameters of the Capsule**

| <i>Parameter</i> | <i>Definition</i>                                     | <i>Description or Significance</i> |
|------------------|---|------------------------------------|
| $\eta_1$         | $\left[1 + \frac{K L^2}{K_1 T H}\right]^{-1}$         | Capsule Design Parameter           |
| $\eta_2$         | $\frac{\Delta\Phi_{\min}}{\Delta\Phi_{\max}}$         | Potential Parameter                |
| $\eta_3$         | $\frac{2 \Delta\Phi_{\min} + \Delta\Phi_{\max}}{3 T}$ | Barrier Gradient Parameter         |
| $\eta_4$         | $\frac{q_s H}{K}$                                     | Flow Parameter                     |

### 3.2.2.4 Physical Significance

Note that, analogous to Eqs (3.5) and (3.6), Eqs (3.17) and (3.18) relate two dimensionless groups of the design variables describing the active capsule. Thus four dimensionless groups, or parameters, are identified to which physical significance is attached. Eq (3.17) relates potential conditions to geometric and material properties of a given capsule design configuration. Eq (3.18) relates the resulting flow quantity to barrier conditions of that configuration. These four parameters are denoted by subscripted  $\eta$ 's, and Table 3 defines and describes each. Making use of these parameters, Eqs (3.17) and (3.18), respectively, are rewritten, now in functional form:

$$\eta_2 = \text{fcn}[\eta_1] \quad (3.19)$$

$$\eta_4 = \text{fcn}[\eta_3] \quad (3.20)$$

Once the two functionals relating the identified parameters are verified and quantified for the defined containment capsule, the physical significance attached to each parameter becomes apparent. For instance, the value of the critical potential difference relative to the maximum potential difference imposed at the outlet is determined through the primary relationship knowing geometric and material properties of the capsule. Thus, by specifying the value of the imposed potential for a certain capsule design, Eq (3.19) is used to determine the critical value of potential difference across the barrier, from which, through the secondary functional relationship of Eq (3.20), the flow rate or capsule discharge is determined. Recall again the similarity between these two functionals and the analytical solution to the one-dimensional case represented by Eqs (3.5) and (3.6).

### 3.3 NUMERICAL ANALYSIS OF CAPSULE HYDRAULICS

A computational algorithm having a central program based on the finite-element method has been developed in the BASIC language to aid in the hydraulic analysis of the capsule. Its primary purpose is to provide the data necessary to verify and evaluate the primary and secondary functional relationships given by Eqs (3.19) and (3.20). In addition to the general finite-element program, the algorithm consists of specialized programs which either generate input data or analyze and present output data for various capsule design scenarios. First described is the finite-element program, core of the solution algorithm, followed by an itemized description of the computational algorithm including the supplemental generation and analysis programs.

The algorithm is tested, among other things, for convergence by increasingly refining the finite-element mesh configurations until acceptable accuracy of the numerical solution is attained. The functionals are then quantified for standard conditions of isotropic material properties and fully penetrating outlet drains. Finally, non-standard conditions are investigated to generate correction factors accounting for anisotropic material conditions and partially penetrating outlet drains.

#### 3.3.1 Finite-Element Analysis of Steady Potential Flow

A closed form solution to potential flow through the two-dimensional capsule as defined in the definition sketch of Figure 3 on page 20 has not been found. Indeed, had one been available, this chapter would have been complete with analytical relationships corresponding to Eqs (3.19) and (3.20) instead of the undefined functionals presented. Lacking this direct solution, however, the finite-element method has been utilized [4] in order to obtain an approximate solution descriptive of capsule hydraulic conditions under various geometric, material and boundary conditions. The program makes use of the Galerkin method of weighted residuals as the required error minimization technique.

Provision for anisotropic seepage [30] [32] has been incorporated in the finite-element program in order to describe the expected differences in principle permeabilities within the disposal cell. Because, under the capsule problem scenario, the identified principle permeabilities axes are always horizontal and vertical, the more general condition of irregular principle axes has not been provided for, but may conceivably be added. This would involve the addition of a cosine multiplier matrix at the local assembly level within the finite-element program. Added input required would be the angle that the principle axis for each element makes with respect to the global coordinate system (always assumed zero in the existing program).

Unique features of the banded, symmetric matrices produced by finite-element solutions can be used to more efficiently compute and store results. However, for simplicity but at the expense of computation time, these unique features have not been taken advantage of in the program developed. Thus, a truly square work matrix of dimension equal to the number of nodal points is generated, to which boundary conditions, both natural and fixed, are applied.

Since the solution is already known for all fixed nodes, removing their corresponding rows from the work matrix does not effect the solution obtained; however, a complex re-numbering scheme would, in general, have to be adopted. To avoid this while still removing from consideration most of the fixed nodal rows, nodal points of the capsule domain are numbered so the largest possible number of fixed nodal points are ordered last. Thus, the order of the matrix corresponding to a certain capsule design may be reduced by a specific amount without effecting the numbering scheme. The reduction in order achieved through this simple procedure saves considerable computation time by reducing the number of simultaneous equations to be solved under the chosen computation scheme [5] [10].

The resulting *BASIC* finite-element program *F.BAS* uses triangular elements and linear interpolating polynomials as basis functions in the numerical solution of partial differential equations describing potential flow. The program is capable of handling two-dimensional, non-homogeneous, anisotropic solution domains of irregular shape. The numeric results are interpreted to represent potential flow through saturated porous media under steady-state conditions. Boundary conditions of either fixed (Dirichlet) or natural (Neumann) types may be specified. Both input

and output data for the finite-element program consists of free-format numerical data describing material properties, nodal geometry and potentials, and elemental connectivities and average velocities. Thus *F.BAS* is the central program of the computational algorithm that has been developed. A listing is given in Appendix A.

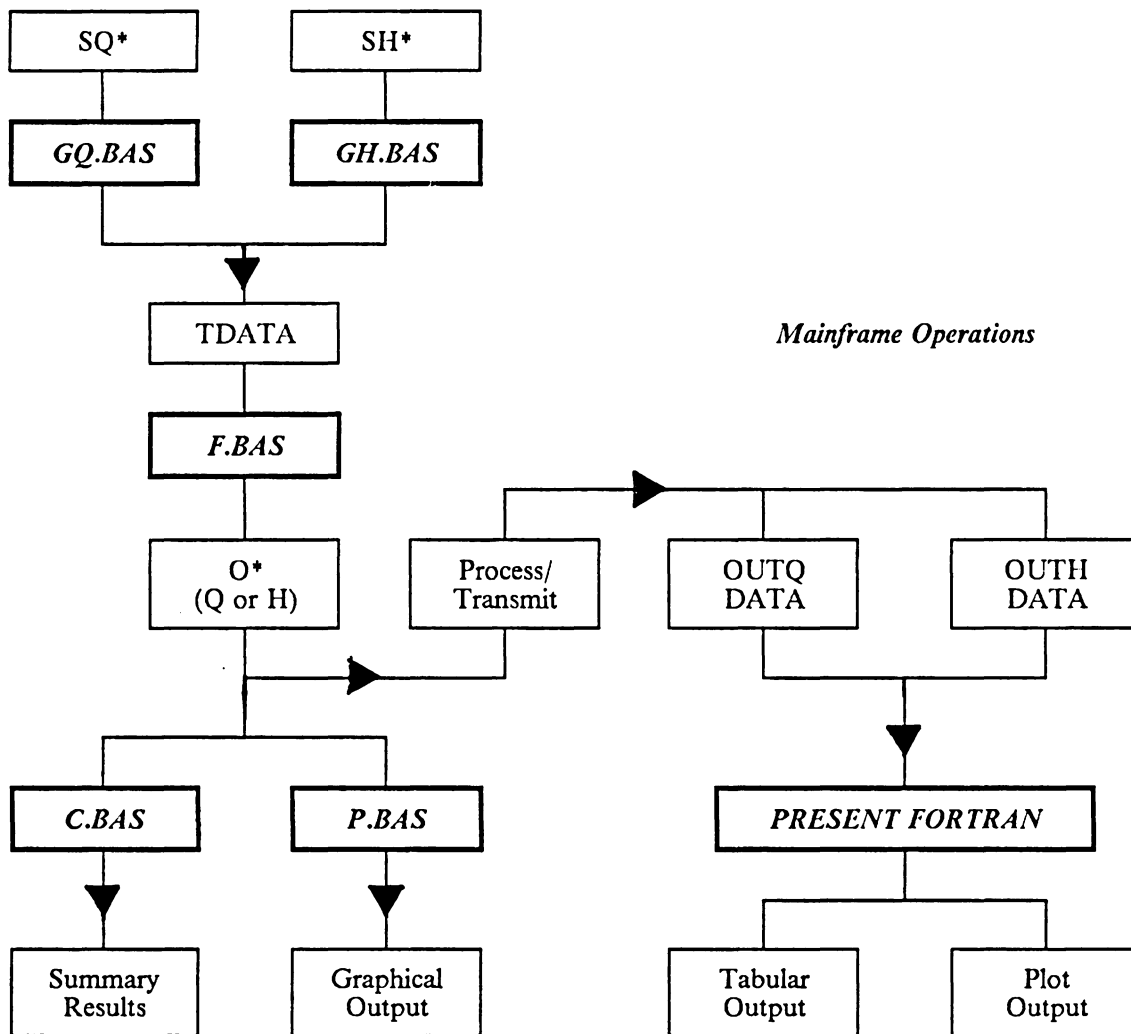
### **3.3.2 The Computational Algorithm**

Specialized generator and analysis programs are used to provide easily obtainable, interpretable results of different design scenarios. They generate and analyze, respectively, the input and output data of the core finite-element program described above. Thus, three steps are required to obtain the dimensionless parameter values for individual cases under differing capsule hydraulic conditions. First, a specialized generator program produces input data for the finite-element program corresponding to specific capsule geometry and material properties, and potential and flow boundary conditions. Second, the finite-element program determines the potential and velocity distributions throughout the solution domain. And third, specialized analysis/presentation programs aid in interpreting the results of the finite-element solution through tabular and graphical presentation of the output. The analysis of the finite-element output includes computation of the dimensionless parameters  $\eta_1$  through  $\eta_4$  as defined in Table 3 on page 27.

**Data Management Programs and Processes:** The auxiliary programs, data files and processes required to carry out the the above mentioned steps and their relationships to the core finite-element program, as well as each other, are illustrated in Figure 4. Items corresponding to programs are represented by walled thicker boxes and the names of these programs are shown in bold italics. An asterisk following a data file indicates that the files of that type are individually named and stored to preserve the results. Each item in the figure is briefly defined or explained. Listings of the auxiliary programs developed in BASIC to solve the quarter capsule are given in Appendix B. The FORTRAN version of the presentation program is also presented.



*Personal Computer Operations*



\* Specification or output data retained for possible review

Figure 4. Schematic of Data Generation Methodology

**Generation of Input Data:** The finite-element program requires a specific input file **TDATA**, a *temporary*, free format file which, under the solution algorithm presented, is created by one of two generator programs developed for this purpose. One generates **TDATA** for cases associated with a quarter-capsule solution and the other for the half-capsule solution. Each requires information on capsule characteristics which is provided by individual capsule specifications data files, one for each case investigated. **TDATA** is considered temporary because each successive application of a generator program reuses this same data file. Should the input data for a particular case have to be reviewed, it can be easily re-generated from the minimal information contained in the corresponding specifications file through application of the appropriate generator program.

- **GQ.BAS** generates input data descriptive of a finite-element mesh representing the symmetrical lower right quarter of the full-capsule solution domain. It is used only for cases having fully penetrating outlet drains (and thus two axes of symmetry). Case specifications are given in specification data files, **SQ\***, describing material properties, geometric configuration, boundary condition data, and finite-element mesh discretization for the quarter-capsule solution domain.
- **GH.BAS** generates input data descriptive of a finite-element mesh representing a symmetrical right half of the full-capsule solution domain. It is used for cases having partially penetrating outlet drains (and thus only one axis of symmetry). Case specifications are given in specification data files, **SH\***, describing material properties, geometric configuration, boundary condition data, and finite-element mesh discretization for the half-capsule solution domain.

**Application of the Finite-Element Program:** The pivotal finite-element program, **F.BAS** previously described, numerically solves potential flow through porous media for various identifiable hydraulic conditions. In order to be as general as possible, its only intended function is to compute nodal potentials and elemental average velocities from material, geometric, and boundary condition data. When used as part of the solution algorithm herein described, the required input is contained in the data file **TDATA** which is generated as above for the special configuration of the capsule solution domain. Output data files for the finite-element program, **O\***, like **TDATA**, are free-format files

and reflect the material and geometric characteristics of the corresponding domain. The results of the finite-element solution, numerical data representing nodal potential and average elemental flow values for each case, are contained in this output.

**Presentation of Results:** Output from the core finite-element program involves simply numerical information including a reflection of material properties, nodal geometry, and elemental connectivities in addition to computed values of nodal potentials and average elemental velocities. In order to present the specialized capsule data in meaningful form, analysis and presentation programs have been written for both P.C. and Mainframe operation.

Because the finite-element program is desired to be general in nature, no provision has been made to pass capsule geometric variables as found in the specifications file through the entire algorithm. Instead, these variables are recomputed from the reflected nodal geometric data knowing characteristics of the standard capsule design for both the quarter-capsule and half-capsule solution domains.

For each case, computations from data in the respective output data file are made in order to obtain numerical values of the dimensionless parameters. Two BASIC programs were written to facilitate this.

- *C.BAS* computes summary data, including the parameters  $\eta_1$  through  $\eta_4$  and the specific discharge  $q_s$ , for individual case results. These summary data are added to summary data files for later quantification of the functionals of Eqs (3.19) and (3.20).
- *P.BAS* uses the graphics capability of the IBM-PC to plot a representation of potential and flow characteristics for individual case results. It is especially useful in that it allows the user to quickly get a pictorial representation of the finite-element results of any particular solution.

The power of the IBM-mainframe and its supported facilities, including the VS Fortran Compiler, the Versatec Plotter, and the GML Script Processor, are used in order to better present output of the various solutions. Successive output data files associated with either a quarter or a half solution domain are assembled into respective **OQ DATA** or **OH DATA** files and transmitted

from PC-diskette to Mainframe-disk storage. The Fortran IV program *PRESENT FORTTRAN* reads these data files, computes values for the dimensionless parameters and specific discharge, and, according to numeric, string or logical information provided in supplemental data files, produces either plot output, tabular output, or both. Thus, summary information as well as the potential and velocity field data may be presented either in tabular or graphical form.

**Computational Facilities:** The VPI & SU Computer Center has a Main Frame consisting of an IBM 3081 Processor Complex along with an IBM 370/158 Central Processor Unit with Attached Processor, two IBM 4341 Central Processor Units, and one Digital VAX 11/780 Central Processor Unit. The 3081 Central Processor Unit runs OS/VS2 Release 3.8 (MVS/SP1) with Job Entry Subsystem 2 (JES2); and VAX11/780 runs MVS. The campus has a hardware network communication system to which an IBM Personal Computer, model IBM PC, is connected linking this stand alone unit to the Main Frame. Peripherals to the PC include an Epson printer, model FX80, and a Hewlett Packard Plotter, model HP7470A. Also available was a Leading Edge microcomputer, model D, with an Epson printer, model FX85.

### **3.3.3 Accuracy of Solution**

Standard values for the design variables were assigned in view of those which might be expected to apply to the tailings disposal area of a uranium milling operation. The proposed design for such an operation in Virginia has been submitted to the Virginia Uranium Administrative Group [19]. The proposal specifies that the de-watered tailings would occupy an actual depth of about 40 feet and would be encapsulated within a 1-foot clay liner of local material. The range of permeabilities of such a barrier material, based on tests performed on remolded samples, is estimated to be between  $3 \times 10^{-8}$  and  $2.9 \times 10^{-7}$  cm/sec. Depending upon the milling process, the resulting tailings are classified as silty sand or very silty sand (SM) in the Unified Soil Classification System.

Based on this information, the values for the design variables given in Table 4(b) are assumed. The half drain spacing, a feature not part of the passive design specified in the report, was chosen so that the resulting value of the design parameter falls near the middle of its possible range of values. That is, a middle value of  $\eta_1 = 0.3333$  was chosen where, by inspection of its definition given in Table 3, the possible range is seen to be  $0 < \eta_1 < 1$ . Design variables which result in low and high values of  $\eta_1$  (0.1111 and 0.8333) are also shown in Table 4, parts (a) and (c), respectively. These values were also used in accuracy considerations to investigate the significance of the value of the design parameter itself.

Upon choosing these standard design variables for a quarter-capsule solution domain, the algorithm was applied in order to evaluate the accuracies to be expected under various degrees of domain refinement. Points explicitly considered are convergence of the solution, the maintenance of flow continuity through the capsule, and the linearity of the solution with respect to potential. From these considerations, the standard finite-element domain discretization is identified. It is refined to a degree sufficient for desired accuracy but not so greatly refined as to be inefficient and computationally burdensome.

**Convergence Considerations:** The number of finite-elements used in the numerical scheme naturally affects the accuracy of the solutions obtained. A series of tests was therefore carried out to assess this effect and the results are summarized in Table 5. Part (a) of the table illustrates the effect of refining the finite-element mesh in the horizontal direction by increasing the number of element columns (increasing NCOL) while holding the number of element rows constant at two (NROW = 2). Part (b) of the table illustrates the effect of refining the finite-element mesh in the vertical direction by changing the number of element rows (varying NROW) while maintaining a constant number of element columns (NCOL = 8).

The error, given in percent, is computed for low, medium and high values of the design parameter  $\eta_1$  from the corresponding converging values of the potential parameter  $\eta_2$ . It is based on the *most accurate* value attained, that is, the one corresponding to the most highly refined finite-element mesh. Specifically, this value corresponds to 20 element columns for  $\eta_1 = 0.1111$  and  $\eta_1$

**Table 4. Values of the Standard Design Variables**

(a)  $\eta_1 = 0.1111$

| <i>Variable</i> | <i>Value</i> | <i>Description</i>   |
|-----------------|--------------|----------------------|
| K               | 1 ft/yr      | Barrier permeability |
| $K_1$           | 10000 ft/yr  | Cell permeability    |
| L               | 800 ft       | Half drain spacing   |
| H               | 4 ft         | Half depth of cell   |
| T               | 2 ft         | Barrier thickness    |

(b)  $\eta_1 = 0.3333$

| <i>Variable</i> | <i>Value</i> | <i>Description</i>   |
|-----------------|--------------|----------------------|
| K               | 1 ft/yr      | Barrier permeability |
| $K_1$           | 10000 ft/yr  | Cell permeability    |
| L               | 800 ft       | Half drain spacing   |
| H               | 16 ft        | Half depth of cell   |
| T               | 2 ft         | Barrier thickness    |

(c)  $\eta_1 = 0.8333$

| <i>Variable</i> | <i>Value</i> | <i>Description</i>   |
|-----------------|--------------|----------------------|
| K               | 1 ft/yr      | Barrier permeability |
| $K_1$           | 100000 ft/yr | Cell permeability    |
| L               | 800 ft       | Half drain spacing   |
| H               | 16 ft        | Half depth of cell   |
| T               | 2 ft         | Barrier thickness    |

**Table 5. Finite-Element Mesh Refinement**

(a.) Horizontal Refinement (NROW = 2)

| NCOL | $\eta_1$ | $\eta_2$ | $\eta_3$ | $\eta_4$ | $q_s$  | Error | Time |
|------|----------|----------|----------|----------|--------|-------|------|
| 02   | 0.1111   | 0.1428   | 2.1426   | 2.1426   | 0.5356 | 21.12 |      |
| 04   | 0.1111   | 0.1245   | 2.0817   | 1.8602   | 0.4651 | 5.60  |      |
| 08   | 0.1111   | 0.1196   | 2.0653   | 1.7827   | 0.4457 | 1.44  | 0:56 |
| 12   | 0.1111   | 0.1185   | 2.0618   | 1.7676   | 0.4419 | 0.51  | 2:33 |
| 16   | 0.1111   | 0.1182   | 2.0607   | 1.7621   | 0.4405 | 0.25  | 5:21 |
| 20   | 0.1111   | 0.1179   | 2.0598   | 1.7590   | 0.4398 | 0.00  | 9:27 |
| 02   | 0.3333   | 0.4706   | 3.2352   | 3.3086   | 0.2068 | 2.46  |      |
| 04   | 0.3333   | 0.4620   | 3.2067   | 3.1837   | 0.1990 | 0.59  |      |
| 08   | 0.3333   | 0.4599   | 3.1996   | 3.1516   | 0.1970 | 0.13  |      |
| 12   | 0.3333   | 0.4594   | 3.1979   | 3.1453   | 0.1966 | 0.02  |      |
| 16   | 0.3333   | 0.4592   | 3.1973   | 3.1413   | 0.1964 | -0.02 | 5:25 |
| 20   | 0.3333   | 0.4593   | 3.1975   | 3.1425   | 0.1964 | 0.00  | 9:50 |
| 02   | 0.8333   | 0.9080   | 4.6933   | 4.7118   | 0.2945 | 0.07  | 0:04 |
| 04   | 0.8333   | 0.9075   | 4.6918   | 4.6956   | 0.2935 | 0.01  |      |
| 08   | 0.8333   | 0.9078   | 4.6927   | 4.6929   | 0.2933 | 0.04  |      |
| 12   | 0.8333   | 0.9074   | 4.6914   | 4.6908   | 0.2932 | 0.00  | 2:33 |

(b.) Vertical Refinement (NCOL = 8)

| NROW | $\eta_1$ | $\eta_2$ | $\eta_3$ | $\eta_4$ | $q_s$  | Error | Time |
|------|----------|----------|----------|----------|--------|-------|------|
| 01   | 0.3333   | 0.4598   | 3.1993   | 3.1513   | 0.1970 | 0.00  | 0:23 |
| 04   | 0.3333   | 0.4598   | 3.1993   | 3.1513   | 0.1970 | 0.00  | 2:40 |

= 0.3333 and to 12 element columns for  $\eta_1 = 0.8333$ . Errors computed in this manner provide a measure of convergence as the mesh is refined by altering the number of mesh divisions in both the horizontal and vertical directions as indicated above.

The computational time required by the personal computer to obtain the numeric potential and velocity distributions within the capsule can be inconvenient if many such solutions are required. The finite-element solution developed generates a number of simultaneous equations equal to the number of nodes in the discretized solution domain. The time required by *F.BAS* to solve these equations in each case is also given in Table 5. The following observations have been made considering the information of this table.

1. For  $NROW = 2$ , convergence for  $\eta_2$  is investigated by varying  $NCOL$  for specific cases corresponding to three different values of  $\eta_1$ . For a medium value of  $\eta_1 = 0.3333$ , the value of  $\eta_2$  is not significantly altered when  $NCOL$  is greater than 8, for which the *accuracy* is 0.5-percent.  $NCOL = 4$  results in 0.6-percent, whereas  $NCOL = 2$  yields 2.5-percent of *inaccuracy* based on the value corresponding to the most highly refined mesh. For a low value of  $\eta_1 = 0.1111$ , the 0.5-percent accuracy level is not attained until  $NCOL = 12$ , with smaller numbers of columns yielding fairly significant inaccuracies, as shown in the table. For a high value of  $\eta_1 = 0.8333$ , on the other hand, refinement of the mesh in the horizontal direction has little effect on the solution and any value of  $NCOL$  provides sufficiently accurate results.
2. When  $NROW$  is varied, the accuracies obtained are not altered significantly. This is as expected and physically meaningful because of the predominantly horizontal flow direction.
3. With  $NROW = 2$ , the most highly refined mesh attempted having  $NCOL = 20$  requires nearly ten minutes to solve the corresponding 84 simultaneous equations. Solution times are about 2.5 minutes for the 52 simultaneous equations resulting from  $NCOL = 12$  and about one minute for the 36 equations resulting from  $NCOL = 8$ .

The 0.5-percent accuracy level referred to here has been arbitrarily chosen to assure that plots generated exhibit no noticeable error. Considering the above points, a standard quarter-capsule solution domain having  $NROW = 2$  and  $NCOL = 8$  is chosen for all solutions with a design



parameter greater than 0.3333. Using the slightly more refined domain with  $NCOL = 12$  should the design parameter fall below 0.3333 will assure that all solutions are within the 0.5-percent accuracy. The increased solution time from one to 2.5 minutes for these few cases has been tolerated.

Maintaining two rows of elements within the cell region of the quarter-capsule is done for two reasons. First, refinement of the cell in the vertical direction will illustrate local velocity vectors in plots more accurately although it will have little effect on the potential and design parameters. Second, vertical division within the cell must be made in order to investigate the effects of partially penetrating drained outlets. Maintaining the number of element rows at two for the present quarter-capsule solution will also allow consistency of solution domain discretization in cases with partially penetrating drains to a factor of one quarter. For these reasons, the additional time required to solve the mesh with  $NROW = 2$  is accepted, even though solution accuracy over meshes with  $NROW = 1$  is not significantly altered.

**Choice of Boundary Type and Continuity Check:** Since the finite-element program accepts both Dirichlet and Neumann boundary conditions, each case may be evaluated and parameter values determined by specifying either potential head or flow velocity at the drained outlet. By assuming uniform flow velocity here,  $q_s$  may be calculated directly from the cell geometry. Two problems arise, however. First, the drained outlet is probably better represented by a uniform potential distribution of Dirichlet type boundary conditions rather than by a uniform velocity distribution as would be specified using Neumann boundary conditions. Second, values of outlet flow velocity which result in practical potential values within the cell are not in general known for specific cases. Thus better results can be attained more easily by assuming Dirichlet boundary conditions at the outlet for various practical cell designs and outlet potentials.

Under this scenario,  $q_s$  must be determined by an indirect method because the finite-element solution yields only the elemental average values of the velocity rather than the true outlet velocity. This indirect method involves calculating discharge through the barrier, element by element, using the average elemental velocities and summing the results to obtain  $q$ , the total discharge through the cell. From this discharge,  $q_s$  is easily found from cell geometry.

Another series of tests were made to indicate whether the finite-element mesh configuration found adequate according to the convergence criteria is sufficiently refined to yield an accurate value for the specific discharge using the preceding indirect procedure. Taking the specific discharges corresponding to the converged low, medium and high values of  $\eta_1$  given in Table 5 to be actual ( $q_{s(\text{act})}$ ), the corresponding true outlet velocities were computed from the geometric variables of Table 4. These velocity values constitute Neumann boundary conditions from which the three cases were solved again to obtain computed values for the specific discharge ( $q_{s(\text{comp})}$ ). Table 6a summarizes the results of these tests, and indicates that the indirect method of computation of  $q_s$  associated with Dirichlet type boundary conditions for solution of various cases is well within the 0.5-percent accuracy tolerance set previously. These tests further verify the correctness of the finite-element solution since close agreement found between the actual outflow and the computed inflow indicates that the solution preserves continuity. Note that specifying a uniform velocity distribution at the outlet (the Neumann boundary condition) does not result in an exactly uniform potential distribution there (as specified for the Dirichlet boundary conditions). The slight differences in the values of corresponding data for Table 6a and Table 5 are attributed to this observation.

**Linearity of solution:** For all previous applications of the solution algorithm, a fixed 10-foot potential difference was imposed at the drained outlet. Doubling and halving this outlet potential, without varying the other standard variables of Table 4b, results in the data of Table 6b. Notice that in both cases, the computed values of  $\eta_1$  and  $\eta_2$  are unchanged from the base values of 0.3333 and 0.4599, respectively. However, the values of  $\eta_3$  and  $\eta_4$  do change, and precisely by factors of 2 and 1/2, respective of doubling and halving the outlet potential. Thus, the relationship of Eq (3.20) is taken to be linear as well as to pass through the origin.

It is well that the pair  $\eta_1$  and  $\eta_2$  behave in like manner since they have been assumed to be functionally related by Eq (3.19). Additionally, because  $\eta_2$  is simply a ratio of potentials (see its definition given in Table 3 on page 27), this independence from the absolute value of the outlet potential is expected. Referring back to the results of the dimensional analysis of Table 2 on page

**Table 6. Other Accuracy Considerations**

(a.) Specifying Flow Into The Outlet Drain

| $\eta_1$ | $\eta_2$ | $\eta_3$ | $\eta_4$ | $Q_{s(comp)}$ | $Q_{s(act)}$ |
|----------|----------|----------|----------|---------------|--------------|
| 0.1111   | 0.1185   | 2.0643   | 1.7698   | 0.4425        | 0.4419       |
| 0.3333   | 0.4600   | 3.2000   | 3.1524   | 0.1970        | 0.1970       |
| 0.8333   | 0.9078   | 4.6998   | 4.7001   | 0.2938        | 0.2933       |

(b.) Linearity of Solution

| $\eta_1$ | $\eta_2$ | $\eta_3$ | $\eta_4$ | $q_s$  | factor |
|----------|----------|----------|----------|--------|--------|
| 0.3333   | 0.4599   | 6.3992   | 6.3033   | 0.3940 | 2      |
| 0.3333   | 0.4599   | 3.1996   | 3.1516   | 0.1970 | 1      |
| 0.3333   | 0.4599   | 1.5998   | 1.5758   | 0.0985 | 1/2    |

23, this seeming independence from absolute potential values is reinforced upon noting that  $\eta_2 = \pi_5/\pi_4$  and is itself a ratio of two of the identified dimensionless numbers which describe capsule characteristics. Thus, varying  $\eta_2$  through its natural range of  $0 < \eta_2 < 1$  is assumed sufficient to produce valid relationships for any potential range.

### **3.3.4 Example Output**

The intermediate results obtained when the solution algorithm is applied to a standard quarter-capsule solution domain are presented and described in Appendix C. This solution that for a quarter capsule which corresponds to the design variables of Table 4b. The following tables and figures illustrate the final results of the algorithm applied to the capsule design having these specifications. They have been produced, essentially, by the program *PRESENT FORTRAN* listed in Appendix B.

Table 7 presents a summary of results and the nodal potentials and Table 8 following presents the average elemental velocities for the same case. These data are illustrated in graphical form in Figure 5. Table 9 and Table 10, along with Figure 6, present similar results for a half-capsule solution under partially penetrating drained outflow conditions for the same standard design variables. Specifically, these two tables and figure represent the solution to a capsule having a drain depth only 1/8 that of the total cell depth.

**Table 7. Quarter-Capsule Solution Domain: Nodal Potentials**

**Input Variables**

| Barrier |           | Cell           |               | Potential         |         |
|---------|-----------|----------------|---------------|-------------------|---------|
| K       | = 1 ft/yr | K <sub>1</sub> | = 10000 ft/yr | ΔΦ <sub>max</sub> | = 10 ft |
| T       | = 2 ft    | L              | = 800 ft      |                   |         |
|         |           | H              | = 16 ft       |                   |         |

**Computed Results**

|                    |  |                   |              |
|--------------------|--|-------------------|--------------|
| critical potential |  | ΔΦ <sub>min</sub> | = 4.599 ft   |
| specific discharge |  | q <sub>s</sub>    | = 0.197 l/yr |

**Dimensionless Parameters**

| η <sub>1</sub> | η <sub>2</sub> | η <sub>3</sub> | η <sub>4</sub> |
|----------------|----------------|----------------|----------------|
| 0.3333         | 0.4599         | 3.1996         | 3.1516         |

**Nodal Results**

| Node | X(ft) | Y(ft) | Φ        | Node | X(ft) | Y(ft) | Φ        |
|------|-------|-------|----------|------|-------|-------|----------|
| 1    | 0     | 0.00  | -4.5988  | 19   | 0     | 16.00 | -4.6007  |
| 2    | 100   | 0.00  | -4.6707  | 20   | 100   | 16.00 | -4.6725  |
| 3    | 200   | 0.00  | -4.8884  | 21   | 200   | 16.00 | -4.8903  |
| 4    | 300   | 0.00  | -5.2588  | 22   | 300   | 16.00 | -5.2609  |
| 5    | 400   | 0.00  | -5.7934  | 23   | 400   | 16.00 | -5.7957  |
| 6    | 500   | 0.00  | -6.5090  | 24   | 500   | 16.00 | -6.5116  |
| 7    | 600   | 0.00  | -7.4278  | 25   | 600   | 16.00 | -7.4308  |
| 8    | 700   | 0.00  | -8.5787  | 26   | 700   | 16.00 | -8.5821  |
| 9    | 800   | 0.00  | -10.0000 | 27   | 800   | 16.00 | -10.0000 |
| 10   | 0     | 8.00  | -4.6002  | 28   | 0     | -2.00 | 0.0000   |
| 11   | 100   | 8.00  | -4.6721  | 29   | 100   | -2.00 | 0.0000   |
| 12   | 200   | 8.00  | -4.8898  | 30   | 200   | -2.00 | 0.0000   |
| 13   | 300   | 8.00  | -5.2603  | 31   | 300   | -2.00 | 0.0000   |
| 14   | 400   | 8.00  | -5.7951  | 32   | 400   | -2.00 | 0.0000   |
| 15   | 500   | 8.00  | -6.5109  | 33   | 500   | -2.00 | 0.0000   |
| 16   | 600   | 8.00  | -7.4301  | 34   | 600   | -2.00 | 0.0000   |
| 17   | 700   | 8.00  | -8.5813  | 35   | 700   | -2.00 | 0.0000   |
| 18   | 800   | 8.00  | -10.0000 | 36   | 800   | -2.00 | 0.0000   |

**Table 8. Quarter-Capsule Solution Domain: Elemental Velocities**

Elemental Results

| Element | Angle(deg) | Velocity(ft/yr) | Element | Angle(deg) | Velocity(ft/yr) |
|---------|------------|-----------------|---------|------------|-----------------|
| 1       | 13.4976    | 7.3910E + 00    | 25      | 0.5795     | 7.1590E + 01    |
| 2       | 13.7038    | 7.3952E + 00    | 26      | 0.6511     | 7.1584E + 01    |
| 3       | 4.5993     | 2.1848E + 01    | 27      | 0.5070     | 9.1927E + 01    |
| 4       | 4.8138     | 2.1849E + 01    | 28      | 0.5789     | 9.1919E + 01    |
| 5       | 2.8331     | 3.7096E + 01    | 29      | 0.4622     | 1.1513E + 02    |
| 6       | 3.0479     | 3.7092E + 01    | 30      | 0.5312     | 1.1512E + 02    |
| 7       | 2.1119     | 5.3516E + 01    | 31      | 0.4313     | 1.4179E + 02    |
| 8       | 2.3273     | 5.3508E + 01    | 32      | 0.0000     | 1.4187E + 02    |
| 9       | 1.7387     | 7.1612E + 01    | 33      | 89.9820    | 2.2994E + 00    |
| 10      | 1.9533     | 7.1599E + 01    | 34      | 90.0000    | 2.3353E + 00    |
| 11      | 1.5209     | 9.1946E + 01    | 35      | 89.9465    | 2.3353E + 00    |
| 12      | 1.7362     | 9.1929E + 01    | 36      | 90.0000    | 2.4442E + 00    |
| 13      | 1.3859     | 1.1515E + 02    | 37      | 89.9131    | 2.4442E + 00    |
| 14      | 1.5967     | 1.1513E + 02    | 38      | 90.0000    | 2.6294E + 00    |
| 15      | 1.2953     | 1.4191E + 02    | 39      | 89.8834    | 2.6294E + 00    |
| 16      | 0.0000     | 1.4213E + 02    | 40      | 90.0000    | 2.8967E + 00    |
| 17      | 4.5754     | 7.2105E + 00    | 41      | 89.8584    | 2.8967E + 00    |
| 18      | 4.6416     | 7.2105E + 00    | 42      | 90.0000    | 3.2545E + 00    |
| 19      | 1.5346     | 2.1788E + 01    | 43      | 89.8382    | 3.2545E + 00    |
| 20      | 1.6066     | 2.1787E + 01    | 44      | 90.0000    | 3.7139E + 00    |
| 21      | 0.9444     | 3.7059E + 01    | 45      | 89.8224    | 3.7139E + 00    |
| 22      | 1.0162     | 3.7056E + 01    | 46      | 90.0000    | 4.2894E + 00    |
| 23      | 0.7040     | 5.3489E + 01    | 47      | 89.8101    | 4.2894E + 00    |
| 24      | 0.7757     | 5.3484E + 01    | 48      | 90.0000    | 5.0000E + 00    |

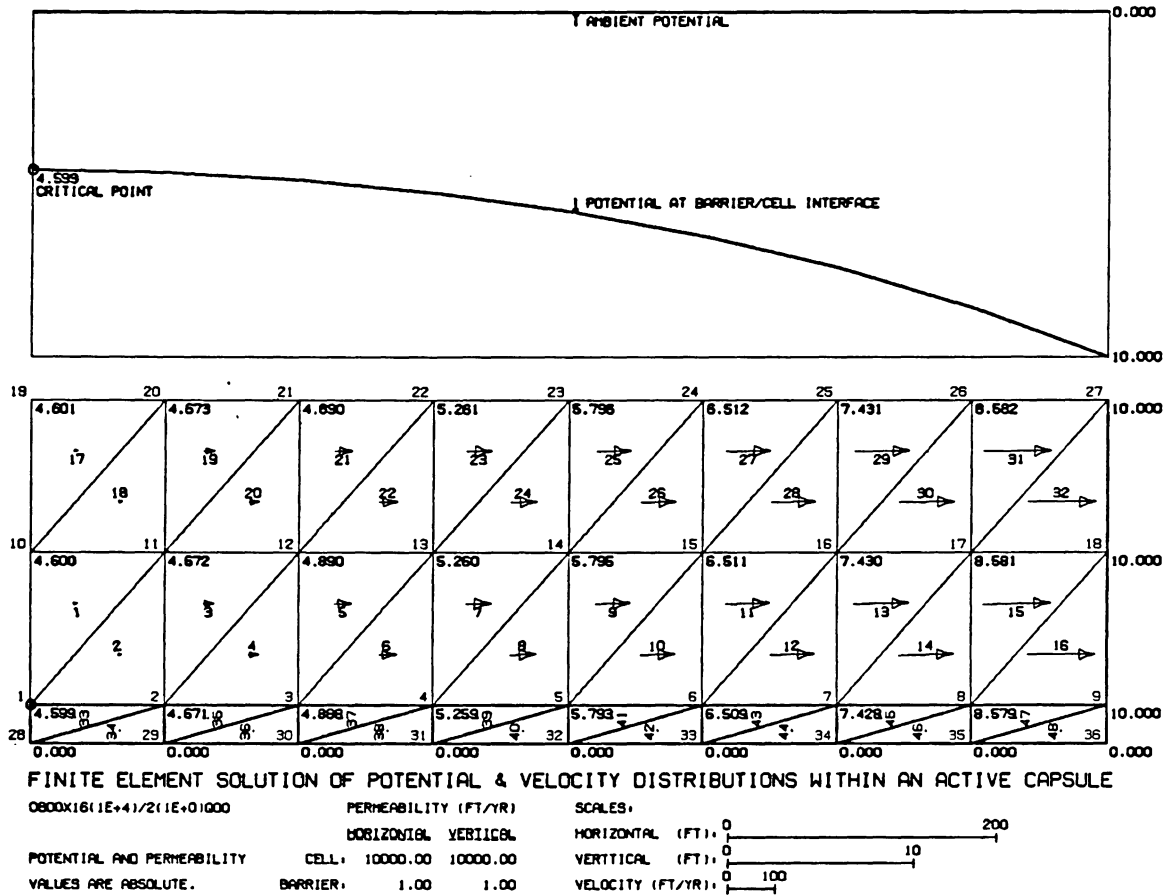


Figure 5. Quarter Capsule Solution Domain

**Table 9. Half-Capsule Solution Domain: Nodal Potentials**

**Input**

| Barrier |   |         | Cell  |   |             | Potential          |   |       |
|---------|---|---------|-------|---|-------------|--------------------|---|-------|
| K       | = | 1 ft/yr | $K_1$ | = | 10000 ft/yr | $\Delta\Phi_{max}$ | = | 10 ft |
| T       | = | 2 ft    | L     | = | 800 ft      |                    |   |       |
|         |   |         | H     | = | 16 ft       |                    |   |       |

**Computed Results**

|                    |                    |   |            |
|--------------------|--------------------|---|------------|
| critical potential | $\Delta\Phi_{min}$ | = | 4.500 ft   |
| specific discharge | $q_s$              | = | 0.193 l/yr |

**Dimensionless Parameters**

| $\eta_1$ | $\eta_2$ | $\eta_3$ | $\eta_4$ |
|----------|----------|----------|----------|
| 0.3333   | 0.4500   | 3.1665   | 3.0925   |

**Nodal Results**

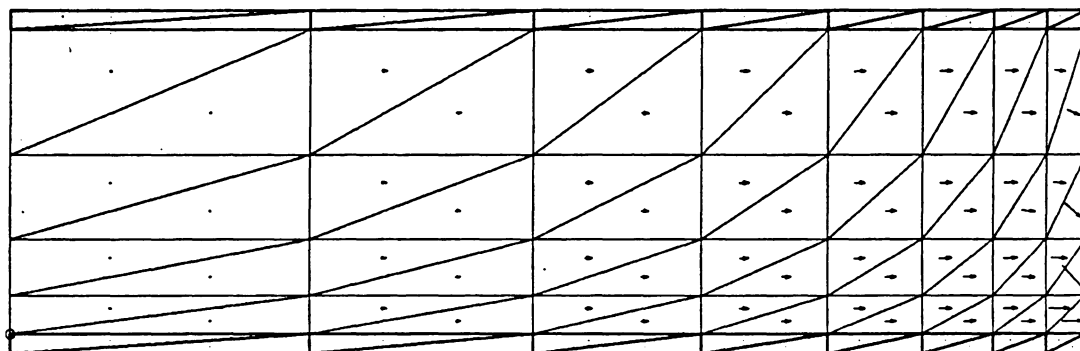
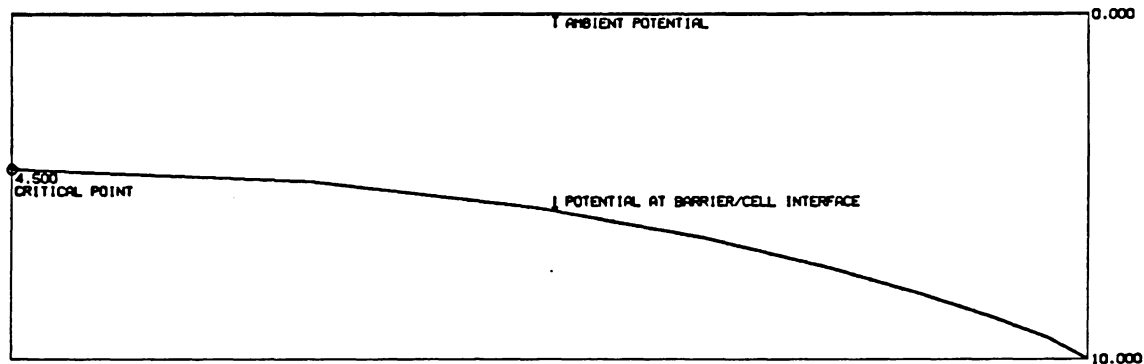
| Node | X(ft)  | Y(ft) | $\Phi$   | Node | X(ft)  | Y(ft) | $\Phi$  |
|------|--------|-------|----------|------|--------|-------|---------|
| 1    | 0.00   | 0.00  | -4.4996  | 33   | 678.04 | 18.81 | -8.1385 |
| 2    | 222.25 | 0.00  | -4.8472  | 34   | 730.78 | 18.81 | -8.8095 |
| 3    | 388.94 | 0.00  | -5.5986  | 35   | 770.33 | 18.81 | -9.3581 |
| 4    | 513.95 | 0.00  | -6.4812  | 36   | 800.00 | 18.81 | -9.7334 |
| 5    | 607.72 | 0.00  | -7.3507  | 37   | 0.00   | 32.00 | -4.4996 |
| 6    | 678.04 | 0.00  | -8.1354  | 38   | 222.25 | 32.00 | -4.8472 |
| 7    | 730.78 | 0.00  | -8.8072  | 39   | 388.94 | 32.00 | -5.5986 |
| 8    | 770.33 | 0.00  | -9.3755  | 40   | 513.95 | 32.00 | -6.4812 |
| 9    | 800.00 | 0.00  | -10.0000 | 41   | 607.72 | 32.00 | -7.3507 |
| 10   | 0.00   | 4.00  | -4.5004  | 42   | 678.04 | 32.00 | -8.1354 |
| 11   | 222.25 | 4.00  | -4.8480  | 43   | 730.78 | 32.00 | -8.8055 |
| 12   | 388.94 | 4.00  | -5.5996  | 44   | 770.33 | 32.00 | -9.3447 |
| 13   | 513.95 | 4.00  | -6.4823  | 45   | 800.00 | 32.00 | -9.6639 |
| 14   | 607.72 | 4.00  | -7.3520  | 46   | 0.00   | 34.00 | 0.0000  |
| 15   | 678.04 | 4.00  | -8.1368  | 47   | 222.25 | 34.00 | 0.0000  |
| 16   | 730.78 | 4.00  | -8.8086  | 48   | 388.94 | 34.00 | 0.0000  |
| 17   | 770.33 | 4.00  | -9.3758  | 49   | 513.95 | 34.00 | 0.0000  |
| 18   | 800.00 | 4.00  | -10.0000 | 50   | 607.72 | 34.00 | 0.0000  |
| 19   | 0.00   | 9.95  | -4.5011  | 51   | 678.04 | 34.00 | 0.0000  |
| 20   | 222.25 | 9.95  | -4.8488  | 52   | 730.78 | 34.00 | 0.0000  |
| 21   | 388.94 | 9.95  | -5.6005  | 53   | 770.33 | 34.00 | 0.0000  |
| 22   | 513.95 | 9.95  | -6.4834  | 54   | 800.00 | 34.00 | 0.0000  |
| 23   | 607.72 | 9.95  | -7.3533  | 55   | 0.00   | -2.00 | 0.0000  |
| 24   | 678.04 | 9.95  | -8.1382  | 56   | 222.25 | -2.00 | 0.0000  |
| 25   | 730.78 | 9.95  | -8.8098  | 57   | 388.94 | -2.00 | 0.0000  |
| 26   | 770.33 | 9.95  | -9.3705  | 58   | 513.95 | -2.00 | 0.0000  |
| 27   | 800.00 | 9.95  | -9.8633  | 59   | 607.72 | -2.00 | 0.0000  |
| 28   | 0.00   | 18.81 | -4.5013  | 60   | 678.04 | -2.00 | 0.0000  |
| 29   | 222.25 | 18.81 | -4.8490  | 61   | 730.78 | -2.00 | 0.0000  |
| 30   | 388.94 | 18.81 | -5.6008  | 62   | 770.33 | -2.00 | 0.0000  |
| 31   | 513.95 | 18.81 | -6.4837  | 63   | 800.00 | -2.00 | 0.0000  |
| 32   | 607.72 | 18.81 | -7.3536  |      |        |       |         |



**Table 10. Half-Capsule Solution Domain: Elemental Velocities**

Elemental Results

| Element | Angle(deg) | Velocity(ft/yr) | Element | Angle(deg) | Velocity(ft/yr) |
|---------|------------|-----------------|---------|------------|-----------------|
| 1       | 7.1737     | 1.5765E + 01    | 49      | -4.8310    | 1.5695E + 01    |
| 2       | 7.7272     | 1.5783E + 01    | 50      | -5.2053    | 1.5710E + 01    |
| 3       | 2.6934     | 4.5138E + 01    | 51      | -1.8112    | 4.5103E + 01    |
| 4       | 3.1086     | 4.5147E + 01    | 52      | -2.0903    | 4.5128E + 01    |
| 5       | 1.9858     | 7.0653E + 01    | 53      | -1.3356    | 7.0617E + 01    |
| 6       | 2.2996     | 7.0655E + 01    | 54      | -1.5457    | 7.0651E + 01    |
| 7       | 1.7506     | 9.2802E + 01    | 55      | -1.1769    | 9.2761E + 01    |
| 8       | 1.9853     | 9.2798E + 01    | 56      | -1.3344    | 9.2803E + 01    |
| 9       | 1.6500     | 1.1165E + 02    | 57      | -1.1099    | 1.1160E + 02    |
| 10      | 1.8256     | 1.1164E + 02    | 58      | -1.2364    | 1.1165E + 02    |
| 11      | 1.5994     | 1.2743E + 02    | 59      | -1.0863    | 1.2708E + 02    |
| 12      | 1.6636     | 1.2742E + 02    | 60      | -1.3851    | 1.2726E + 02    |
| 13      | 1.4779     | 1.4343E + 02    | 61      | -1.2926    | 1.3636E + 02    |
| 14      | 0.3287     | 1.4367E + 02    | 62      | -4.1845    | 1.3906E + 02    |
| 15      | 0.2244     | 2.1041E + 02    | 63      | -5.3874    | 1.0807E + 02    |
| 16      | 0.0000     | 2.1052E + 02    | 64      | -22.6014   | 1.3701E + 02    |
| 17      | 4.6393     | 1.5696E + 01    | 65      | -90.0000   | 2.2498E + 00    |
| 18      | 4.9970     | 1.5702E + 01    | 66      | -89.9630   | 2.4236E + 00    |
| 19      | 1.7365     | 4.5116E + 01    | 67      | -90.0000   | 2.4236E + 00    |
| 20      | 2.0046     | 4.5116E + 01    | 68      | -89.9077   | 2.7993E + 00    |
| 21      | 1.2801     | 7.0640E + 01    | 69      | -90.0000   | 2.7993E + 00    |
| 22      | 1.4839     | 7.0634E + 01    | 70      | -89.8751   | 3.2406E + 00    |
| 23      | 1.1295     | 9.2792E + 01    | 71      | -90.0000   | 3.2406E + 00    |
| 24      | 1.2792     | 9.2781E + 01    | 72      | -89.8554   | 3.6754E + 00    |
| 25      | 1.0636     | 1.1164E + 02    | 73      | -90.0000   | 3.6754E + 00    |
| 26      | 1.1700     | 1.1163E + 02    | 74      | -89.8428   | 4.0677E + 00    |
| 27      | 1.0254     | 1.2736E + 02    | 75      | -90.0000   | 4.0677E + 00    |
| 28      | 0.8886     | 1.2739E + 02    | 76      | -89.8346   | 4.4027E + 00    |
| 29      | 0.7985     | 1.4177E + 02    | 77      | -90.0000   | 4.4027E + 00    |
| 30      | -3.5183    | 1.4365E + 02    | 78      | -89.8328   | 4.6724E + 00    |
| 31      | -3.0380    | 1.6634E + 02    | 79      | -90.0000   | 4.6723E + 00    |
| 32      | -47.4976   | 3.1143E + 02    | 80      | -89.8724   | 4.8319E + 00    |
| 33      | 0.8422     | 1.5647E + 01    | 81      | 89.9601    | 2.2498E + 00    |
| 34      | 0.8941     | 1.5647E + 01    | 82      | 90.0000    | 2.4236E + 00    |
| 35      | 0.3102     | 4.5098E + 01    | 83      | 89.8934    | 2.4236E + 00    |
| 36      | 0.3592     | 4.5097E + 01    | 84      | 90.0000    | 2.7993E + 00    |
| 37      | 0.2294     | 7.0626E + 01    | 85      | 89.8554    | 2.7993E + 00    |
| 38      | 0.2662     | 7.0623E + 01    | 86      | 90.0000    | 3.2406E + 00    |
| 39      | 0.2026     | 9.2778E + 01    | 87      | 89.8360    | 3.2406E + 00    |
| 40      | 0.2292     | 9.2775E + 01    | 88      | 90.0000    | 3.6754E + 00    |
| 41      | 0.1905     | 1.1162E + 02    | 89      | 89.8260    | 3.6754E + 00    |
| 42      | 0.1985     | 1.1162E + 02    | 90      | 90.0000    | 4.0677E + 00    |
| 43      | 0.1742     | 1.2722E + 02    | 91      | 89.8205    | 4.0677E + 00    |
| 44      | -0.1511    | 1.2734E + 02    | 92      | 90.0000    | 4.4036E + 00    |
| 45      | -0.1388    | 1.3869E + 02    | 93      | 89.8130    | 4.4036E + 00    |
| 46      | -5.6517    | 1.4245E + 02    | 94      | 90.0000    | 4.6877E + 00    |
| 47      | -6.3284    | 1.2727E + 02    | 95      | 89.7427    | 4.6878E + 00    |
| 48      | -41.4427   | 2.2158E + 02    | 96      | 90.0000    | 5.0000E + 00    |



**FINITE ELEMENT SOLUTION OF POTENTIAL & VELOCITY DISTRIBUTIONS WITHIN AN ACTIVE CAPSULE**

CASE: 0.00/AR=.02/PF=0.125

PERMEABILITY (FT/YR)

SCALES:

HORIZONTAL 10000.00

VERTICAL 10000.00

HORIZONTAL (FT): 0 200

VERTICAL (FT): 0 20

POTENTIAL AND PERMEABILITY

CELL: 10000.00 10000.00

VELOCITY (FT/YR): 0 200

VALUES ARE ABSOLUTE.

BARRIER: 1.00 1.00

**Figure 6. Half Capsule Solution Domain**

### 3.3.5 Capsule Characteristic Curve

The data of Table 11 has been generated by application of the solution algorithm for various geometric configurations and different material properties under different potential conditions. The code associated with each case indicates the various input values. To the left of the slash mark are values of variables descriptive of the cell. The half cell length  $L$  is separated from the half cell depth  $H$  by "x" and these geometric properties are followed by the value of cell permeability  $K_1$  in parentheses. To the right of the slash, the barrier thickness  $T$ , is followed by barrier permeability  $K$ , the later also in parentheses. The final three characters of the code indicate case type (Q for quarter-capsule) and case number (0 to 20).

Each solution resulted in numerical values for the design and potential parameters symbolized by  $\eta_1$  and  $\eta_2$ , respectively, which have been inferred by Eq (3.19) to be functionally related. Also, numerical values for the barrier gradient and the discharge parameters,  $\eta_3$  and  $\eta_4$  respectively, inferred to be functionally related by Eq (3.20), are provided. These data are plotted in Figure 7 to establish these relationships. This figure illustrates the primary functional relationship between the design  $\eta_1$  and the potential parameter  $\eta_2$  as well as the secondary functional relationship between the barrier gradient parameter  $\eta_3$  and the flow parameter  $\eta_4$ .

Interestingly, the relationship between  $\eta_3$  and  $\eta_4$ , in addition to being linear as has been previously observed, is found to be essentially an equality, excepting cases corresponding to low values of  $\eta_1$ . In fact, it is for this reason that the 1/3 factor of Eq (3.18) was retained in the derivation of this relationship.

It seems that, for cases corresponding to lower values of the design parameter, the assumed parabolic surface of depression along the barrier/cell interface is less valid. Data points for  $\eta_3$  and  $\eta_4$  corresponding to  $\eta_1$  values of 0.2 and below exhibit scatter when plotted. Figure 7 illustrates this by plotting data corresponding to these low values of  $\eta_1$  with triangular symbols. From the first relationship, it is noted that low values of  $\eta_1$  also correspond to low values of  $\eta_2$ , and that a low value for the this parameter indicates a steep, inefficient curve describing the potential variation along the barrier/cell interface. Thus, this scatter occurs only under conditions

**Table 11. Data For Standard Potential-Flow Characteristic Curves**

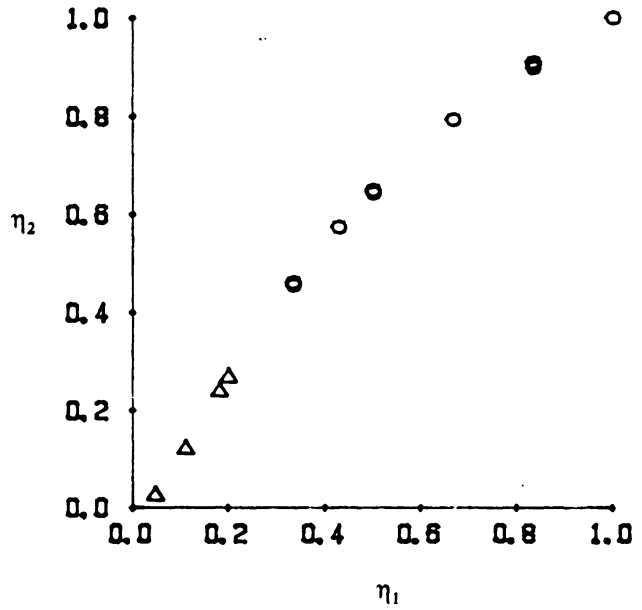
| $\eta_1$ | $\eta_2$ | $\eta_3$ | $\eta_4$ | $q_s$  | code                            |
|----------|----------|----------|----------|--------|---------------------------------|
| 0.3333   | 0.4599   | 3.1996   | 3.1516   | 0.1970 | 0800x16(1.00E + 4)/2(1E + 0)Q00 |
| 0.1818   | 0.2371   | 2.4568   | 2.2988   | 0.1437 | 1200x16(1.00E + 4)/2(1E + 0)Q01 |
| 0.6667   | 0.7932   | 4.3107   | 4.3075   | 0.2692 | 0400x16(1.00E + 4)/2(1E + 0)Q02 |
| 0.1111   | 0.1185   | 2.0618   | 1.7676   | 0.4419 | 0800x04(1.00E + 4)/2(1E + 0)Q03 |
| 0.4286   | 0.5737   | 3.5791   | 3.5547   | 0.1481 | 0800x24(1.00E + 4)/2(1E + 0)Q04 |
| 0.0476   | 0.0235   | 1.7450   | 1.1360   | 0.0710 | 0800x16(1.00E + 3)/2(1E + 0)Q05 |
| 0.8333   | 0.9078   | 4.6927   | 4.6929   | 0.2933 | 0800x16(1.00E + 5)/2(1E + 0)Q06 |
| 0.2000   | 0.2664   | 5.1091   | 4.8347   | 0.3022 | 0800x16(1.00E + 4)/1(1E + 0)Q07 |
| 0.5000   | 0.6483   | 1.9138   | 1.9067   | 0.1192 | 0800x16(1.00E + 4)/4(1E + 0)Q08 |
| 0.0476   | 0.0235   | 1.7450   | 1.1361   | 0.7100 | 0800x16(1.00E + 4)/2(1E + 1)Q09 |
| 0.8333   | 0.9078   | 4.6927   | 4.6928   | 0.0293 | 0800x16(1.00E + 4)/2(1E-1)Q10   |
| 0.9983   | 0.9992   | 2.4986   | 2.4987   | 0.0104 | 0400x24(1.00E + 5)/4(1E-1)Q11   |
| 0.3333   | 0.4595   | 3.1982   | 3.1478   | 0.1312 | 0400x24(1.67E + 3)/2(1E + 0)Q12 |
| 0.8333   | 0.9076   | 4.6921   | 4.6920   | 0.1955 | 0400x24(1.67E + 4)/2(1E + 0)Q13 |
| 0.5000   | 0.6479   | 3.8264   | 3.8111   | 0.1588 | 0400x24(3.33E + 3)/2(1E + 0)Q14 |
| 0.3333   | 0.4605   | 3.2018   | 3.1543   | 0.7886 | 1200x04(9.00E + 4)/2(1E + 0)Q15 |
| 0.8333   | 0.8978   | 4.6594   | 4.6596   | 1.1649 | 1200x04(9.00E + 5)/2(1E + 0)Q16 |
| 0.5000   | 0.6441   | 3.8138   | 3.7986   | 0.9496 | 1200x04(1.80E + 5)/2(1E + 0)Q17 |
| 0.3333   | 0.4555   | 3.1850   | 3.1103   | 0.1296 | 0120x24(1.50E + 2)/2(1E + 0)Q18 |
| 0.8333   | 0.9057   | 4.6856   | 4.6828   | 0.1951 | 0120x24(1.50E + 3)/2(1E + 0)Q19 |
| 0.5000   | 0.6434   | 3.8112   | 3.7828   | 0.1576 | 0120x24(3.00E + 2)/2(1E + 0)Q20 |

(a.) Primary Relationship

Capsule Design Parameter

-vs-

Potential Parameter



(b.) Secondary Relationship

Barrier Gradient Parameter

-vs-

Flow Parameter

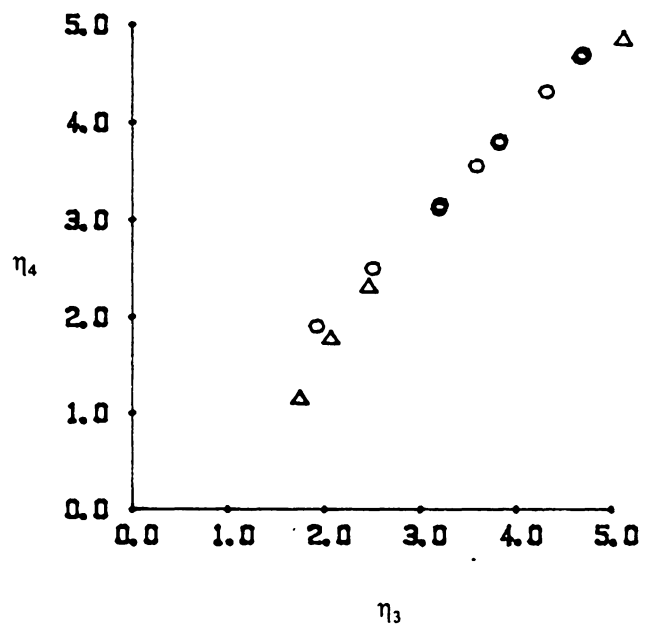


Figure 7. Containment Capsule Characteristic Curves: Quantification of the primary and secondary parametric relationships.

which are undesirable at best and it is not seen as a particular problem in the practical sense. In fact, no great loss is anticipated even if all cases in which the design parameter is below 0.2 were not considered in further development of descriptive relationships. Thus, the valid range of the design parameter involved in all further developments is specified to be  $0.2 < \eta_1 < 1$ . The effect is to avoid undesirable conditions while validating the simple relationship between the barrier gradient parameter and the discharge parameter of  $\eta_4 = \eta_3$  for all practical cases.

### **3.3.6 Ranges of Validity**

The relationships of Eqs (2.19) and (2.20) have been graphically quantified in Figure 7 by plotting the numerical data of Table 11. Some consideration should be made concerning the ranges for which these relationships are valid. This is done by again considering the physically significant dimensionless numbers of Table 2 on page 23.

Comparing the definitions of the first three dimensionless numbers of Table 2 on page 23 with the data of Table 11, the ranges indicated in Table 12 on page 54, under which the data has been generated and for which it is valid, have been identified. Should a capsule be defined so that the value of one of these physically significant dimensionless numbers fall outside of its valid range, results obtained from relationships based on this data, although not necessarily invalid, should be questioned for that particular case.

As indicated previously, because  $\eta_2 = \pi_5/\pi_4$  is a ratio of potentials, it, and thus  $\eta_1$  to which it is linked, are independent of absolute potentials as well as  $\pi_4$  and  $\pi_5$ .

**Table 12. Valid Ranges of the Dimensionless Numbers**

| <i>Range</i>            | <i>Grouping</i> | <i>Significance</i>        |
|-------------------------|-----------------|----------------------------|
| $150 < \pi_1 < 10,0000$ | $\frac{K_1}{K}$ | Permeability ratio         |
| $0.0033 < \pi_2 < 0.2$  | $\frac{H}{L}$   | Aspect ratio               |
| $0.0625 < \pi_3 < 0.5$  | $\frac{T}{H}$   | Relative barrier thickness |

### 3.3.7 Correction Factors for Non-Standard Conditions

The standard curve of Figure 7a was developed for isotropic conditions within the cell and drains which penetrate the cell completely. Deviations from these standard conditions in regard to both anisotropy and partial penetration result in a downward shift of this curve. It has been found that this shift can be described by introducing correction factors, multipliers for the potential parameter which are functions of the degrees of either partial penetration or anisotropy as well as the capsule aspect ratio ( $H/L$ ) and  $\eta_1$

#### 3.3.7.1 Anisotropic Conditions

Improved capsule operational characteristics can result from increasing the value of the capsule permeability in the horizontal direction. Assuming that the disposal material has a certain base permeability  $K_b$ , the horizontal permeability  $K_1$  can be increased by systematically adding layers of a material of greater permeability  $K_a$ . The resulting permeability of the layered structure will depend on, in addition to  $K_b$  and  $K_a$ , the thickness of the base material  $t_b$ , and the added material  $t_a$ . The resulting effective horizontal and vertical permeabilities of such a layered structure will no longer be equal giving rise to anisotropic conditions. These principle permeabilities can be expressed as follows [Bouwer]:

$$K_1 = \frac{K_a t_a + K_b t_b}{t_a + t_b} \quad (3.21)$$

$$K_2 = \frac{t_a + t_b}{t_a/K_a + t_b/K_b} \quad (3.22)$$

For the cell with a two layer repetitive pattern in the direction of the half capsule depth as has been described, the volume of added material can be related to the total disposal volume to provide a factor useful in later investigations.



$$f_h = \frac{t_a}{t_a + t_b} \quad (3.23)$$

Using this factor, Eq (3.21) is rewritten as follows:

$$K_1 = K_b + f_h (K_a - K_b) \quad (3.24)$$

Also, the degree of anisotropy is defined as  $f_a = \frac{K_2}{K_1}$ . Thus, making use of the above:

$$\frac{1}{f_a} = f_h^2 + \left[ \frac{K_a}{K_b} + \frac{K_b}{K_a} \right] (1 - f_h) f_h + (1 - f_h)^2 \quad (3.25)$$

These relationships have been developed to describe how increasing cell permeability might be accomplished to improve operation of the capsule. The factor  $f_h$  and thus the degree of anisotropy  $f_a$  can be optimized for specific capsule conditions. These results will be referenced from Chapter 5 in this regard.

The layered cell structure described above is interpreted as an anisotropic medium within the capsule design. Therefore, the data of Appendix D for anisotropic conditions has been generated by applying the solution algorithm to the capsule and varying the degree of anisotropy  $f_a$ . Figure 8 was produced by comparing this data to the corresponding isotropic data given in Table 11. It illustrates the correction factors to be applied to  $\eta_2$  for the isotropic conditions of Figure 7a so that it and the secondary relationship, Figure 7b, are corrected for conditions of anisotropy. Dependencies on both the design parameter  $\eta_1$  and the aspect ratio  $H/L$  are noted.

The final relationship of Figure 8 is produced to illustrate that, even for highly anisotropic conditions, the relationship between  $\eta_3$  and  $\eta_4$  is still very nearly an equality. The effect of anisotropy within the cell seems to be simply a shift in the surface of depression which does not invalidate the assumed parabolic shape of the surface.

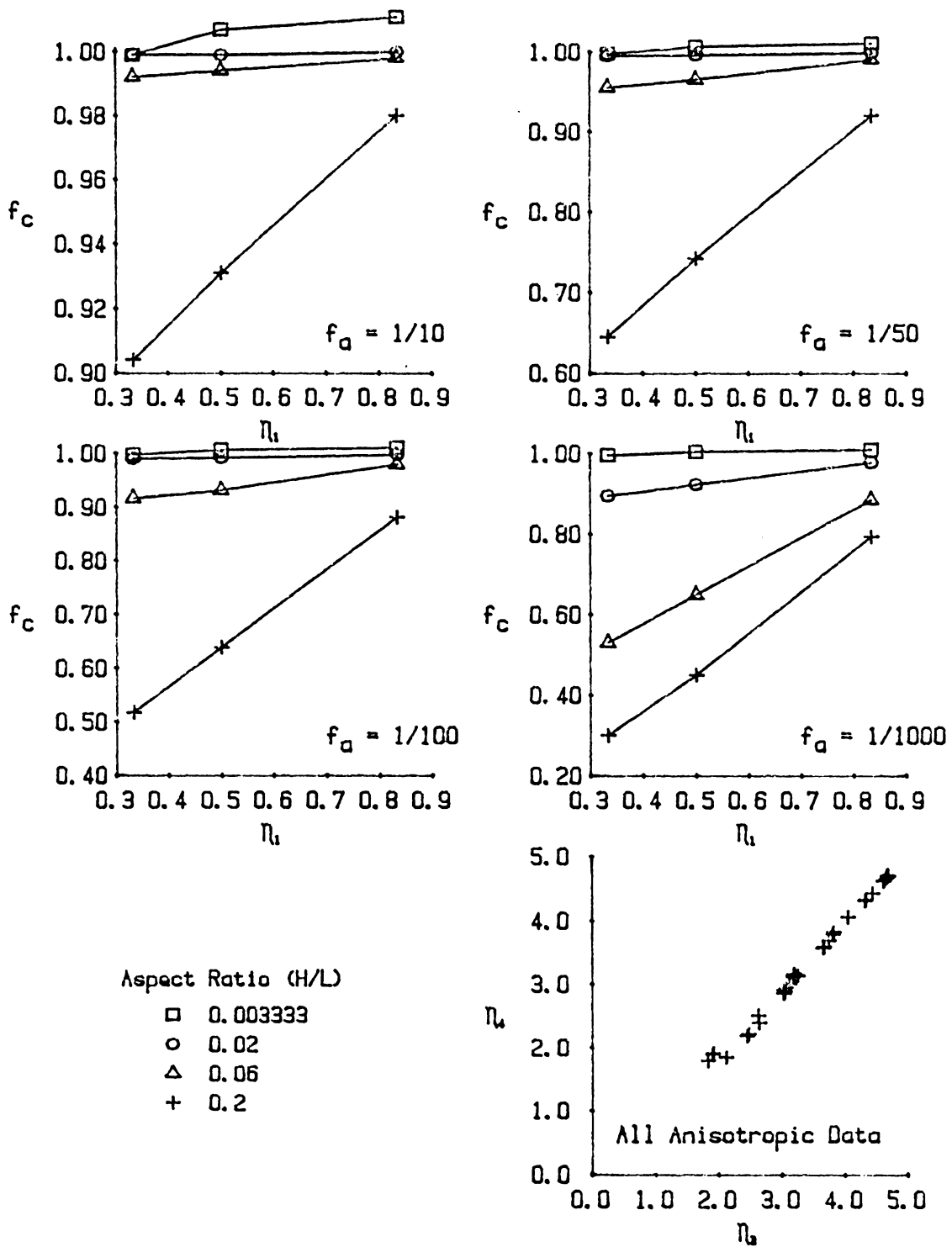


Figure 8. Anisotropic Conditions: Correction factors applied to the potential parameter.

### 3.3.7.2 Partially Penetrating Outlet Drains

It has been found that correction factors for partial penetration can be formulated in a manner analogous to that used for conditions of anisotropy. Following a similar procedure, the data of Appendix E has been generated by applying the solution algorithm to the capsule with various degrees of drain penetration  $f_p$ . Figure 9 was produced by comparing this data to the corresponding full penetration data given in Table 11. It illustrates the correction factors to be applied to  $\eta_2$  for the full penetration conditions of Figure 7a so that it and the secondary relationship, Figure 7b, are corrected for conditions of partial penetration. Again, dependencies on both the design parameter  $\eta_1$  and the aspect ratio  $H/L$  are noted.

The final relationship of Figure 9 is produced to illustrate the accuracy of the assumed relationship  $\eta_4 = \eta_3$  under partially penetrating conditions. The inability of the assumed parabolic potential surface within the cell to describe the effect of non-standard conditions at the boundary (the partially penetrating outlet drain) is the probable cause of the poorer fit as compared to the similar relationship of Figure 8. By inspection of the data of Appendix E, it can be seen that data pairs corresponding to smaller  $f_p$  and larger aspect ratios ( $H/L$ ) deviate more from the assumed equality. Even so, the relationship is not so bad so that the equality cannot be used for most practical conditions, especially if care is energized in it's application.

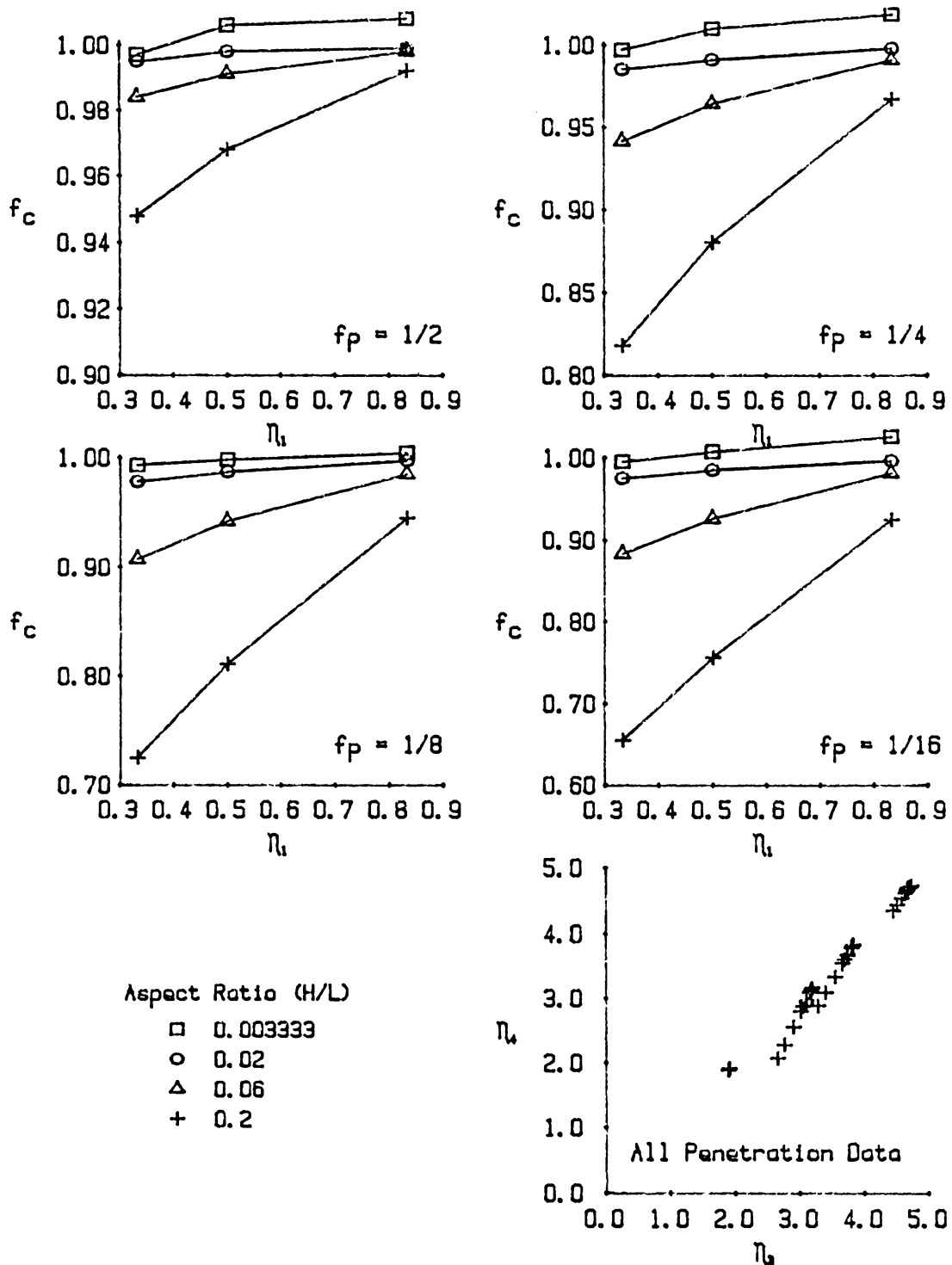


Figure 9. Partially Penetrating Drains: Correction factors applied to the potential parameter.

## CHAPTER 4

# CONCENTRATION PROFILES WITHIN THE BARRIER

The *containment capsule* described in Chapter 3 consists of a permeable region with a certain level of resident concentration completely encapsulated by a low permeability barrier and placed entirely within a saturated, permeable groundwater environment. A lower potential head is imposed within the capsule relative to that of the surrounding ambient region. Thus, a potential difference exists across the barrier for all points along the perimeter of the capsule so that the potential for convective flow through the barrier is everywhere inward. The practical application of this posed problem is immediately seen upon realizing that the dispersive migration potential of the resident concentration within the capsule will be inhibited, and possibly effectively eliminated, by this convective inflow potential from the surrounding ambient region. This section develops a mathematical representation of the resulting one dimensional concentration profile which will develop across the barrier under steady state conditions. Definitions of terms not already defined in Chapter 3 are added to the notation.

Since each profile indicates the barrier performance under certain conditions, the model predicts operational characteristics under various design conditions. Thus, barrier design criteria can be developed. The ultimate goal is, of course, to maintain ambient water quality by allowing only negligible amounts of the contained resident concentration through the barrier.

## 4.1 NOTATION

|            |  |
|------------|--|
| $C(s)$     | = Steady state variation of concentration across the barrier [-] |
| $C_0$      | = Ambient or background level of contaminant concentration [-]   |
| $\Delta C$ | = Total change in concentration across the barrier [-]           |
| $d$        | = Dispersivity of the barrier material [L]                       |
| $D$        | = Dispersion coefficient of the barrier material [ $L^2/T$ ]     |
| $n$        | = Porosity of the barrier material [-]                           |
| $\Phi(s)$  | = Variation of the potential across the barrier [L]              |
| $s$        | = Spatial coordinate across the barrier [L]                      |
| $t$        | = Time [T]   |
| $u$        | = Average pore water velocity within the barrier [L/T]           |

## 4.2 PROBLEM IDENTIFICATION

The idealized conditions surrounding the barrier at the critical point of the capsule are illustrated in Figure 10. A containment region of saturated material having certain imposed values of potential head and resident concentration is separated from the ambient region by a barrier of thickness  $T$ , also of saturated material with a porosity value  $n$ . Further, both permeability and dispersion coefficients of the barrier material,  $K$  and  $D$  respectively, have values which are relatively much lower than those of either the ambient or imposed regions. Due to this relatively low barrier permeability, values of potential within the cell adjust quickly relative to the potential values within the barrier. Thus, an effectively constant potential difference across the barrier  $\Delta\Phi_{\min}$  resulting from the steady state potential curve  $\Phi(s)$  may be imposed by pumping from the cell, even though from a location remote to the barrier. When the resulting flow from the ambient region significantly reduces dispersive migration through the barrier, the assumed constant concentration at the boundaries becomes practicable, and a fair representation of the proposed steady state problem re-

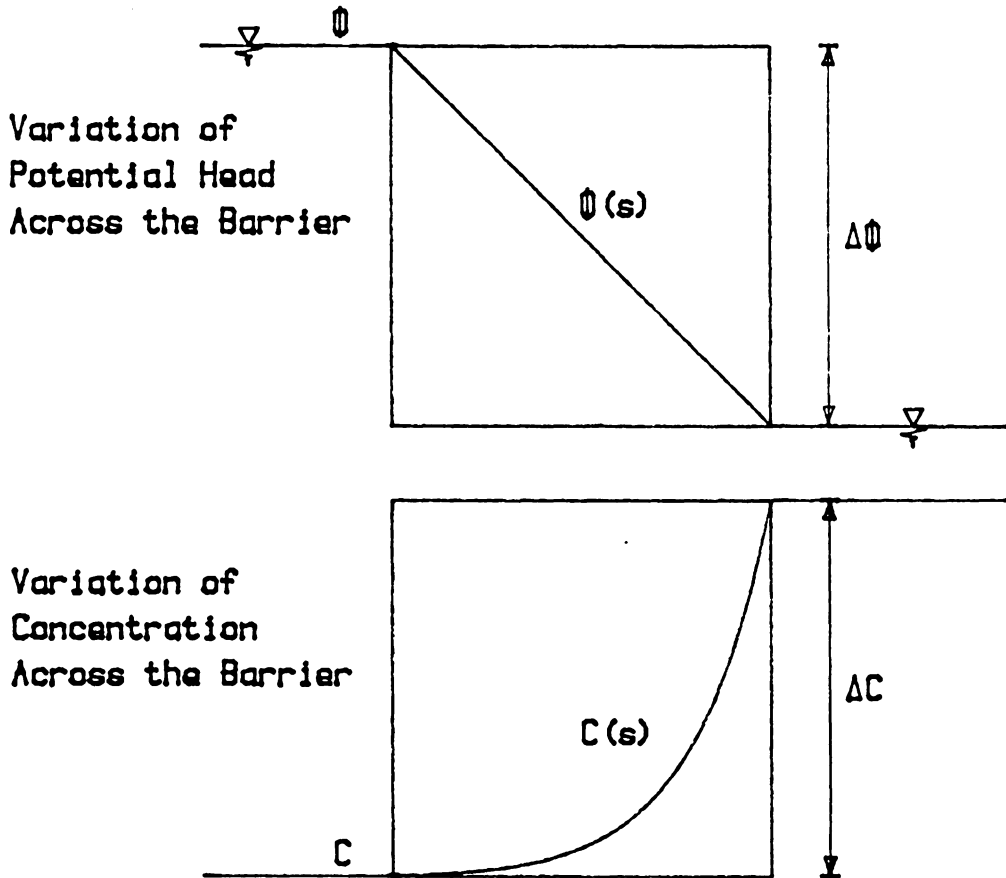
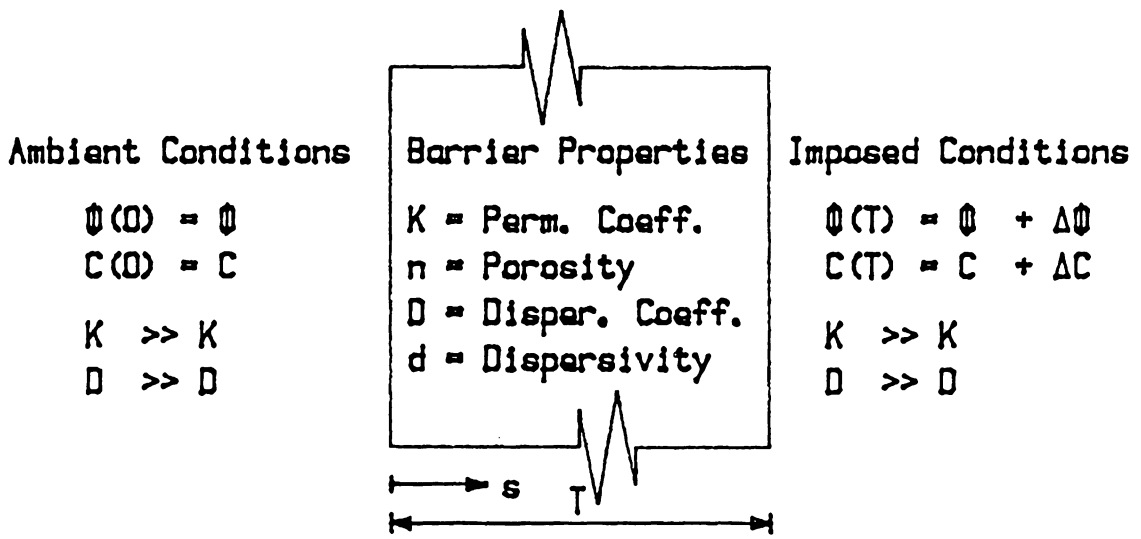


Figure 10. The Barrier Problem: Definition sketch with steady state boundary conditions.

sults. For simplicity of analysis, several complicating factors have been neglected [26]. Among them:

- Dilution of the concentration at the barrier/cell interface will obviously occur with constant inflow but this effect is assumed small due to the relatively high dispersion coefficient of the cell region as well as its comparatively greater volume. (Refer to Figure 3 on page 20). Additionally, the following chapter will identify design characteristics which minimize total costs, the operational costs of which are certainly directly related to flow volume.
- Unaccounted for chemical or radiological decay, or otherwise general reduction of concentration by any other means (including dilution over time), may be observed. Appropriate adjustments to the imposed boundary conditions as indicated by these observations can be made when necessary to provide steady conditions to which equilibrium will adjust.
- The natural affinity of contaminants toward soil (or even the barrier itself) provides a sink in transport problems. However, this point has far less applicability when the migration problem is analyzed from the containment perspective, as in this work.

Under these simplifications, the steady state concentration profile  $C(s)$  is solved analytically for all possible variations of the assumed boundary conditions, including convective conditions that promote migration. It is when this solution corresponds to practical problem constraints of the proposed active capsule design (that is, significantly reduced outward migration achieved with minimal inflow) that the results obtained may be used to develop minimum allowable concentration migration criteria.

### 4.3 ANALYTICAL SOLUTION

Since both potential and concentration conditions are held constant for all time at the barrier boundaries, resident concentration level within the barrier,  $C(s)$ , is a function only of position within the barrier. The one-dimensional partial differential steady-state convection-dispersion



equation involving the variation of this concentration with respect to the direction normal to the barrier may be written [2] [3] [7]:

$$\frac{\partial}{\partial s} \left[ D \frac{\partial}{\partial s} [C(s)] \right] - u \frac{\partial}{\partial s} [C(s)] = 0 \quad (4.1)$$

Two other equations exist corresponding to the two other mutually perpendicular cartesian coordinate directions along the barrier orthogonal to  $s$ . In these directions, concentration is constant, and thus both of its first and second partial derivatives with respect to these directions must identically equal zero. Therefore, they add no information to the solution at hand and are not further considered.

Darcy's Law defined by Eq (3.1) is again used to determine the average velocity through the barrier. However, since dispersion effects are being considered, this equation is corrected by the porosity factor  $n$  to evaluate the average *pore* velocity [1] [26].

$$u = - \frac{K}{n} \frac{\partial}{\partial s} [\Phi(s)] \quad (4.2)$$

Further, it is assumed that under equilibrium conditions, the values of the material properties  $D$ ,  $K$ , and  $n$  are constant. Applying these assumptions to the convection-dispersion equation, the following second-order differential equation is obtained which describes equilibrium convection-dispersion through a barrier having constant material properties.

$$D \frac{\partial^2}{\partial s^2} [C(s)] + \frac{K}{n} \frac{\partial}{\partial s} [\Phi(s)] \frac{\partial}{\partial s} [C(s)] = 0 \quad (4.3)$$

Rearranging so that the  $C(s)$  differentials are grouped together into a single term on the left-hand side by moving all other variables to the right-hand side results in the following:

$$\frac{\frac{\partial^2}{\partial s^2} [C(s)]}{\frac{\partial}{\partial s} [C(s)]} = - \frac{K}{n D} \frac{\partial}{\partial s} [\Phi(s)]. \quad (4.4)$$

Now, consider the right-hand side of this equation. In addition to  $D$ ,  $K$ , and  $n$  all having been assumed constant, continuity of flow under the special steady conditions of Darcy's law applied to this problem requires that the differential of  $\Phi(s)$  must also be constant. Thus, the entire right hand side consists of constant variables and must itself be constant. By defining this constant as  $\sigma$ , two separated differential equations result which are linked by  $\sigma$ , referred to as the separation constant. The first is:

$$\frac{\frac{\partial^2}{\partial s^2}[C(s)]}{\frac{\partial}{\partial s}[C(s)]} = \sigma \quad (4.5)$$

and the second:

$$\frac{\partial}{\partial s}[\Phi(s)] = -\frac{nD}{K}\sigma \quad (4.6)$$

These can be solved independently of each other by applying the boundary conditions illustrated in Figure 10 on page 62. An expression involving  $C(s)$  is obtained by solving the second-order differential Eq (4.5) making use of the two boundary conditions related to concentration.

$$C(s=0) = C_0 \quad (4.7)$$

$$C(s=T) = C_0 + \Delta C \quad (4.8)$$

Through implicit integration, exponentiation, and again implicit integration, Eq (4.5) yields

$$C(s) = \frac{e^A}{\sigma} e^{\sigma s} + B \quad (4.9)$$

where  $A$  and  $B$  are constants of integration. From the boundary condition of Eq (4.7), these constants can to be related:

$$B = C_0 - \frac{e^A}{\sigma} \quad (4.10)$$

Next, the term containing A is evaluated using Eq (4.8).

$$\frac{e^A}{\sigma} = \frac{\Delta C}{e^{\sigma T} - 1} \quad (4.11)$$

Finally, through appropriate substitutions and rearranging, the following non-dimensionalized equation is obtained. It describes the concentration profile across the barrier as a function of  $\sigma$ .

$$\frac{C(s) - C_0}{\Delta C} = \frac{e^{\sigma s} - 1}{e^{\sigma T} - 1} \quad (4.12)$$

The separation constant  $\sigma$ , and the linear potential distribution across the barrier  $\Phi(s)$ , are evaluated by solving the first-order differential Eq (4.6) making use of the boundary conditions related to potential, also illustrated in Figure 10 on page 62.

$$\Phi(s = 0) = \Phi_0 \quad (4.13)$$

$$\Phi(s = T) = \Phi_0 + \Delta\Phi_{\min} \quad (4.14)$$

The solution of this system, Eqs (4.6), (4.13) and (4.14), is straightforward from which the two equations result:

$$\sigma = - \frac{K \Delta\Phi_{\min}}{n D T} \quad (4.15)$$

$$\frac{\Phi(s) - \Phi_0}{\Delta\Phi_{\min}} = \frac{s}{T} \quad (4.16)$$

Thus, the potential head varies linearly across the barrier and flow and dispersion parameters are linked through the constant  $\sigma$  defined in Eq (4.15). Rewriting Eq (4.12) making use of this definition yields the following:

$$\frac{C(s) - C_0}{\Delta C} = \frac{\exp\left[\left[-\frac{K \Delta\Phi_{\min}}{n D}\right]\left[\frac{s}{T}\right]\right] - 1}{\exp\left[-\frac{K \Delta\Phi_{\min}}{n D}\right] - 1} \quad (4.17)$$

#### 4.4 PHYSICAL SIGNIFICANCE

Several simplifying assumptions have been used in investigating the practical problem described. First, long-term containment of contaminants was assumed under constant imposed potential head within the cell and constant barrier properties. This implied constant boundary conditions, or equilibrium conditions, for which a steady-state solution was obtained. Two additional constraints required for the solution to be a valid representation of the practical nature of the containment capsule problem are:

1. Minimal convective inflow so as not to significantly dilute the resident concentrations within the containment region, and
2. Negligible dispersive migration of this concentration into and through the barrier so as not to degrade barrier characteristics or affect ambient concentration levels.

By inspection of Eq (4.17), three physically meaningful dimensionless parameters, denoted by  $\mu_1$ ,  $\mu_2$ , and  $\mu_3$ , may be identified. The first two describe, respectively, the *relative penetration* into and the *relative concentration* within the barrier. The third relates physical and material *barrier properties*, consisting of convection and dispersion related variables, and critical potential conditions. Table 13 describes and defines these dimensionless parameters. Using these definitions, the following non-dimensionalized expression can be written for the concentration profile:

$$\mu_2 = \frac{e^{\mu_3 \mu_1} - 1}{e^{\mu_3} - 1} \quad (4.18)$$

**Table 13. Characteristic Barrier Design Parameters**

| Parameter | Definition                                | Description or Significance  |
|-----------|---|------------------------------|
| $\mu_1$   | $s/T$                                     | Relative Penetration         |
| $\mu_2$   | $\frac{C(s) - C_0}{\Delta C}$             | Relative Concentration       |
| $\mu_3$   | $-\frac{K \Delta\Phi_{min}}{n D} (= T/d)$ | Barrier Properties Parameter |

This relationship has been used to generate a family of performance curves for a low permeability barrier separating two regions having different levels of resident concentration. These curves are illustrated in Figure 11.

An alternative interpretation of  $\mu_3$  is made by noting that the dispersion coefficient  $D$  is not truly constant for a material under varying potential conditions but that the quotient  $D/u$  does approximate a constant [11] [25]. Thus the dispersivity of a material is defined as follows:

$$d = \frac{D}{u} \quad (4.19)$$

It can be shown that heretofore derivations are equally as valid so long as the potential distribution across the barrier is linear which, of course, has already been assumed under Darcy flow. That is, from Eq (4.2) [26]:

$$u = - \frac{K}{n} \frac{\Delta\Phi_{min}}{T} \quad (4.20)$$

Making appropriate substitutions,  $\mu_3$  becomes simply  $T/d$  as indicated in parentheses in Table 13.

The numeric value of this parameter corresponds to the barrier's containment effectiveness. This is seen by the dramatic shifts of the concentration profiles of Figure 11 resulting from various values of this parameter. It follows that for a barrier having a known dispersivity  $d$ ,  $T$  can be adjusted to provide any value of  $\mu_3$  and thus any level of protection as indicated by the shifting concentration profiles of Figure 11. Conservative barrier operating criteria may be developed from these results.

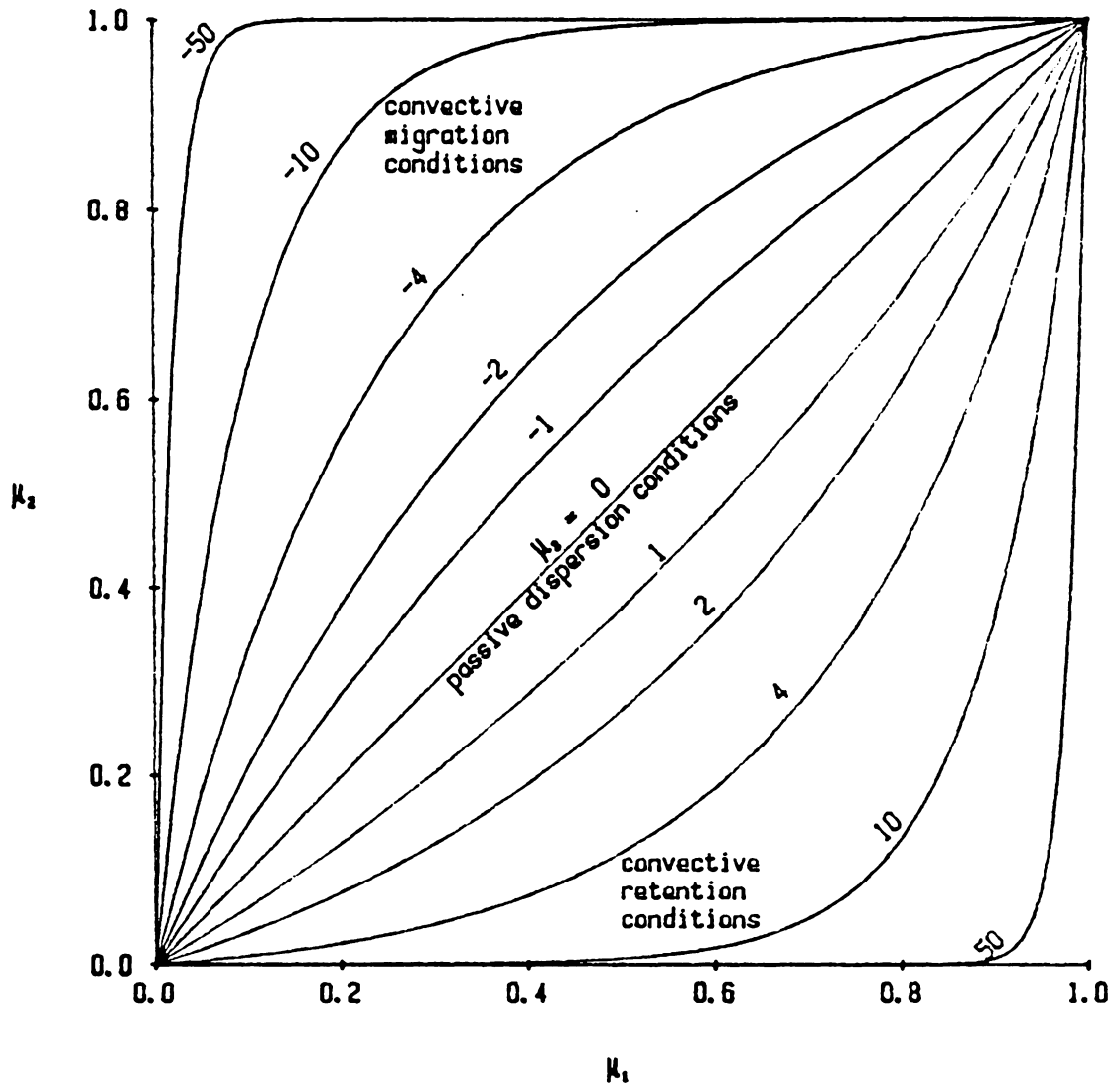


Figure 11. Barrier Performance Curves: Non-dimensionalized solution of the barrier problem.

## CHAPTER 5

# ECONOMIC OPTIMIZATION OF THE CAPSULE

A total cost function describing the effect of varying capsule design features on the total capsule cost is developed. In order to accomplish this, six initial cost coefficients ( $\alpha_1 - \alpha_6$ ), each related to a different aspect of construction, and five annual cost coefficients ( $\beta_1 - \beta_5$ ), each related to a different aspect of operation or maintenance, are introduced. Each coefficient converts a characteristic component or feature of the capsule, defined by the design variables developed in Chapter 3, into the specific cost of that component or feature. These eleven coefficients are more fully explained as the function is developed. By minimizing the total cost function with respect to these design variables, economically optimum conditions are identified. The coefficients and terms required to describe capsule economics, but not defined in Chapters 3 or 4, have been added to the notation.

The analysis is made primarily to indicate the potential for optimizing trends and relationships within the active capsule design. Because each coefficient is linked to its associated design feature through an assumed linear relationship, economies of scale have not been accounted for in development of the cost function. Thus, values of the cost coefficients should be chosen keeping in mind that they are scale dependent, and may need to be revised upon final evaluation of the scale of the problem addressed.



## 5.1 NOTATION

- a,b,c = Coefficients of a parabolic function relating  $\eta_2$  to  $\eta_1$  [-]
- $C_\alpha$  = Specific initial capital costs relative to unit volume protected [ $\$/L^3$ ]
- $C_\beta$  = Specific annual operating and maintenance costs relative to unit volume protected [ $\$/L^3$ ]
- $C_s$  = Total specific cost function [ $\$/L^3$ ]
- $f_c(f_a, f_p)$  = Combined correction factor for anisotropy and partial penetration [-]
- $f_q$  = Factor to obtain gross capsule discharge from net [-]
- i = Marginal rate of return (cost of money) [-]
- j = Rate of change of gradient series (inflation rate) [-]
- N = Project design life [T]
- $r(i,j,N)$  = Present worth reduction factor for an annual series [T]
- W = Half width of drain [L]
- $\alpha_1$  = Barrier construction cost per volume [ $\$/L^3$ ]
- $\alpha_2$  = Cell construction cost per volume [ $\$/L^3$ ]
- $\alpha_3$  = Drain construction cost per volume [ $\$/L^3$ ]
- $\alpha_4$  = Cost per volume of high permeability additive [ $\$/L^3$ ]
- $\alpha_5$  = Pumping facilities construction cost per discharge [ $\$/L^3$ ]
- $\alpha_6$  = Treatment facilities construction cost per discharge [ $\$/L^3$ ]
- $\beta_1$  = Pumping cost per volume [ $\$/L^3$ ]
- $\beta_2$  = Treatment cost per volume [ $\$/L^3$ ]
- $\beta_3$  = Pumping facilities maintenance cost per discharge per year [ $\$/L^3$ ]
- $\beta_4$  = Treatment facilities maintenance cost per discharge per year [ $\$/L^3$ ]
- $\beta_5$  = Capsule maintenance cost per volume per year [ $\$/L^3T$ ]
- $\gamma$  = Combined cost coefficient related to capsule annual discharge volume [ $\$/L^3$ ]
- $\lambda$  = Grouping of design and cost variables [L]

## 5.2 THE SPECIFIC COST FUNCTION

Relationships for the total *initial* capital cost and the total *annual* operating and maintenance costs required to assure safe operating conditions are developed individually. For generality of solution and so that cases of different aspect ratios may be easily compared, all total component costs are divided by the total containment region volume and thus define specific cost per unit volume protected. The total present value cost per unit volume protected, or the *combined specific cost function*  $C$ , may then be expressed as the sum of these costs, the specific initial cost  $C_a$  and the specific annual cost  $C_b$  reduced to its present worth by the present worth factor  $r$ .

The basic idea behind development of the cost function is that the costs of individual capsule components, whether capital construction costs, or annual operation and maintenance costs, can be related to specific features of that component, for example, to the component's volume or the capsule operational discharge. In order to simplify the optimization, these relationships are assumed linear. As a consequence, the cost coefficients of proportionality used in these relationships become scale dependent. That is, even though the coefficients represent *specific* quantities, the values chosen to describe a 2-acre chemical hazardous waste disposal facility would be expected to vary significantly from those representing a 220-acre uranium mill tailing disposal facility.

Further development of the cost function might include means to handle these expected economies of scale as well as possible cost differences with respect to geographical region. For the present study, however, the linear assumptions are adequate to illustrate optimizing trends with respect to various design conditions.

### 5.2.1 Initial Capital Costs

The individual cost of each capsule component is assumed to be proportional to the volume of that capsule component region through the associated cost coefficient. Thus,  $\alpha_1$ ,  $\alpha_2$  and  $\alpha_3$  are introduced as coefficients of proportionality for the capital costs associated with construction of the

barrier, the cell, and the drain, respectively. They may simply be considered as the unit cost of construction for each of these component regions.

The coefficient  $\alpha_4$  describes the cost of layering a unit volume of the more highly permeable material within the cell in order to obtain more favorable flow characteristics. The intent is to increase the permeability in the horizontal direction, the preferred flow direction, and the effective result is anisotropic conditions within the cell as discussed in Chapter 3. Eq (3.24) defines the fraction of additional material  $f_h$  which, when multiplied by the total cell volume, produces the total volume of material added. The cost coefficient  $\alpha_4$  is assumed proportional to this product. The resulting cost is considered to be in addition to the cell construction cost associated with  $\alpha_2$ .

The proportionality coefficient  $\alpha_5$  relates the capital cost associated with construction of the pumping facility to the *gross* capsule discharge. Gross discharge is stressed since the capsule discharge  $q$ , discussed in Chapter 3, was defined without consideration of the possibility of re-circulating the capsule discharge. Thus, it represents the net outflow from the capsule required to maintain safe operating conditions. This net discharge is corrected by the factor  $f_q$  to obtain the gross discharge, the actual amount required to be pumped considering re-circulation. The possibility for re-circulation is provided primarily because treatment cost are expected to be less under this type of scenario.

Similar to pumping facilities, the construction cost of treatment facilities is assumed to be proportional to the *net* outflow from the capsule. Since  $q$  represents the actual amount to be treated and disposed of, no correction is provided in the  $\alpha_6$  term which quantifies this cost. Thus, by basing the pumping cost on gross and the treatment costs on net discharge, the factor  $f_q > 1$  which relates the two is defined.

Applying appropriate values to each coefficient results in the total initial capital cost of the capsule, represented by the numerator of Eq (5.1) below. This sum is divided by the size of the containment region to obtain the specific initial capital cost per unit volume protected,  $C_\alpha$ .

$$C_\alpha = \frac{\alpha_1 T L + \alpha_2 H L + \alpha_3 W H f_p + \alpha_4 H L f_h + \alpha_5 q f_q + \alpha_6 q}{H L} \quad (5.1)$$

**Table 14. Components of the Initial Capital Cost Coefficients**

|   |
|---|
| $\alpha_1$ : Specific barrier construction cost [\$/L <sup>3</sup> ]  |
| <p>cost of the barrier material<br/> excavation and reclamation of the barrow region<br/> transportation to and placement at the capsule site</p> |
| $\alpha_2$ : Specific cell construction cost [\$/L <sup>3</sup> ]   |
| <p>excavation and reclamation of the cell volume<br/> placement of waste material<br/> engineering and design contingencies</p>                   |
| $\alpha_3$ : Specific drain construction cost [\$/L <sup>3</sup> ]  |
| <p>cost of the drain material<br/> transportation to the capsule site<br/> construction including screened wells</p>                              |
| $\alpha_4$ : Specific cost of material additive [\$/L <sup>3</sup> ]  |
| <p>cost of porous additive<br/> cost of lost disposal volume</p>  |
| $\alpha_5$ : Pumping facilities construction cost per discharge [\$/L <sup>3</sup> ]  |
| <p>the cost of construction of pumping facilities<br/> engineering and design contingencies for these facilities</p>                              |
| $\alpha_6$ : Treatment facilities construction cost per discharge [\$/L <sup>3</sup> ]  |
| <p>the cost of construction of treatment facilities<br/> engineering and design contingencies for these facilities</p>                            |

Table 14 describes the capital cost coefficients and lists the principle factors that should be considered in estimating their value.

### **5.2.2 Annual Operating and Maintenance Costs**

The annual operating costs is related primarily to the amount of discharge drawn from the capsule for treatment or disposal. Hence,  $\beta_1$  and  $\beta_2$  are assumed to represent coefficients of proportionality linking this net outflow discharge to the pumping costs and treatment costs. Their respective values are determined by the specific cost of physically pumping or treating a unit volume of discharge. The coefficients  $\beta_3$  and  $\beta_4$  are similarly introduced to relate the net outflow to the costs of maintaining the pumping and treatment facilities, respectively.

Conceptually, the treated discharge may be either simply discharged to the environment, or alternatively recycled through the capsule at a lower volume but higher concentration. It is the second recycling alternative which has made necessary the introduction of the factor  $f_q$  to account for the increased pumping rates while still relating the treatment cost to the net outflow. Thus, the net outflow is corrected by  $f_q$  to reflect a gross value for the discharge which is related to costs of operation and maintenance of the pumping facility through the cost coefficients  $\beta_1$  and  $\beta_3$ , respectively. No corrections are made to the net discharge applied to cost coefficients associated with operation and maintenance of the treatment facility,  $\beta_2$  and  $\beta_4$ , respectively.

Finally, the maintenance cost of the encapsulation is assumed to be proportional to the size of the encapsulation itself and  $\beta_5$  to represents the associated cost coefficient of proportionality. Thus, the total annual operational and maintenance cost of the capsule is denoted by the numerator of Eq (5.2) below. As before, this sum is divided by the size of the containment region to obtain the specific annual cost per unit volume protected.

$$C_\beta = \frac{\beta_1 q f_q + \beta_2 q + \beta_3 q f_q + \beta_4 q + \beta_5 H L}{H L} \quad (5.2)$$

**Table 15. Components of the Annual Operating and Maintenance Cost Coefficients**

|   |
|---|
| $\beta_1$ : Pumping cost per volume [ $\$/L^3$ ]  |
| energy required to pump the gross discharge   |
| $\beta_2$ : Treatment cost per volume [ $\$/L^3$ ]                                      |
| treatment of the net discharge  |
| $\beta_3$ : Pumping facility maintenance cost per gross discharge per year [ $\$/L^3$ ] |
| maintaining the pumping facilities  |
| $\beta_4$ : Treatment facility maintenance cost per net discharge per year [ $\$/L^3$ ] |
| maintaining the treatment facilities  |
| $\beta_5$ : Capsule maintenance cost per volume per year [ $\$/L^3 T$ ]                 |
| maintaining the capsule itself  |

Table 15 describes these cost coefficients and lists the principle factors that should be considered in estimating their values.

### 5.2.3 Combined Cost Function

The total present value of the cost per unit volume protected may be written as  $C_s = C_a + r C_p$ , where the present worth factor  $r$  converts the annual series represented by  $C_p$  to its corresponding present worth value. This factor can be used in association with either a uniform annual series or a gradient annual series [31]. A uniform annual series requires information about the cost of money  $i$  and the project design life  $N$ . A gradient annual series requires additional information concerning the rate of increase of the series  $j$  to account for the rate of inflation, for example. The following equation defines the present worth factor for a gradient annual series but is also valid for a uniform series by setting  $j = 0$ .

$$r = \begin{cases} \frac{1 - (1 + j)^N / (1 + i)}{i - j} & i \neq j \\ \frac{N}{1 + i} & i = j \end{cases} \quad (5.3)$$

A new cost coefficient can be defined to combine those coefficients associated with the capsule discharge. Note that the dimension of this new coefficient is that of specific cost.

$$\gamma = \frac{\alpha_5 f_q + \alpha_6}{r} + \beta_1 f_q + \beta_2 + \beta_3 f_q + \beta_4 \quad (5.4)$$

Using the preceding relationships to combine Eqs (5.1) and (5.2) and simplifying while recalling the definition of the specific discharge  $q_s = \frac{q}{HL}$  introduced in Chapter 3, the total present worth specific cost function is obtained as follows:

$$C_s = \alpha_1 \frac{T}{H} + \alpha_2 + \alpha_3 \frac{W f_p}{L} + \alpha_4 f_h + \gamma q_s r + \beta_5 r \quad (5.5)$$

It was explained in Chapter 3 that  $\eta_3 = \eta_4$  for practical cases where  $0.2 < \eta_1 < 1$ . Using the definitions of  $\eta_3$  and  $\eta_4$  given in Table 3 on page 27, the definition of the net specific discharge may thus be written as follows:

$$q_s = \frac{K}{H T} \left[ \frac{2 \Delta\Phi_{\min} + \Delta\Phi_{\max}}{3} \right] \quad (5.6)$$

Similarly, the definition of the potential parameter  $\eta_2$  yields the following relationships for the potential difference across the barrier at the drain,  $\Delta\Phi_{\max}$ , in terms of the potential difference across the barrier at the critical point,  $\Delta\Phi_{\min}$ :

$$\Delta\Phi_{\max} = \frac{\Delta\Phi_{\min}}{\eta_2} \quad (5.7)$$

Back substituting this expression for  $\Delta\Phi_{\max}$  of Eq (5.7) into Eq (5.6), and the resulting expression for  $q_s$  into Eq (5.5) and simplifying, a new expression for the combined cost function is obtained.

$$C_s = \alpha_1 \frac{T}{H} + \alpha_2 + \alpha_3 \frac{W f_p}{L} + \alpha_4 f_h + \gamma \frac{\lambda}{T} \left[ 2 + \frac{1}{\eta_2} \right] + \beta_5 r \quad (5.8)$$

The term  $\lambda$  has been introduced to replace a group of variables which is often repeated in the subsequent developments. Its dimension is that of length and it is defined as follows:

$$\lambda = \frac{r K \Delta\Phi_{\min}}{3 H} \quad (5.9)$$

According to the primary relationship of Figure 7a, the potential parameter  $\eta_2$  is related to the design parameter  $\eta_1$  in a curvilinear, monotonically increasing manner for standard conditions of isotropy and full penetration. This relationship is corrected for deviations from standard conditions through a correction factor  $f_c$ . Figure 8 and Figure 9 illustrate the values of this correction factor for various degrees of anisotropic ( $f_a$ ) and partially penetrating ( $f_p$ ) conditions, respectively. Assuming that a, b, and c are coefficients of the second-degree polynomial describing this relationship within the practical range of interest, the following generalization is made.



$$\eta_2 = f_c (a \eta_1^2 + b \eta_1 + c) \quad (5.10)$$

Recall that the capsule design parameter  $\eta_1$  is itself a function of  $K$ ,  $L$ ,  $T$ , and  $H$  in addition to  $K_1$  as indicated by its definition taken from Table 3 on page 27 (see Eq (3.24) also):

$$\eta_1 = \left[ 1 + \frac{K L^2}{K_1 T H} \right]^{-1} \quad (5.11)$$

Thus, in addition to cost coefficients, the total cost function of Eq (5.8) is seen to depend upon the critical potential across the barrier  $\Delta\Phi_{\min}$ , the penetration factor  $f_p$ , the factor  $f_h$  which is related to  $f_a$  and  $K_1$ , and five capsule design variables  $K$ ,  $L$ ,  $T$ ,  $H$ , and  $W$ . The potential parameter  $\eta_2$  itself can be expressed in terms of, and thus is completely defined by, several of these eight variables. Optimum capsule design criteria, which in some cases must be tempered by practical considerations, are established by minimizing the total cost function with respect to these eight design variables. Special consideration is given to the optimization of the degree of partial penetration,  $f_p$ , due to the complex effect that this factor has on  $\eta_2$  through  $f_c$  of Figure 9 on page 59.

### 5.3 OPTIMUM CAPSULE DESIGN CRITERIA

The effect of several of the design variables appearing on the right hand side of Eq (5.8) (with proper regard given to  $\lambda$  as defined in Eq (5.9)) on the total cost function can be seen by simple inspection, neglecting momentarily their effect on the design parameter  $\eta_1$ . For example, because  $H$  appears only in the denominator, even though in two of the terms, its value should be maximized within practical limitations to reduce  $C_t$ . Since  $W$ , and  $K$  appear only in the numerator, the values of these variables should be minimized to the extent practical in order to reduce the total cost function. The inspection of Eq (5.8) (and Eq (5.9)) also suggests that  $\Delta\Phi_{\min}$  should be minimized; however, the relationships developed in Chapter 4 must be considered to insure that a minimum contaminant migration criterion at the critical point is met.

Since the  $\eta_1$  as defined in Eq (5.11) is not dependent upon either  $W$  or  $\Delta\Phi_{\min}$ , the optimizing trends identified for these two variables is general. It can also be shown from Eq (5.11) that reducing  $K$  and increasing  $H$  both tend to increase  $\eta_1$ . Eq (5.8) implies, on the other hand, that an increase in  $\eta_1$  reduces the cost function, because the polynomial defined by the coefficients  $a$ ,  $b$ , and  $c$  is monotonically increasing with respect to  $\eta_1$  (see also Figure 7a). Thus the above identified optimizing trends with respect to these two variables are also verified.

The optimizing trends defined by simply maximizing or minimizing these four variables can hardly be considered as optimization criteria. However, because they describe physically meaningful design features, practical or natural considerations which limit the range of possible values can be viewed as constraining criteria. Thus, practical, natural or derived constraints on the values of  $H$ ,  $W$ ,  $K$ , and  $\Delta\Phi_{\min}$  are taken as optimizing criteria for the capsule design. These criteria may be summarized as follows:

1. In maximizing the half capsule thickness (or depth)  $H$ , the feasibility of increasing excavation depth into the saturated groundwater zone must be taken into account. This is a practical consideration which would seem to be site specific, depending upon, among other things, site geology.
2. The half drain width  $W$  must be at least wide enough to allow placement of screened wells into the drain so that constant, below ambient potential may be maintained at the edge of the containment region. Within this practical constraint,  $W$  should be minimized.
3. The value of the barrier permeability  $K$  falls within a natural range for various suitable barrier materials. The optimum material, other economic conditions being equal, is the one with the lowest  $K$  value.
4. Maintaining safe operational conditions at the capsule design critical point is fundamental to the active landfill design. The value of  $\Delta\Phi_{\min}$  must be maintained above a certain value in order to assure negligible dispersion at this point. The suggested criterion for minimum contaminant migration developed earlier in Chapter 4 will be used to investigate the economics of capsule operation.

Again referring to Eq (5.8), the barrier thickness  $T$ , which appears both in the numerator and the denominator of the total cost function, can be optimized to minimize  $C_s$ . Additionally, because of their effect on the design parameter  $\eta_1$ , the capsule length,  $L$ , and the factor corresponding to the addition of porous cell material,  $f_h$ , can also be optimized. Thus a fifth, a sixth and a seventh optimization criteria are developed to minimize the total cost function  $C_s$  with respect to  $L$ ,  $T$  and  $f_h$ .

### 5.3.1 Optimum Capsule Length

The fifth cost optimizing criterion is developed by investigating the effect of the capsule length on the cost function. Taking the first partial derivative of Eq (5.8) with respect to the capsule length results in the following partial differential equation:

$$\frac{\partial}{\partial L} [C_s] = -\frac{\alpha_3 W f_p}{L^2} + \frac{\gamma \lambda}{T} \frac{\partial}{\partial L} \left[ \frac{1}{\eta_2} \right] \quad (5.12)$$

Carrying out the differentiation through repeated application of the chain rule while recalling the definition of  $\eta_2$  and  $\eta_1$  given in Eqs (5.10) and (5.11), respectively, yields:

$$\frac{\partial}{\partial L} \left[ \frac{1}{\eta_2} \right] = \left[ \frac{f_c (2a \eta_1 + b)}{\eta_2^2} \right] \left[ \left[ 1 + \frac{K L^2}{K_1 H T} \right]^{-2} \left[ \frac{2 K L}{K_1 H T} \right] \right] \quad (5.13)$$

Again making use of the definition of  $\eta_1$  and simplifying results in:

$$\frac{\partial}{\partial L} \left[ \frac{1}{\eta_2} \right] = \frac{f_c (2a \eta_1 + b) (1 - \eta_1) \eta_1}{\eta_2^2} \frac{2}{L} \quad (5.14)$$

In order to simplify the preceding and the following results, a new potential parameter  $\eta_2'$  is defined as a function of the potential parameter, the design parameter and the coefficients and correction factors which link the two as follows:

$$\frac{1}{\eta_2'} = \frac{f_c (2a\eta_1 + b)(1 - \eta_1)\eta_1}{\eta_2^2} \quad (5.15)$$

Thus, the right hand side of Eq (5.14) is reduced to  $\frac{2}{L\eta_2'}$  and Eq (5.12) becomes:

$$\frac{\partial}{\partial L}[C_s] = -\frac{\alpha_3 W f_p}{L^2} + \frac{\gamma \lambda}{T L} \frac{2}{\eta_2'} \quad (5.16)$$

Eq (5.16) describes the change in the cost function with respect to L. Thus, setting it equal to zero will define a relationship between the various design variables involved which result in an extreme (either maximum or minimum) total cost. This condition is necessary, but technically not sufficient, to guarantee the minimum cost with varying L. An argument to verify that this relationship will indeed define a minimum cost condition will be presented later. But for now, assuming that this minimizing tendency is valid and setting  $\frac{\partial}{\partial L}[C_s] = 0$ , Eq (5.16), after judicious manipulation, becomes:

$$\frac{L}{T} = \frac{W f_p}{\lambda} \frac{\alpha_3}{\gamma} \frac{\eta_2'}{2} \quad (5.17)$$

### 5.3.1.1 Physical Significance

Eq (5.17) implies that the optimum capsule length relative to the barrier thickness (L/T) is directly related to three dimensionless groups, the first of already optimized design variables and  $f_p$ , the second of cost coefficients, and the third  $\eta_2'$ . This relationship can be illustrated for a isotropic capsule with a fully penetrating drain under varying potential conditions.

From Eq (5.15), note that  $\eta_2'$  is dependent upon  $\eta_2$  and  $\eta_1$ , and from Eq (5.10), that the value of one determines the other for unique values of a, b, and c. Applying curve-fitting techniques to the data for fully penetrating isotropic cases ( $f_p = 1$  and  $f_c = 1$ ) given in Table 11 on page 51, the coefficients of the second-degree polynomial of Eq (5.10) are found to be  $a = -0.67$ ,  $b = 1.69$  and

$c = -0.03$ . Adopting these values and varying the potential parameter  $\eta_2$  through a range of values roughly corresponding to  $0.2 < \eta_1 < 1$ , Eq (5.17) is used to produce Figure 12.

This figure, a graphical representation of the first optimum capsule design relationship for relative length, can be used to find the economically optimum drain spacing ( $2L$ ) relative to the barrier thickness ( $T$ ) under assumed cost variables and for the four otherwise practically optimum design conditions already identified. Note the sensitivity of this relationship to the value of the potential parameter  $\eta_2$ .

### 5.3.1.2 Verification of Minimizing Conditions

In order to verify that the relationship described by Eq (5.17) and illustrated in Figure 12 does indeed correspond to optimum capsule design characteristics, the following argument is offered.

Taking the derivative of Eq (5.16) again with respect to  $L$  results in the second partial of the cost function  $C_s$ :

$$\frac{\partial^2}{\partial L^2} [C_s] = \frac{2\alpha_3 W f_p}{L^3} - \frac{\gamma \lambda}{T L^2} \frac{2\eta_1'}{\eta_2'} \quad (5.18)$$

where  $\eta_1'$  is the following complex function of  $\eta_1$ , and the coefficients  $a$ ,  $b$  and  $c$ :

$$\eta_1' = \left[ \frac{2[-6a\eta_1^2 + 2(2a-b)\eta_1 + b]}{2a\eta_1 + b} - \frac{4[-2a\eta_1^3 + (2a-b)\eta_1^2 + b\eta_1]}{a\eta_1^2 + b\eta_1 + c} \right] \quad (5.19)$$

To show that Eq (5.18) is positive for all valid values of  $\eta_1$  would provide the additional sufficient condition necessary to prove that Eq (5.16), when set equal to zero, describes a cost minimizing relationship between the design variables. However, the complexity of Eq (5.18), with its dependence upon  $\eta_1'$  as defined in Eq (5.19), makes difficult this determination by simple inspection alone. Thus, a more detailed yet indirect analysis is used to show that a minimizing trend with respect to  $L$  has been identified. To accomplish this, Eq (5.16) is set to zero to define the necessary condition for the cost function to be extreme, and Eq (5.18) is assumed to be greater than zero to

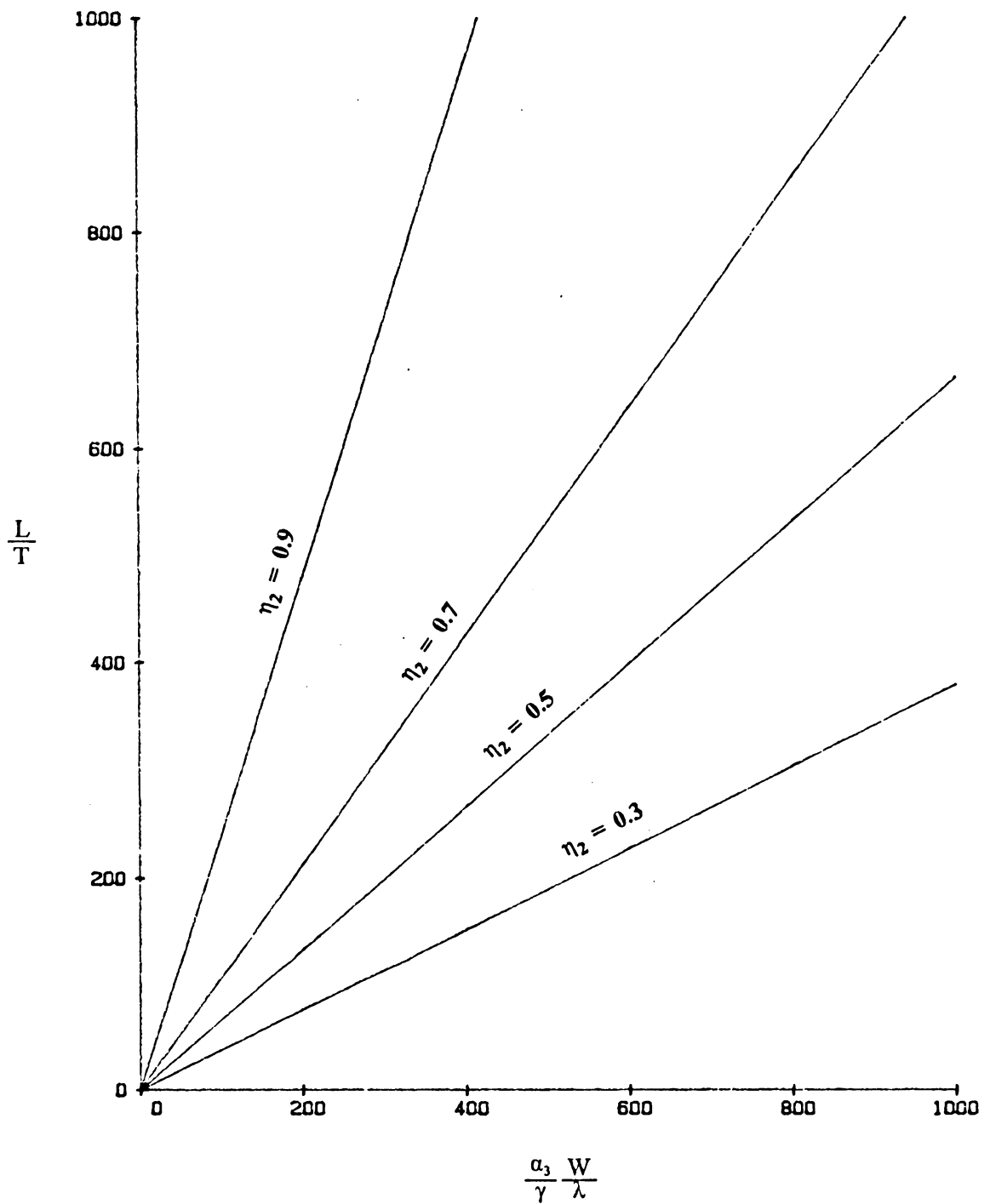


Figure 12. Optimum Capsule Length Relative To Barrier Thickness: Generated for isotropic cell and fully penetrating drain ( $f_c = 1$ ).

provide the sufficient condition for this extreme to be a minimum. The two respective relationships which result are:

$$\frac{\gamma \lambda}{T L} \frac{2}{\eta_2'} = \frac{\alpha_3 W f_p}{L^2} \quad (5.20)$$

$$\frac{\alpha_3 W f_p}{L^2} \stackrel{?}{>} \frac{L}{2} \frac{\gamma \lambda}{T L^2} \frac{2 \eta_1'}{\eta_2'} \quad (5.21)$$

Combining Eqs (5.19) and (5.20) and simplifying produces the following relation which, if true, is the necessary and sufficient condition for the identified cost minimizing relationship to be valid.

$$\eta_1' \stackrel{?}{<} 2 \quad (5.22)$$

This relationship is tested numerically for the meaningful range of  $0.2 < \eta_1 < 1$ . As before, the coefficients a, b and c are approximated by the values -0.67, 1.69 and -0.03, respectively, for this range. Now, considering the definition given in Eq (5.19), the data in Table 16 is generated. Since for the valid range of  $\eta_1$ ,  $\eta_1'$  never exceeds 2, the relative length relationship of Eq (5.17) is shown to be cost minimizing, as has been assumed.

### **5.3.2 Optimum Barrier Thickness**

A sixth cost optimizing criterion is developed by investigating the effect of the barrier thickness on the cost function given by Eq (5.8). Because T appears both in the numerator and the denominator of different terms of the cost function, an optimum barrier thickness relationship can be obtained through minimization of C, with respect this variable. Following is an outline of this minimization process which is similar to that performed with respect to L.

Taking the first partial derivative of Eq (5.8) with respect to the barrier thickness T:

**Table 16. Numerical Test of Minimizing Conditions**

| $\eta_1$ | $\eta_1'$ |
|----------|-----------|
| 0.200    | -2.338    |
| 0.300    | -2.233    |
| 0.400    | -2.213    |
| 0.500    | -2.232    |
| 0.600    | -2.271    |
| 0.700    | -2.314    |
| 0.800    | -2.337    |
| 0.900    | -2.282    |
| 1.000    | -2.000    |



$$\frac{\partial}{\partial T}[C_s] = \frac{\alpha_1}{H} + \gamma \lambda \frac{\partial}{\partial T} \left[ \frac{2 + \eta_2^{-1}}{T} \right] \quad (5.23)$$

The remaining partial differentiation is carried out through repeated application of the chain rule while noting the definitions of  $\eta_2$  and  $\eta_1$  given in Eqs (5.10) and (5.11), respectively:

$$\frac{\partial}{\partial T} \left[ \frac{2 + \eta_2^{-1}}{T} \right] = \frac{1}{T^2} \left[ \left[ \frac{f_c (2a\eta_1 + b)}{\eta_2^2} \right] \left[ 1 + \frac{KL^2}{K_1 HT} \right]^{-2} \left[ \frac{-KL^2}{K_1 HT} \right] - \left[ 2 + \frac{1}{\eta_2} \right] \right] \quad (5.24)$$

Again from the definition of  $\eta_1$ , Eq (5.24) is simplified, resulting in:

$$\frac{\partial}{\partial T} \left[ \frac{2 + \eta_2^{-1}}{T} \right] = \frac{-1}{T^2} \left[ \frac{f_c (2a\eta_1 + b) (1 - \eta_1) \eta_1}{\eta_2^2} + 2 + \frac{1}{\eta_2} \right] \quad (5.25)$$

Simplifying further using Eq (5.15):

$$\frac{\partial}{\partial T} \left[ \frac{2 + \eta_2^{-1}}{T} \right] = \frac{-1}{T^2} \left[ \frac{1}{\eta_2'} + 2 + \frac{1}{\eta_2} \right] \quad (5.26)$$

The results of Eq (5.26) is used to replace the differential in Eq (5.23).

$$\frac{\partial}{\partial T}[C_s] = \frac{\alpha_1}{H} - \frac{\gamma \lambda}{T^2} \left[ \frac{1}{\eta_2'} + 2 + \frac{1}{\eta_2} \right] \quad (5.27)$$

As before, economically optimum conditions may be identified by setting  $\frac{\partial}{\partial T}[C_s]$  to zero. Recalling the definition of  $\lambda$  given in Eq (5.9) and solving for T, the following is obtained:

$$T^2 = \frac{r K \Delta \Phi_{\min}}{3} \frac{\gamma}{\alpha_1} \left[ \frac{1}{\eta_2'} + 2 + \frac{1}{\eta_2} \right] \quad (5.28)$$

### 5.3.2.1 Physical Significance

It can be shown, in a fashion analogous to that used in the capsule length optimization, that the relationship developed here also describes cost minimum conditions. Again for isotropic, fully penetrating conditions, Eq (5.28) may be used to generate Figure 13, illustrating a second capsule design relationship relating optimum barrier thickness  $T$  to economic and already optimized design variables. Thus, between these first two optimum capsule design relationships, the optimizations of both  $L$  and  $T$  are complete. Note the lesser dependence of this relationship upon the value of  $\eta_2$ .

Alternatively, choosing the value of  $\mu_3$  associated with a desired concentration profile from Figure 11 on page 70, the barrier thickness  $T$  is fixed for known barrier dispersivity  $d$  (recall the definition of  $\mu_3$  from Table 13 on page 68). Now Eq (5.28) can be used to determine the optimum potential to be imposed at the barrier critical design point, that is  $\Delta\Phi_{\min}$ , for specific cost parameters.

### 5.3.3 Optimum Containment Region Permeability

A seventh cost optimizing criterion is developed by investigating the effect that creating anisotropic conditions within the cell has on the cost function. First recall from Chapter 3 that the effective horizontal permeability of a layered cell scenario is related to the base material permeability  $K_b$ , the permeability of the added material  $K_a$ , and the relative amount of these two materials described by the factor  $f_h$ . For convenience, Eq (3.24) is rewritten:

$$K_1 = K_b + f_h (K_a - K_b) \quad (5.29)$$

Now, taking the first partial derivative of Eq (5.8) with respect to  $f_h$ .

$$\frac{\partial}{\partial f_h} [C_s] = \alpha_4 + \frac{\gamma \lambda}{T} \frac{\partial}{\partial f_h} \left[ \frac{1}{\eta_2} \right] \quad (5.30)$$

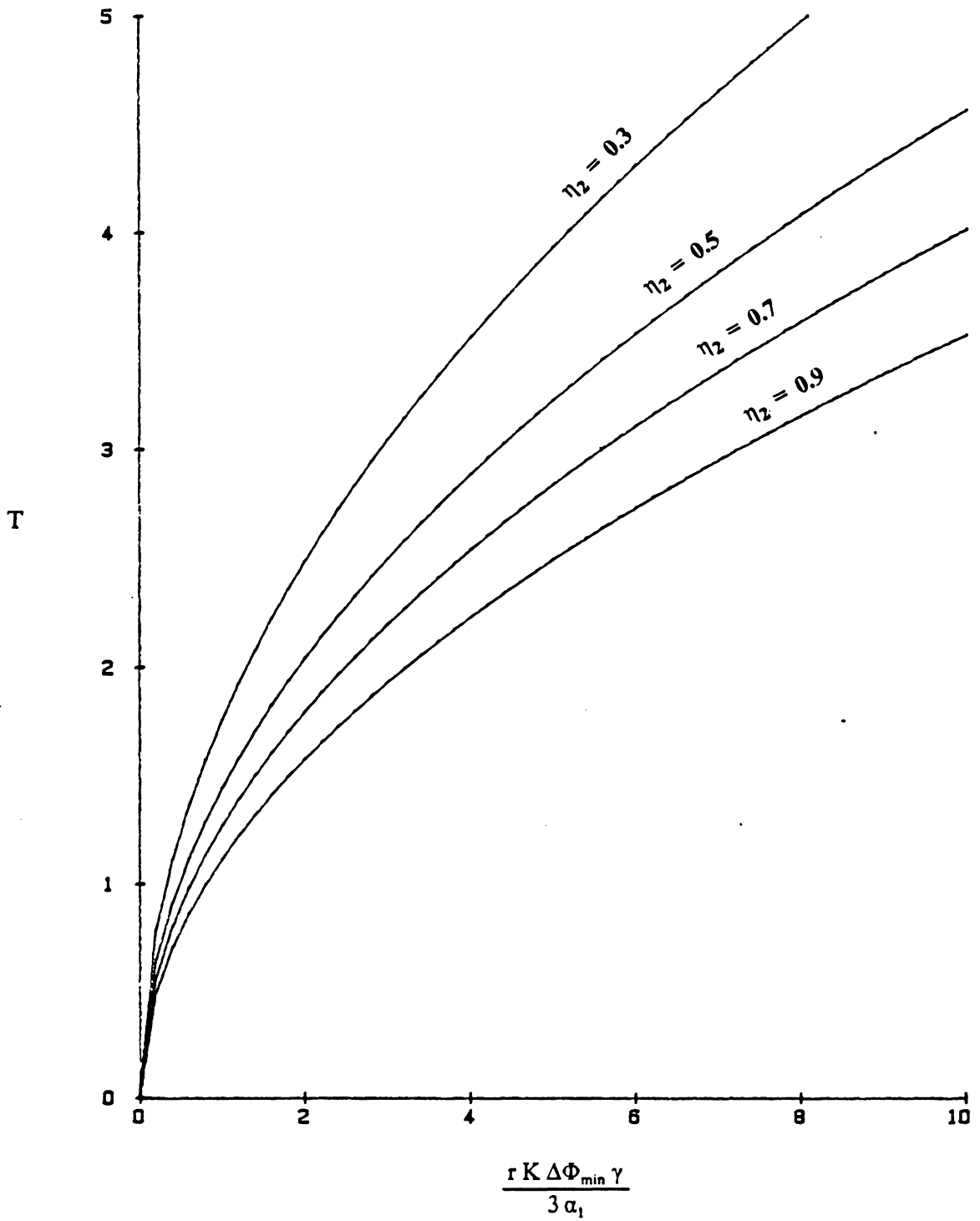


Figure 13. Optimum Barrier Thickness: Generated for anisotropic cell and fully penetrating drain ( $f_c = 1$ ).

Repeatedly applying the chain rule while again referring to the definitions of Eqs (5.10) and (5.11) in addition to Eq (5.29) results in:

$$\frac{\partial}{\partial f_h} \left[ \frac{1}{\eta_2} \right] = \left[ \frac{f_c(2a\eta_1 + b)}{\eta_2^2} \right] \left[ 1 + \frac{KL^2}{K_1 HT} \right]^{-2} \left[ \frac{-KL^2}{K_1^2 HT} \right] [K_a - K_b] \quad (5.31)$$

Upon further simplification:

$$\frac{\partial}{\partial f_h} \left[ \frac{1}{\eta_2} \right] = \frac{-f_c(2a\eta_1 + b)(1 - \eta_1)\eta_1}{\eta_2^2} \frac{K_a - K_b}{K_1} \quad (5.32)$$

Using this result and Eq (5.15), Eq (5.30) becomes:

$$\frac{\partial}{\partial f_h} [C_s] = \alpha_4 - \frac{\gamma \lambda}{T} \frac{K_a - K_b}{K_1} \frac{1}{\eta_2'} \quad (5.33)$$

Setting this equation equal to zero establishes a third optimum capsule design relationship, this time for cell permeability.

$$\frac{K_1}{K_a - K_b} = \frac{\gamma \lambda}{\alpha_4 T} \frac{1}{\eta_2'} \quad (5.34)$$

### 5.3.3.1 Physical Significance

From the preceding, the optimum amount of modifying material to be added,  $f_h$ , can now be expressed in terms of the optimum cell permeability  $K_1$  as defined by Eq (5.34). Rewriting Eq (5.29):

$$f_h = \frac{K_1 - K_b}{K_a - K_b} \quad (5.35)$$

In turn, the optimum degree of anisotropy can be determined using Eq (3.25) which is rewritten here for convenience.

$$\frac{1}{f_a} = f_h^2 + \left[ \frac{K_a}{K_b} + \frac{K_b}{K_a} \right] (1 - f_h) f_h + (1 - f_h)^2 \quad (5.36)$$

It is from this value of  $f_a$  and through the relationship of Figure 8 on page 57 that that part of the combined correction factor  $f_c$  due to cell anisotropy may be found.

Again from Chapter 3, the definition of  $f_h$  given in Eq (3.23) is rewritten:

$$t_b = \frac{t_a}{f_h} - t_a \quad (5.37)$$

Thus, an optimum depth for each layer of the base material  $t_b$  can be determined from the optimized value of  $f_h$  for a chosen depth of the added material  $t_a$ . The resulting two layer alternating pattern comprising the cell will have differing effective permeabilities in the horizontal and vertical directions,  $K_1$  and  $K_2$ , respectively. This anisotropy provides optimum potential and flow conditions which minimize the total specific cost.

Note that through Eq (5.34), these relationships, like previous optimization results represented by Figure 12 on page 85 and Figure 13 on page 90, ultimately depend upon the value of  $\eta_z$ . Iteration will quite likely be required before consistent results between these relationships and those descriptive of the capsule flow itself are achieved.

### **5.3.4 Optimum Drain Penetration**

The the eighth and final criterion involving the penetration factor  $f_p$  is somewhat more vague than the preceding developments. Taking the partial derivative, as above, would involve differentiating the graphical relationship of Figure 9 on page 59 with respect to  $f_p$ . Alternatively, since this is the last design variable considered for optimization, by optimizing all other variables according to the seven criteria already developed for various values of  $f_p$ , the value corresponding to minimum cost may be found indirectly.

## 5.4 EVALUATION OF THE OPTIMUM CAPSULE DESIGN

The eight conditions identified in this section which must be met so that capsule cost, as specified by the cost function of Eq (5.8), is minimized are inter-related in a complex fashion. Additionally, the potential-flow relationships developed in Chapter 3, specifically, the relationships represented by Figure 7 on page 52, Figure 8 on page 57, and Figure 9 on page 59, must be satisfied and due regard must be given to the concentration profiles of Chapter 4 (Eq 4.19). In order to satisfy simultaneously all these requirements, a predictor-corrector methodology has been adopted. It has been incorporated in a computerized optimization program which, with user input and decision making regarding graphical relationships for correction factors, is capable of achieving an optimum solution by repeated iteration toward simultaneously satisfying these relationships.

An outline of the methodology followed in the program *OPTM.BAS* follows. Discussion of an illustrative problem, including development of input based on a 220-acre uranium mill tailing disposal facility [19] and analysis of the BASIC output, follows this outline. The program listing and an example solution are given in Appendix F.

### 5.4.1 Outline of the Optimization Methodology

1. Choose the minimum possible or practical values of the barrier material permeability  $K$  and the half drain width  $W$ .
2. Choose the maximum possible or practical half depth of excavation  $H$ .
3. Set the barrier thickness  $T = \mu_3 d$  according to the desired concentration profile as illustrated in Figure 9 on page 59.
4. Assume the degree of penetration  $f_p$ .
5. Assume the combined correction factor  $f_c$ .
6. Assume a value of the capsule design parameter ( $0.2 < \eta_1 < 1$ ) and compute  $\eta_2$  by Eq (5.10) and  $\eta_z$  by Eq (5.15).

7. Optimize individually the values of (a) the critical potential across the barrier  $\Delta\Phi_{\min}$  by Eq (5.28), (b) the half drain spacing  $L$  by Eqs (5.17) and (5.9), and (c) the cell permeability  $K_1$  by Eq (5.34).
8. Check the assumed value of  $\eta_1$  using Eq (5.11). Revise and repeat as required.
9. Determine the value of the cell degree of anisotropy  $f_a$  by Eqs (5.35) and (5.36).
10. Check the assumed value of  $f_c$  using Figure 8 on page 57 and Figure 9 on page 59. Revise and repeat as required.
11. Check that the values of the dimensionless numbers fall within the ranges as indicated by Table 12 on page 54.
12. Vary the penetration factor  $f_p$  iteratively and repeat as required until the minimum cost is found.

#### **5.4.2 Illustrative Problem**

As in Chapter 3, the specifications for a proposed 220-acre uranium mill tailing disposal facility [19] are used to illustrate use of *OPTM.BAS* to approximate the design of an active capsule. Specific input is required and is found or assumed as follows.

First, the typical values of the  $\alpha$  and  $\beta$  coefficients, which are intended to be descriptive of capital and operational costs of a 220-acre uranium mill tailing disposal area, are chosen [27] [14] [29]. The values selected, indicated in the input data of *OPTM.BAS*, have been chosen to be used solely for illustrative purposes. Actual values may vary significantly under a more detailed analysis. Additionally, the rate of return on money (discount rate) is assumed at 10 percent over a 100 year design period, thus  $r = 10$  yrs.

Next, design variables for the barrier are assumed. Taking the higher (more conservative) value of permeability given in the proposal for local re-compacted clay,  $K = 2.9 \times 10^{-7}$  cm/sec or 0.3 ft/yr. Data for a more porous media [11] is used to extrapolate a probable value for dispersivity in clay with the results  $d = 0.12$  ft. (See also [25]). Choosing the concentration profile corresponding to

$\mu_3 = 10$  as illustrated in Figure 11 on page 70, the barrier thickness is found as the product of this parameter and the dispersivity. Thus,  $T = \mu_3 \times d = 1.2$  ft.

Cell design variables are taken from the proposal. Depth of disposal cell is 40 feet, therefore  $H = 20$  ft. The base disposal material, a silty sand, is assumed to have  $K_b = 100$  ft/yr [3] [17] with an additional material of  $K_a = 10000$  ft/yr available (sand for example) to modify this permeability if desirable. The half width of the drain is assumed to be  $W = 1$  ft to assure that room is available for the construction of screened wells.

Applying the optimization program, a total cost of  $\$0.0556/\text{ft}^3$  of disposal volume is found under fully penetrating drains. Essentially no correction is required for anisotropic conditions, even though, for optimum flow, 4 percent of the disposal volume should be composed of the porous additive. Half drain spacing is found to be 197 ft.

A cost reducing trend is observed for lesser and lesser degrees of drain penetration, until at 1/8 penetration, the total cost is  $\$0.0524/\text{ft}^3$  of disposal volume. This value was attained with a total correction factor  $f_c = 0.80$  and for a aspect ratio  $H/L = 0.30$ . Recall that this is the outside the range for which the relationships have been developed (Table 12 on page 54).

This cell design consists of an optimum 0.87 percent added material of permeability  $K_a = 10,000$  ft/yr. This corresponds to an effective anisotropic factor, as per Eq (3.25), of  $f_a = \frac{K_2}{K_1} = 0.542$ . Also of interest is the inverse of  $q_e$  which corresponds to the equivalent evacuation time of the cell under steady pumping, 12.9 years for this example. The capsule conditions are created by imposing a 5.43 ft potential difference across the 1.2 ft barrier at the critical point. Since  $\eta_1 = 0.772$ ,  $\eta_2 = 0.875$  by Eq (5.10), and the required potential difference to be imposed at the outlet drain  $\Delta\Phi_{\max}$  is 6.2 ft. Optimum half length  $L$  is now only 67.5 ft.

Comparisons may be made between costs of individual components. Notably, the capital cost of barrier construction has the greatest present worth cost ( $\$0.0180/\text{ft}^3$ ) of all capsule components for the assumed problem. This cost plus cell construction cost ( $\$0.01/\text{ft}^3$ ) together approximate the cost of a corresponding passive system. Their sum constitutes 53 percent of the total present worth active system cost, both capital and operating, designed for a 100 year period.



Finally, the capsule design can be applied to the site specific conditions of the proposed tailing disposal area. Due to the high groundwater of the designated location, the proposed 220-acre tailing disposal area (TDA) was to be of the above grade (passive) design and located on the approximately 2000-foot wide "Meadows" area between and along Mill Creek and Dry Branch. This high groundwater table can be used to create the conditions necessary for an active design by lowering the entire waste encapsulation into saturated conditions. Thus, the above optimized capsule may be interpreted as follows.

The parallel drains are assumed to run perpendicular to the streams and thus are about 2000 feet long, the width of the "Meadows". The length of the encapsulation, about 4800 ft to provide the specified waste disposal volume, is divided into about 36 capsules by parallel drains spaced at 133-foot intervals. Total discharge, found from the specific discharge  $q_s$  and volume, is 0.94 cfs. Total cost, found from the specific cost  $C_s$  and volume, is \$20 million. Using the above determined 53 percent factor, a comparable passive design would cost about \$11 million.

**APPENDIX A**  
**FINITE-ELEMENT PROGRAM LISTING**

```

10 OPTION BASE 1
20 DEFINT I-N
22 '
25 OPEN "TDATA" FOR INPUT AS #1
26 PRINT"Output file";:INPUT OT$:OPEN OT$ FOR OUTPUT AS #2
28 INPUT#1,CASE$
30 '
31 INPUT#1,NPROP,NNODE,NELEM,NSURF, IOR
41 DIM PROP(NPROP),FCT(NPROP)
42 DIM X(NNODE),Y(NNODE),Z(NNODE),KODE(NNODE),RHS(NNODE),WORK(NNODE,NNODE+1)
44 DIM II(NELEM),JJ(NELEM),KK(NELEM),MM(NELEM),C2(NELEM,3),C3(NELEM,3)
50 '
150 FOR I=1 TO NPROP:INPUT#1,PROP(I),FCT(I):NEXT
320 FOR I=1 TO NNODE:INPUT#1,X(I),Y(I),Z(I),KODE(I):NEXT
370 '
400 PRINT "Coefficient matrix assembly"
425 '
500 FOR IELE=1 TO NELEM
600 INPUT#1,LI,LJ,LK,LM
601 II(IELE)=LI:JJ(IELE)=LJ:KK(IELE)=LK:MM(IELE)=LM
602 A2=X(LI)*Y(LJ)-Y(LI)*X(LJ)+X(LJ)*Y(LK)-Y(LJ)*X(LK)+X(LK)*Y(LI)-Y(LK)*X(LI)
650 'compute coefficients
680 TMP1=PROP(LM)/A2:TMP2=TMP1*FCT(LM)
684 E21=Y(LJ)-Y(LK):C2(IELE,1)=E21*TMP1
685 E22=Y(LK)-Y(LI):C2(IELE,2)=E22*TMP1
686 E23=Y(LI)-Y(LJ):C2(IELE,3)=E23*TMP1
687 E31=X(LK)-X(LJ):C3(IELE,1)=E31*TMP2
688 E32=X(LI)-X(LK):C3(IELE,2)=E32*TMP2
689 E33=X(LJ)-X(LI):C3(IELE,3)=E33*TMP2
699 'local assembly
700 TMP1=TMP1/2:TMP2=TMP2/2
701 B11=TMP1*E21^2 +TMP2*E31^2
702 B12=TMP1*E22*E21+TMP2*E32*E31
703 B13=TMP1*E23*E21+TMP2*E33*E31
704 B21=TMP1*E21*E22+TMP2*E31*E32
705 B22=TMP1*E22^2 +TMP2*E32^2
706 B23=TMP1*E23*E22+TMP2*E33*E32
707 B31=TMP1*E21*E23+TMP2*E31*E33
708 B32=TMP1*E22*E23+TMP2*E32*E33
709 B33=TMP1*E23^2 +TMP2*E33^2
710 'global assembly
711 WORK(LI,LI)=WORK(LI,LI)+B11
712 WORK(LI,LJ)=WORK(LI,LJ)+B12
713 WORK(LI,LK)=WORK(LI,LK)+B13
714 WORK(LJ,LI)=WORK(LJ,LI)+B21
715 WORK(LJ,LJ)=WORK(LJ,LJ)+B22
716 WORK(LJ,LK)=WORK(LJ,LK)+B23
717 WORK(LK,LI)=WORK(LK,LI)+B31
718 WORK(LK,LJ)=WORK(LK,LJ)+B32
719 WORK(LK,LK)=WORK(LK,LK)+B33
748 NEXT IELE
805 '
900 PRINT"Application of boundary conditions"
903 '
905 'apply neuman b.c.'s
910 FOR ISUR=1 TO NSURF
925 INPUT#1,IFM,ITO,SRFX
940 TMP=SQR((X(ITO)-X(IFM))^2+(Y(ITO)-Y(IFM))^2)*SRFX/2
960 RHS(IFM)=RHS(IFM)+TMP
967 RHS(ITO)=RHS(ITO)+TMP
970 NEXT ISUR
1005 'apply dirchlet b.c.'s
1010 FOR INOD=1 TO NNODE:IF KODE(INOD)=0 THEN 1070
1030 RHS(INOD)=Z(INOD)
1040 FOR JNOD=1 TO NNODE
1050 IF JNOD=INOD THEN WORK(INOD,JNOD)=1 ELSE RHS(JNOD)=RHS(JNOD)-WORK(INOD,JNOD)*Z(INOD):WORK(INOD,JNOD)=0:WORK(JNOD,INOD)=0
1060 NEXT JNOD
1070 NEXT INOD
1200 '

```

```

1500 PRINT"Solution of system of equations"
1600 '
2500 TIN$=TIME$
3000 NEQN=NNODE-10R
3100 NQP1=NEQN+1
3200 NQM1=NEQN-1
3300 FOR I=1 TO NEQN:WORK(I,NQP1)=RHS(I):NEXT
4100 SIGN=1
4125 '
4140 FOR I=1 TO NQM1
4155 MAX=I
4160 AMAX=ABS(WORK(I,I))
4170 IP1=I+1
4180 FOR K=IP1 TO NEQN
4190 IF ABS(WORK(K,I)) <= AMAX THEN 4220
4200 MAX=K
4210 AMAX=ABS(WORK(K,I))
4220 NEXT K
4240 IF MAX=I THEN 4330
4260 L=I-1
4270 FOR L=I TO NQP1
4280 TEMP= WORK(I,L):WORK(I,L)=WORK(MAX,L):WORK(MAX,L)=TEMP
4290 NEXT L
4310 SIGN= -SIGN
4330 FOR J=IP1 TO NEQN
4340 IF WORK(J,I)=0 THEN 4410
4350 CST= -WORK(J,I)/WORK(I,I)
4370 FOR L=I TO NQP1:WORK(J,L)=WORK(J,L)+WORK(I,L)*CST:NEXT L
4410 NEXT J
4420 NEXT I
4435 '
4610 FOR K=NEQN TO 1 STEP -1
4620 Z(K)=WORK(K,NQP1)
4630 IF K=NEQN THEN 4692
4640 KP1=K+1
4650 FOR J=KP1 TO NEQN:Z(K)=Z(K)-WORK(K,J)*Z(J):NEXT J
4692 IF WORK(K,K)=0 THEN STOP
4695 Z(K)=Z(K)/WORK(K,K)
4713 NEXT K
4800 TOUT$=TIME$
4900 '
5100 ERASE KODE,RHS,WORK
5300 DIM VX(NELEM),VY(NELEM)
5400 '
5500 PRINT"Secondary quantities"
5600 '
6000 FOR I=1 TO NELEM
6040 DPDX=Z(II(I))*C2(I,1)+Z(JJ(I))*C2(I,2)+Z(KK(I))*C2(I,3)
6045 VX(I)=DPDX
6050 DPDY=Z(II(I))*C3(I,1)+Z(JJ(I))*C3(I,2)+Z(KK(I))*C3(I,3)
6055 VY(I)=DPDY
6090 NEXT I
6500 '
6600 PRINT"Output"
6700 '
7000 PRINT#2,CASE$
8000 PRINT#2,NPROP;NNODE;NELEM
8100 FOR I=1 TO NPROP:PRINT#2,PROP(I);FCT(I):NEXT
8200 FOR I=1 TO NNODE:PRINT#2,X(I);Y(I);Z(I):NEXT
8300 FOR I=1 TO NELEM:PRINT#2,II(I);JJ(I);KK(I);MM(I);VX(I);VY(I):NEXT
8990 '
8999 PRINT"Time in matrix solver"
9000 PRINT TOUT$:PRINT TIN$
9100 END

```

**APPENDIX B**

**SAMPLE AUXILIARY PROGRAM LISTINGS**

## The PC Data Generator Program

*GQ.BAS*

```
19 CLS
22 PRINT "Specifications file";:INPUT IN$:OPEN IN$ FOR INPUT AS #2
30 PRINT "Generated data file is TDATA":OPEN "TDATA" FOR OUTPUT AS #1
85 '
86 'input specifications
90 INPUT #2,CASE$
91 INPUT #2,NCOL,CL
92 INPUT #2,NRC,TC,DKC,SKC
93 INPUT #2,NRB,TB,DKB,SKB
94 INPUT #2,ITYPE,BCIMP
95 IF ITYPE=0 THEN BCIMP=CL*BCIMP
96 AMBPOT=0!
105 '
110 'determine cell characteristics
125 NNC=(NRC+1)*(NCOL+1)
127 IOR=NCOL+1
140 NNODE=NNC+NRB*(NCOL+1)
141 NELEM=2*(NRC+NRB)*(NCOL)
147 IF ITYPE=1 THEN NSURF=0 ELSE NSURF=NRC
150 PRINT USING"Total number of nodes      = ####";NNODE
151 PRINT USING"Reduction of order        = ####";IOR
152 PRINT USING"Total number of elements = ####";NELEM
154 PRINT USING"Number of columns         = ####";NCOL
170 '
175 'cell characteristics and material properties
180 PRINT#1,CASE$
195 PRINT#1,2;NNODE;NELEM;NSURF;IOR
198 PRINT#1,DKC;SKC
199 PRINT#1,DKB;SKB
202 '
205 '***generate node data***
209 INOD=0
211 '(cell)
212 DX=CL/NCOL:DY=TC/NRC
216 YTMP=-DY
220 FOR I=1 TO NRC+1
225 XTMP=-DX
227 YTMP=YTMP+DY
230 FOR J=1 TO NCOL+1
240 INOD=INOD+1
250 XTMP=XTMP+DX
270 TMP=0!:ITMP=0 'free nodes within cell
275 IF ITYPE=1 AND J=NCOL+1 THEN TMP=BCIMP:ITMP=1 'imposed head
280 PRINT #1,XTMP;YTMP;TMP;ITMP
290 NEXT
295 NEXT
300 IF INOD<>NNC THEN PRINT"error in counting nodes":STOP
```

```

400 '(barrier)
405 DY=TB/NRB
415 YTMP=0
417 FOR I=1 TO NRB
418 XTMP=-DX
419 YTMP=YTMP-DY
420 FOR J=1 TO NCOL+1
425 XTMP=XTMP+DX
430 INOD=INOD+1
440 PRINT#1,XTMP;YTMP;:IF YTMP=-TB THEN PRINT#1,AMBPOI;1 ELSE PRINT#1,0;0
450 NEXT
455 NEXT
530 'check
531 IF INOD<>NNODE THEN PRINT "error in counting nodes":STOP
575 '
600 '***generate element data***
603 IELE=0
605 '(cell)
620 FOR I=1 TO NRC
621 C4(1)=(I-1)*(NCOL+1)+1
622 C4(2)=C4(1)+1
623 C4(3)=C4(1)+NCOL+1
624 C4(4)=C4(3)+1
650 FOR J=1 TO NCOL
661 PRINT#1,C4(3);C4(1);C4(4);1
662 PRINT#1,C4(4);C4(1);C4(2);1
670 IELE=IELE+2
675 FOR K=1 TO 4:C4(K)=C4(K)+1:NEXT
680 NEXT J
690 NEXT I
695 '(barrier)
699 FOR I=1 TO NRB
701 C4(1)=NNC+(I-1)*(NCOL+1)+1
702 C4(2)=C4(1)+1
703 C4(3)=C4(1)-NCOL-1
704 C4(4)=C4(3)+1
705 IF I=1 THEN C4(3)=1:C4(4)=2
709 FOR J=1 TO NCOL
710 PRINT#1,C4(3);C4(1);C4(4);2
720 PRINT#1,C4(4);C4(1);C4(2);2
745 IELE=IELE+2
750 FOR K=1 TO 4:C4(K)=C4(K)+1:NEXT
760 NEXT J
765 NEXT I
770 '(check)
780 IF NELEM<>IELE THEN PRINT "error in counting elements":STOP
790 '
835 '***generate surface data***
840 IF ITYPE<>0 THEN GOTO 999
860 FOR I=1 TO NSURF
861 NFM=I*(NCOL+1)
862 NTO=NFM+NCOL+1
865 PRINT#1,NFM;NTO;BCIMP
870 NEXT
999 END

```

## The PC Plot Program

*P.BAS*

```
5 SCREEN 1:COLOR 1,0
10 PRINT"INPUT PLOT DATA FILE";:INPUT PL$:OPEN PL$ FOR INPUT AS #1
20 PRINT"Quarter solution...Press Q"
22 PRINT"Half solution.....Press H"
25 IF "Q"=INKEY$ OR "q"=INKEY$ THEN FLAG=4:GOTO 30
27 IF "H"=INKEY$ OR "h"=INKEY$ THEN FLAG=2:GOTO 30
29 GOTO 25
30 CLS
35 INPUT#1,CASE$
40 INPUT#1,NPROP,NNODE,NELEM
55 DIM X(NNODE),Y(NNODE),Z(NNODE)
60 DIM II(NELEM),JJ(NELEM),KK(NELEM),MM(NELEM),VX(NELEM),VY(NELEM)
62 FOR I=1 TO NPROP:INPUT#1,PROP,FCT:NEXT
67 '
70 XMAX=-1000:XMIN=1000
72 YMAX=-1000:YMIN=1000
74 ZMAX=-1000:ZMIN=1000
90 FOR I=1 TO NNODE
100 INPUT#1,X(I),Y(I),Z(I)
110 IF X(I)>XMAX THEN XMAX=X(I):NPOT=I
120 IF Y(I)>YMAX THEN YMAX=Y(I)
125 IF Z(I)>ZMAX THEN ZMAX=Z(I)
130 IF X(I)<XMIN THEN XMIN=X(I)
140 IF Y(I)<YMIN THEN YMIN=Y(I)
145 IF Z(I)<ZMIN THEN ZMIN=Z(I)
150 NEXT I
155 '
172 SX=300/XMAX
174 SY=190/(YMAX-YMIN)
176 SZ=YMAX*SY/(-ZMIN)
180 TX=10
190 TY=195+YMIN*SY
200 '
310 VMAX=0
320 FOR I=1 TO NELEM
322 INPUT#1,II(I),JJ(I),KK(I),MM(I),VX(I),VY(I)
324 TMP=SQR(VX(I)^2+VY(I)^2)
326 IF TMP>VMAX THEN VMAX=TMP
327 NEXT I
328 '
329 ARRLTH=(X(NPOT)-X(NPOT-1))*SX*.015
330 SVX=ARRLTH*17/VMAX
332 SVY=SVX*.75
340 '

```



```

349 FOR I=1 TO NELEM
350 AX=TX+(X(II(I))+X(JJ(I))+X(KK(I)))*SX/3
360 AY=TY-(Y(II(I))+Y(JJ(I))+Y(KK(I)))*SY/3
370 FMX=TX+X(II(I))*SX
380 FMY=TY-Y(II(I))*SY
390 TOX=FMX+(X(JJ(I))-X(II(I)))*SX
400 TOY=FMY-(Y(JJ(I))-Y(II(I)))*SY
410 LINE (FMX,FMY)-(TOX,TOY)
450 TOX=TOX+(X(KK(I))-X(JJ(I)))*SX
460 TOY=TOY-(Y(KK(I))-Y(JJ(I)))*SY
470 LINE -(TOX,TOY)
480 TOX=TOX+(X(II(I))-X(KK(I)))*SX
490 TOY=TOY-(Y(II(I))-Y(KK(I)))*SY
500 LINE -(TOX,TOY)
520 CX=VX(I)*SVX
530 CY=VY(I)*SVY
535 PAINT (AX,AY),MM(I),3
540 LINE (AX-CX,AY+CY)-(AX+CX,AY-CY),0
545 CIRCLE (AX+CX,AY-CY),1,0
550 NEXT
560 IF ""=INKEY$ THEN 560 ELSE 570
570 '
590 'special output
595 '
600 FOR I=2 TO NPOT
620 LINE (TX+X(I-1)*SX,5-Z(I-1)*SZ)-(TX+X(I)*SX,5-Z(I)*SZ),0
630 NEXT
700 '
710 LOCATE 1,2:PRINT CASE$
725 LOCATE (5-Z(NPOT)*SZ)/8,34
750 PRINT USING"##.###";ABS(Z(NPOT));
775 LOCATE (5-Z(1)*SZ)/8,1
780 PRINT USING"##.###";ABS(Z(1))
900 '
920 DCH2=0:XLG=X(2):FCOL=(X(3)-X(2))/X(2)
925 FMBOT=NELEM-(NPOT-1)*2
927 FMTOP=FMBOT-(NPOT-1)*2
930 FOR I=1 TO NPOT-1
932 DCH2=DCH2+(VY(FMBOT+I*2-1)+VY(FMBOT+I*2))*XLG*FCOL^(I-1)
935 IF FLAG=2 THEN DCH2=DCH2-(VY(FMTOP+I*2-1)+VY(FMTOP+I*2))*XLG*FCOL^(I-1)
940 NEXT
943 IF FLAG=2 THEN TC=YMAX+YMIN ELSE TC=YMAX
945 SPDCH=.5*DCH2/XMAX/TC
952 LOCATE 5,20
955 PRINT USING"SPDCH =##.###";SPDCH
992 IF ""=INKEY$ THEN 992 ELSE 993
993 STOP
998 ERASE X,Y,Z,II,JJ,KK,MM,VX,VY
999 GOTO 30

```

## The Mainframe Presentation Program

### PRESENT FORTRAN

```
C   SPECIALIZED PRESENTATION OF RESULTS OF FINITE ELEMENT PROGRAM
C   TO INTERPRET PERFORMANCE OF ACTIVE DISPOSAL CAPSULES
C
C SPECIAL NOTES
C -HORIZONTAL AND VERTICAL COORDINATES ORIGINATE AT THE CRITICAL POINT
C -HORIZONTAL AXIS IS ALONG THE BARRIER/CELL INTERFACE
C -VERTICAL AXIS IS POSITIVE IN CELL, NEGATIVE IN LOWER BARRIER
C -AMBIENT POTENTIAL (OUTSIDE THE BARRIER). IS ZERO
C
C PROGRAM CONTROL (LOGICAL) VARIABLES ARE PROVIDED FROM UNIT #1
C   LPLT = SPECIFIES PLOT OUTPUT
C   LTAB = SPECIFIES TABULAR OUTPUT
C   LHALF = INDICATES IF THE DATA REPRESENTS A HALF CAPSULE SOLUTION
C   LNUM = SPECIFIES NUMBERING OF NODES AND ELEMENTS ON THE PLOT
C
C VARIABLE FORMATS (F0-F5) FOR GML MARKUP ARE PROVIDED FROM UNIT #2
C
C VARIABLES DESCRIBING PLOT CHARACTERISTICS ARE PROVIDED FROM UNIT #3
C   XDIM = HORIZONTAL DIMENSION OF THE SOLUTION DOMAIN
C   YDIM = VERTICAL DIMENSION OF THE SOLUTION DOMAIN
C   SZLNGD = SIZE OF THE LEGEND
C   GAP = SPACE BETWEEN POTENTIAL CURVE AND THE SOLUTION DOMAIN
C   HT = HEIGHT OF CHARACTERS
C   FACT = FACTOR TO SCALE FINAL PLOT
C
C DATA FROM EACH FINITE ELEMENT SOLUTION IS PROVIDED FROM UNIT #5
C   NPROP = NUMBER OF MATERIALS WITH DIFFERENT PERMEABILITIES
C   NNODE = NUMBER OF NODES IN THE SOLUTION DOMAIN
C   NELEM = NUMBER OF ELEMENTS IN THE SOLUTION DOMAIN
C   PROP(NPROP,2) = ARRAY CONTAINING PRIMARY PERMEABILITY AND
C                 DEGREE OF ANISOTROPY FOR EACH MATERIAL
C   X(NNODE) = VECTOR OF NODAL VALUES FOR THE HORIZONTAL DIRECTION
C   Y(NNODE) = VECTOR OF NODAL VALUES FOR THE VERTICAL DIRECTION
C   Z(NNODE) = VECTOR OF NODAL VALUES FOR THE POTENTIAL
C   II(NELEM) = VECTOR OF FIRST CONNECTIVITY FOR EACH ELEMENT
C   JJ(NELEM) = VECTOR OF SECOND CONNECTIVITY FOR EACH ELEMENT
C   KK(NELEM) = VECTOR OF THIRD CONNECTIVITY FOR EACH ELEMENT
C   MM(NELEM) = VECTOR SPECIFYING MATERIAL NUMBER FOR EACH ELEMENT
C   VX(NELEM) = VECTOR OF HORIZONTAL VELOCITIES
C   VY(NELEM) = VECTOR OF VERTICAL VELOCITIES
C
C COMPUTED OR DETERMINED VARIABLES DESCRIPTIVE OF CAPSULE GEOMETRY
C   XMIN = MINIMUM HORIZONTAL COORDINATE VALUE WITHIN SOLUTION DOMAIN
C   IXMIN = LOWEST NODE NUMBER CORRESPONDING TO XMIN
C   XMAX = MAXIMUM HORIZONTAL COORDINATE VALUE WITHIN SOLUTION DOMAIN
C   IXMAX = LOWEST NODE NUMBER CORRESPONDING TO XMAX
C   YMIN = MINIMUM VERTICAL COORDINATE VALUE WITHIN SOLUTION DOMAIN
C   IYMIN = LOWEST NODE NUMBER CORRESPONDING TO YMIN
C   YMAX = MAXIMUM VERTICAL COORDINATE VALUE WITHIN SOLUTION DOMAIN
C   IYMAX = LOWEST NODE NUMBER CORRESPONDING TO YMAX
C   YOUT = ILLUSTRATED THICKNESS OF OUTLET
C   SOLNT = ILLUSTRATED THICKNESS OF CELL
C   HALFT = HALF THICKNESS OF CELL
C   NCOL = NUMBER OF ELEMENTAL COLUMNS IN THE SOLUTION DOMAIN
C   XLFT = WIDTH OF THE LEFT MOST COLUMN
C   FCOL = REDUCTION FACTOR FOR SUCCESSIVE COLUMNS TO RIGHT
C   IBOT = BEGINNING ELEMENT NUMBER FOR LOWER BARRIER
C   ITOP = BEGINNING ELEMENT NUMBER FOR UPPER BARRIER
C   DCH2 = TWICE CAPSULE DISCHARGE
C   SPDCH = SPECIFIC DISCHARGE
C   ETA1 = DESIGN PARAMETER
C   ETA2 = POTENTIAL PARAMETER
C   ETA3 = BARRIER GRADIENT PARAMETER
C   ETA4 = DISCHARGE PARAMETER
```

```

C
C *****
C *
C *
C *
C *
C *****
    LOGICAL*1 LPLT,LTAB,LHALF,LNUM
    COMMON CASE(6),NPROP,NNODE,NELEM,PROP(5,2),X(120),Y(120),Z(120),
    * II(200),JJ(200),KK(200),MM(200),VX(200),VY(200),
    * XMAX,YMIN,YMAX,IXMAX,YOUT,SOLNT,HALFT,SPDCH,ETA1,ETA2,ETA3,ETA4
    COMMON/T/F0(20),F1(260),F2(60),F3(20),F4(60),F5(20)
    COMMON/P/XDIM,YDIM,SZLGND,GAP,HT,FACT
1  FORMAT(20A4)

C...SET PARAMETERS ACCORDING TO LOGICAL VARIABLES
READ(1,*)LTAB,LPLT,LHALF,LNUM
IF(LTAB)THEN
    READ(2,1)F0,F1,F2,F3,F4,F5
    WRITE(7,F0)
ENDIF
IF(LPLT)THEN
    READ(3,*)XDIM,YDIM,SZLGND,GAP,HT,FACT
    IF(10.5/FACT-YDIM-SZLGND.LE.0.)STOP
    CALL PLOTS(0,0,50)
    CALL FACTOR(FACT)
ENDIF

C...READ DATA FOR ONE SOLUTION
5  READ(5,1,END=999)CASE
    READ(5,*)NPROP,NNODE,NELEM
    READ(5,*)(PROP(I,1),PROP(I,2),I=1,NPROP)
    READ(5,*)(X(I),Y(I),Z(I),I=1,NNODE)
    READ(5,*)(II(I),JJ(I),KK(I),MM(I),VX(I),VY(I),I=1,NELEM)

C...MAKE CALCULATIONS FOR SUMMARY VALUES
CALL SEARCH(X,NNODE,XMIN,IXMIN,XMAX,IXMAX)
CALL SEARCH(Y,NNODE,YMIN,IYMIN,YMAX,IYMAX)
IF(LHALF)THEN
    YOUT=Y(2*IXMAX)
    SOLNT=YMAX+YMIN
    HALFT=SOLNT/2
ELSE
    YOUT=YMAX
    SOLNT=YMAX
    HALFT=SOLNT
ENDIF
NCOL=IXMAX-1
XLFT=X(2)-X(1)
FCOL=(X(3)-X(2))/XLFT
IBOT=NELEM-(NCOL)*2
ITOP= IBOT-(NCOL)*2

```

```

DCH2=0.
DO 200 I=1,NCOL
  IF(LHALF)DCH2=DCH2
  *          -(VY(ITOP+I*2-1)+VY(ITOP+I*2))*XLFT*FCOL**(I-1)
200 DCH2=DCH2  +(VY(IBOT+I*2-1)+VY(IBOT+I*2))*XLFT*FCOL**(I-1)
  SPDCH=.5*DCH2/XMAX/SOLNT
  ETA1=1./(1.-PROP(2,1)*PROP(2,2)/PROP(1,1)*XMAX**2/HALFT/YMIN)
  ETA2=Z(1)/Z(IXMAX)
  ETA3=(2.*Z(1)+Z(IXMAX))/3./YMIN
  ETA4=SPDCH*HALFT/ABS(PROP(2,1)*PROP(2,2))

C...CALL DESIRED SUBROUTINES
  IF(LTAB)CALL TAB
  IF(LPLT)CALL PLT(LNUM)
  GOTO 5
999 IF(LPLT)CALL PLOT(0.,0.,999)
  STOP
  END

C *****
C *
C *          SUBROUTINE TO GENERATE A TABULAR PRESENTATION
C *          VIA IBM-GML AND THE 3800 LASER PRINTER
C *
C *****

SUBROUTINE TAB
COMMON CASE(6),NPROP,NNODE,NELEM,PROP(5,2),X(120),Y(120),Z(120),
* II(200),JJ(200),KK(200),MM(200),VX(200),VY(200),
* XMAX,YMIN,YMAX,IXMAX,YOUT,SOLNT,HALFT,SPDCH,ETA1,ETA2,ETA3,ETA4
COMMON/T/F0(20),F1(260),F2(60),F3(20),F4(60),F5(20)

WRITE(7,F1)CASE,XMAX,PROP(1,1),PROP(1,1)*PROP(1,2),HALFT,
*PROP(2,1),PROP(2,1)*PROP(2,2),ABS(YMIN),
*Z(NNODE)-Z(IXMAX),Z(NNODE)-Z(1),SPDCH,ETA1,ETA2,ETA3,ETA4

WRITE(7,F2)
NN2=.5*NNODE+.6
DO 1 I=1,NN2
  IF(I.LT.NN2.OR.MOD(NNODE,2).EQ.0)THEN
    WRITE(7,F3)I,X(I),Y(I),Z(I),NN2+I,X(NN2+I),Y(NN2+I),Z(NN2+I)
  ELSE
    WRITE(7,F3)I,X(I),Y(I),Z(I)
  ENDIF
1 CONTINUE

WRITE(7,F4)CASE
NE2=NELEM/2+.6
DO 2 I=1,NE2
  A1=ATAN(VY(I)/VX(I))*57.29578
  V1=SQRT(VX(I)**2+VY(I)**2)
  A2=ATAN(VY(NE2+I)/VX(NE2+I))*57.29578
  V2=SQRT(VX(NE2+I)**2+VY(NE2+I)**2)
2  WRITE(7,F5)I,A1,V1,NE2+I,A2,V2
RETURN
END

```

```

C *****
C *
C *      SUBROUTINE TO GENERATE A GRAPHICAL PRESENTATION      *
C *      VIA IBM VERSATEC PLOTTER                               *
C *
C *
C *****

      SUBROUTINE PLT(LNUM)
      LOGICAL*1 LNUM
      COMMON CASE(6), NPROP, NNODE, NELEM, PROP(5,2), X(120), Y(120), Z(120),
      * II(200), JJ(200), KK(200), MM(200), VX(200), VY(200),
      * XMAX, YMIN, YMAX, IXMAX, YOUT, SOLNT, HALFT, SPDCH, ETA1, ETA2, ETA3, ETA4
      COMMON/P/XDIM, YDIM, SZLGND, GAP, HT, FACT

C
C...SOLUTION DOMAIN
      CALL SCALE(X, NNODE, XDIM, XMIN, XMAX, XSCALE)
      CALL SCALE(Y, NNODE, YDIM, YMIN, YMAX, YSCALE)
      SMAX=X(IXMAX)-X(IXMAX-1)
      VSCALE=SMAX/2/VX(2*(IXMAX-1))
      CALL PLOT(1.5-XMIN*XSCALE, SZLGND-YMIN*YSCALE+5.25*(1.-FACT)+.8, -3)

C...NODES
      IF(LNUM)THEN
      DO 150 I=1, NNODE
      CALL NEWPEN(1)
      CALL NUMBER(X(I)-HT*(.5+INT(ALOG10(FLOAT(I))+1.001)), Y(I)+.5*HT,
      * HT, FLOAT(I), 0., -1)
      CALL NEWPEN(3)
150  CALL NUMBER(X(I)+.5*HT, Y(I)-1.5*HT, HT, ABS(Z(I)), 0., 3)
      ENDIF
      CALL SYMBOL(X(1), Y(1), HT, 1, 0., -1)

C...ELEMENTS
      DO 300 I=1, NELEM
      IF(MM(I).EQ.1)THEN
      CALL NEWPEN(1)
      ELSE
      CALL NEWPEN(3)
      ENDIF
      CALL TRIELE(II(I), JJ(I), KK(I), XAVE, YAVE, X, Y, NNODE)
      CALL NEWPEN(1)
      CALL ARROW(VX(I)*VSCALE, VY(I)*VSCALE, XAVE, YAVE, SMAX*.5, THETA)
      IF(LNUM)THEN
      CALL NEWPEN(2)
      CALL ELEN0(I, XAVE, YAVE, THETA, HT)
      ENDIF
300  CONTINUE

C...OUTLET
      CALL NEWPEN(3)
      CALL PLOT(XMAX*XSCALE, 0., 3)
      CALL PLOT(XMAX*XSCALE, YOUT*YSCALE, 2)

C
C...POTENTIAL DIFFERENCE ACROSS MEMBRANE
      TMPY=10.5-SZLGND-GAP-YDIM
      IF(TMPY.LE.0.)STOP
      CALL PLOT(0., YMAX*YSCALE+GAP+TMPY, -3)

C...BOX
      CALL NEWPEN(4)
      CALL PLOT(XDIM, 0., 2)
      CALL NEWPEN(1)
      CALL PLOT(XDIM, -TMPY, 2)
      CALL PLOT(0., -TMPY, 2)
      CALL PLOT(0., 0., 2)
      CALL NEWPEN(3)
      CALL SYMBOL(XDIM/2., -HT*1.5, HT*1.5, 127, 0., -1)
      CALL SYMBOL(XDIM/2.+2.*HT, -HT*1.5, HT, 'AMBIENT POTENTIAL', 0., 17)

```

```

C...CURVE
  CALL SEARCH(Z,NNODE,ZMIN,ZMAX,IZMAX,IZMIN)
  SMNO=1E-50
  IF(-SMNO.LT.ZMAX.AND.ZMAX.LT.SMNO)ZMAX=0.
  CALL SCALE(Z,NNODE,TMPY,ZMIN,ZMAX,ZSCALE)
  CALL LINE(X,Z,IXMAX)
  DO 11 I=1,IXMAX
    IF(X(I)-XDIM/2.)11,12,12
  11  CONTINUE
  12  YTEMP=Z(I-1)+(XDIM/2.-X(I-1))/(X(I)-X(I-1))*(Z(I)-Z(I-1))
  CALL SYMBOL(XDIM/2.,YTEMP,HT*1.5,126,0.,-1)
  CALL SYMBOL(XDIM/2.+2.*HT,YTEMP+.5*HT,HT,
  *      'POTENTIAL AT BARRIER/CELL INTERFACE',0.,35)
C...CRITICAL POINTS
  CALL NUMBER(XDIM+.5*HT,Z(IXMAX)-HT/2,HT,ABS(Z(IXMAX)/ZSCALE),0.,3)
  CALL NUMBER(XDIM+.5*HT,ZMAX-.5*HT,HT,ABS(ZMAX),0.,3)
  CALL SYMBOL(0.,Z(1),HT,1,0.,-1)
  IF(ABS(Z(1)/TMPY).GE..5)THEN
    CALL SYMBOL(.5*HT,Z(1)+2.*HT,HT,'CRITICAL POINT',0.,14)
    CALL NUMBER(.5*HT,Z(1)+.5*HT,HT,ABS(Z(1)/ZSCALE),0.,3)
  ELSE
    CALL SYMBOL(.5*HT,Z(1)-3.*HT,HT,'CRITICAL POINT',0.,14)
    CALL NUMBER(.5*HT,Z(1)-1.5*HT,HT,ABS(Z(1)/ZSCALE),0.,3)
  ENDIF
C
C...LEGEND
  CALL PLOT(0.,-TMPY-GAP-YDIM-SZLGND,-3)
  CALL NEWPEN(3)
  CALL SYMBOL(0.,1.5,1.5*HT,'FINITE ELEMENT SOLUTION OF POTENTIAL &
  *VELOCITY DISTRIBUTIONS WITHIN AN ACTIVE CAPSULE',0.,86)
C...NOTATIONS
  CALL NEWPEN(2)
  CALL SYMBOL(0.,1.2,HT,CASE,0.,24)
  CALL SYMBOL(0.,.6,HT,'POTENTIAL AND PERMEABILITY',0.,26)
  CALL SYMBOL(0.,.3,HT,'VALUES ARE ABSOLUTE.',0.,20)
C...PERMEABILITIES
  PX=30.*HT
  CALL SYMBOL(PX,1.2,HT,'          PERMEABILITY (FT/YR)',0.,28)
  CALL SYMBOL(PX,.9,HT,'          HORIZONTAL  VERTICAL',0.,28)
  CALL SYMBOL(PX,.85,HT,'          _____',0.,28)
  CALL SYMBOL(PX,.6,HT,'          CELL:',0.,8)
  CALL NUMBER(PX+HT*(14-INT(ALOG10(ABS(PROP(1,1)))+.001)),
  *      .6,HT,ABS(PROP(1,1)),0.,2)
  CALL NUMBER(PX+HT*(24-INT(ALOG10(ABS(PROP(1,1)*PROP(1,2)))+.001)),
  *      .6,HT,ABS(PROP(1,1)*PROP(1,2)),0.,2)
  CALL SYMBOL(PX,.3,HT,'BARRIER:',0.,8)
  CALL NUMBER(PX+HT*(14-INT(ALOG(ABS(PROP(2,1)))+.001)),
  *      .3,HT,ABS(PROP(2,1)),0.,2)
  CALL NUMBER(PX+HT*(24-INT(ALOG(ABS(PROP(2,1)*PROP(2,2)))+.001)),
  *      .3,HT,ABS(PROP(2,1)*PROP(2,2)),0.,2)
C...SCALES
  SX=65.*HT
  CALL SYMBOL(SX,1.2,HT,'SCALES:',0.,7)
  CALL SYMBOL(SX,.9,HT,'HORIZONTAL (FT):',0.,17)
  CALL SYMBOL(SX,.6,HT,'VERTICAL (FT):',0.,17)
  CALL SYMBOL(SX,.3,HT,'VELOCITY (FT/YR):',0.,17)
  BX=83.*HT
  BMAX=XDIM-HT*(83.-0.)
  CALL BAR(XSCALE,BMAX,BX,.9)
  CALL BAR(YSCALE,SOLNT*YSCALE,BX,.6)
  CALL BAR(VSCALE,SMAX*.5,BX,.3)
C...PREPARE FOR NEXT PLOT
  CALL PLOT(XMAX+5.,-5.25*(1.-FACT)+.8,-3)
  RETURN
  END

```

```

C *****
C *
C *          VARIOUS SUPPLEMENTAL SUBROUTINES
C *
C *****

      SUBROUTINE SEARCH(A,NA,AMIN,IAMIN,AMAX,IAMAX)
C
C RETURNS MIN/MAX VALUES OF VECTOR A(NA) AND RESPECTIVE POSITIONS
C
      DIMENSION A(NA)
      AMAX=-1E50
      AMIN= 1E50
      DO 1 I=1,NA
        IF(A(I).GT.AMAX)THEN
          AMAX=A(I)
          IAMAX=I
        ENDIF
        IF(A(I).LT.AMIN)THEN
          AMIN=A(I)
          IAMIN=I
        ENDIF
      1 CONTINUE
      RETURN
      END

C
C -----
C
      SUBROUTINE SCALE(A,NA,ADIM,AMIN,AMAX,ASCALE)
C
C RETURNS ASCALE CORRESPONDING TO AMIN AND AMAX AND SCALED A(NA)
C
      DIMENSION A(NA)
      ASCALE=ADIM/(AMAX-AMIN)
      DO 2 I=1,NA
      2 A(I)=A(I)*ASCALE
      RETURN
      END

C
C -----
C
      SUBROUTINE TRIELE(N1,N2,N3,CX,CY,X,Y,N)
C
C PLOTS TRIANGULAR ELEMENT AND RETURNS CENTROID COORDINATES
C
      DIMENSION X(N),Y(N)
      CALL PLOT(X(N1),Y(N1),3)
      CALL PLOT(X(N2),Y(N2),2)
      CALL PLOT(X(N3),Y(N3),2)
      CALL PLOT(X(N1),Y(N1),2)
      CX=(X(N1)+X(N2)+X(N3))/3
      CY=(Y(N1)+Y(N2)+Y(N3))/3
      RETURN
      END

```

```

C
C
SUBROUTINE ARROW(DX,DY,XC,YC,AMAX,THETA)
C
C PLOTS SYMBOLIC VELOCITY ARROW AT ELEMENT CENTRIOD
C
  THETA=ATAN(DY/DX)
  ALPHA=. 2
  BETA=. 3
  TMP=SQRT(DX**2+DY**2)
  TMP=TMP*(1.-.75*TMP/AMAX)
  IF(TMP.GT.AMAX*.25)TMP=AMAX*.25
  XA=XC-DX/2
  YA=YC-DY/2
  XB=XA+DX
  YB=YA+DY
  X1=XB-.5*TMP*COS(THETA-ALPHA)
  Y1=YB-.5*TMP*SIN(THETA-ALPHA)
  X2=XB-.5*TMP*COS(THETA+ALPHA)
  Y2=YB-.5*TMP*SIN(THETA+ALPHA)
  X3=XB-TMP*COS(THETA-BETA)
  Y3=YB-TMP*SIN(THETA-BETA)
  X4=XB-TMP*COS(THETA+BETA)
  Y4=YB-TMP*SIN(THETA+BETA)
  CALL PLOT(XA,YA,3)
  CALL PLOT(XB,YB,2)
  CALL PLOT(X1,Y1,2)
  CALL PLOT(X3,Y3,2)
  CALL PLOT(X4,Y4,2)
  CALL PLOT(X2,Y2,2)
  CALL PLOT(XB,YB,2)
  RETURN
  END
C
C
SUBROUTINE ELENO(N,XC,YC,THETA,HT)
C
C IDENTIFIES ELEMENT BY NUMBER
C
  R=N
  IF(MOD(N,2).EQ.0)THEN
    GAMMA=ATAN(1./INT(ALOG10(R)+1.001))
    TMP=.5*HT/SIN(GAMMA)
    CALL NUMBER(XC-TMP*COS(THETA-GAMMA),YC-TMP*SIN(THETA-GAMMA),
  *           HT,R,THETA*57.3,-1)
  ELSE
    GAMMA=ATAN(3./INT(ALOG10(R)+1.001))
    TMP=1.5*HT/SIN(GAMMA)
    CALL NUMBER(XC-TMP*COS(THETA+GAMMA),YC-TMP*SIN(THETA+GAMMA),
  *           HT,R,THETA*57.3,-1)
  ENDIF
  RETURN
  END

```



```

C
C
SUBROUTINE LINE(X,Y,N)
C
C   PLOTS LINE RELATING TWO CORRESPONDING 1-D VECTORS
C
  DIMENSION X(N),Y(N)
  CALL PLOT(X(1),Y(1),3)
  DO 1 I=2,N
1 CALL PLOT(X(I),Y(I),2)
  RETURN
  END
C
C
SUBROUTINE BAR(ASCALE,BARMAX,X,Y)
C
C   DRAWS LONGEST POSSIBLE BAR SCALE TO 50, 20, OR 10 SCALE
C
  TMP=ALOG10(BARMAX/ASCALE)
  IF(TMP.LT.0.)THEN
    N=INT(TMP-1.)
  ELSE
    N=INT(TMP)
  ENDIF
  IF(5.*10.**N*ASCALE.LE.BARMAX)THEN
    AVAL=5.*10.**N
    GOTO 10
  ELSEIF(2.*10.**N*ASCALE.LE.BARMAX)THEN
    AVAL=2.*10.**N
    GOTO 10
  ELSEIF(10.**N*ASCALE.LE.BARMAX)THEN
    AVAL=10.**N
    GOTO 10
  ENDIF
  STOP
10 XX=X+AVAL*ASCALE
  CALL SYMBOL(X,Y,.1,13,0.,-1)
  CALL SYMBOL(XX,Y,.1,13,0.,-1)
  CALL PLOT(X,Y,3)
  CALL PLOT(XX,Y,2)
  CALL NUMBER(X-.05,Y+.1,.1,0.,0.,-1)
  IF(N)2,1,1
1 CALL NUMBER(XX-.05*(N+1),Y+.1,.1,AVAL,0.,-1)
  RETURN
2 CALL NUMBER(XX-.05*(ABS(N)+1),Y+.1,.1,AVAL,0.,ABS(N))
  RETURN
  END

```

**APPENDIX C**

**EXAMPLE INTERMEDIATE RESULTS OF THE**

**SOLUTION ALGORITHM**

The following specifications data file **SQ00** illustrates input format for the generator program **GQ.BAS**.

```
0800X16(1E + 4)/2(1E + 0)Q00
8 800.
2 16. -1.E+4 1.
1 2. -1.E+0 1.
1 -10.
```

The following free format data file **TDATA** was generated applying the generator program **GQ.BAS** of Appendix B to the specifications file **SQ00** above. It is an example of the input required for the finite-element program **F.BAS** listed in Appendix A.

```
0800X16(1E + 4)/2(1E + 0)Q00
2 36 48 0 9
-10000 1
-1 1
0 0 0 0
100 0 0 0
200 0 0 0
300 0 0 0
400 0 0 0
500 0 0 0
600 0 0 0
700 0 0 0
800 0 -10 1
0 8 0 0
100 8 0 0
200 8 0 0
300 8 0 0
400 8 0 0
500 8 0 0
600 8 0 0
700 8 0 0
800 8 -10 1
0 16 0 0
100 16 0 0
200 16 0 0
300 16 0 0
400 16 0 0
500 16 0 0
600 16 0 0
700 16 0 0
800 16 -10 1
0 -2 0 1
100 -2 0 1
200 -2 0 1
300 -2 0 1
400 -2 0 1
500 -2 0 1
600 -2 0 1
700 -2 0 1
800 -2 0 1
```

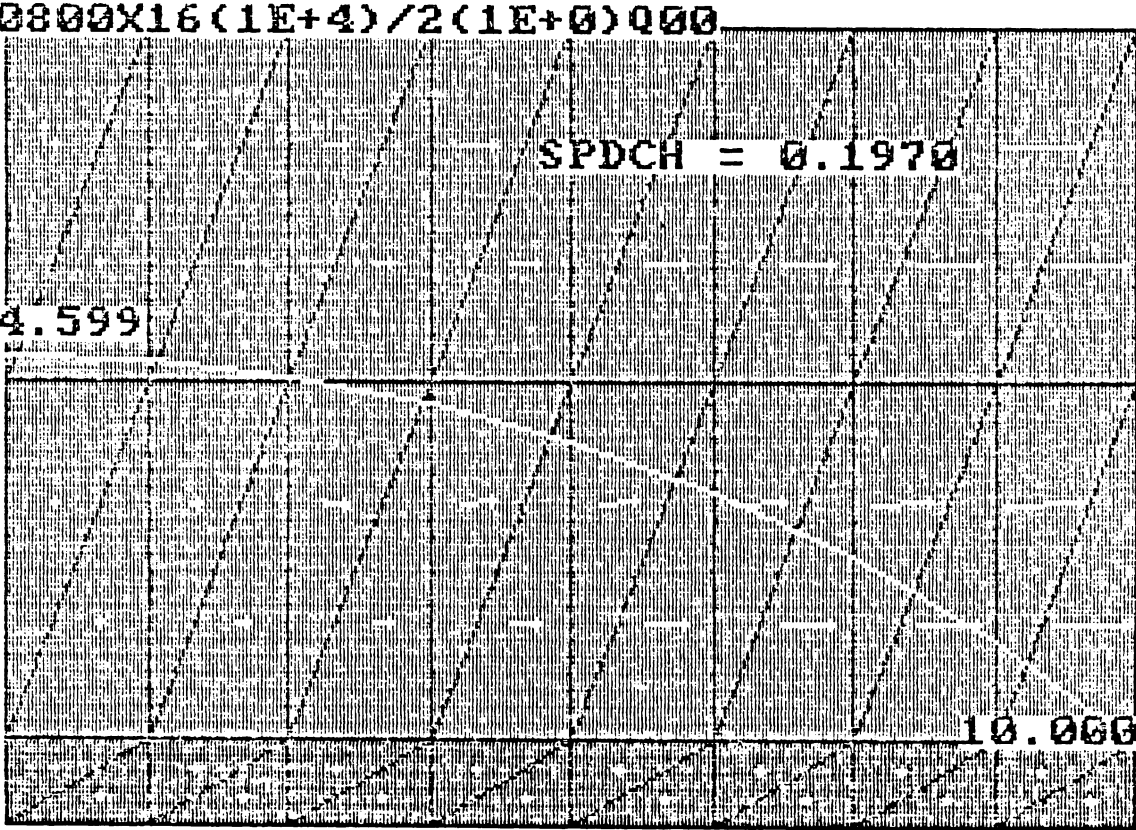
10 1 11 1  
11 1 2 1  
11 2 12 1  
12 2 3 1  
12 3 13 1  
13 3 4 1  
13 4 14 1  
14 4 5 1  
14 5 15 1  
15 5 6 1  
15 6 16 1  
16 6 7 1  
16 7 17 1  
17 7 8 1  
17 8 18 1  
18 8 9 1  
19 10 20 1  
20 10 11 1  
20 11 21 1  
21 11 12 1  
21 12 22 1  
22 12 13 1  
22 13 23 1  
23 13 14 1  
23 14 24 1  
24 14 15 1  
24 15 25 1  
25 15 16 1  
25 16 26 1  
26 16 17 1  
26 17 27 1  
27 17 18 1  
1 28 2 2  
2 28 29 2  
2 29 3 2  
3 29 30 2  
3 30 4 2  
4 30 31 2  
4 31 5 2  
5 31 32 2  
5 32 6 2  
6 32 33 2  
6 33 7 2  
7 33 34 2  
7 34 8 2  
8 34 35 2  
8 35 9 2  
9 35 36 2

The following data file OQ00 is the free format output data of the finite-element program *F.BAS* listed in Appendix A which corresponds to the specifications file SQ00 above.

```
0800X16(1E + 4)/2(1E + 0)Q00
 2 36 48
-10000 1
-1 1
 0 0 -4.598812
 100 0 -4.67066
 200 0 -4.888376
 300 0 -5.258769
 400 0 -5.793404
 500 0 -6.508981
 600 0 -7.427845
 700 0 -8.578702
 800 0 -10
 0 8 -4.600192
 100 8 -4.672061
 200 8 -4.889842
 300 8 -5.260347
 400 8 -5.795142
 500 8 -6.510933
 600 8 -7.430073
 700 8 -8.581268
 800 8 -10
 0 16 -4.600652
 100 16 -4.672528
 200 16 -4.890331
 300 16 -5.260873
 400 16 -5.795722
 500 16 -6.511584
 600 16 -7.430816
 700 16 -8.582122
 800 16 -10
 0 -2 0
 100 -2 0
 200 -2 0
 300 -2 0
 400 -2 0
 500 -2 0
 600 -2 0
 700 -2 0
 800 -2 0
 10 1 11 1 7.18689 1.725098
 11 1 2 1 7.184723 1.751953
 11 2 12 1 21.77811 1.751953
 12 2 3 1 21.77158 1.833496
 12 3 13 1 37.05048 1.833496
 13 3 4 1 37.03931 1.972168
 13 4 14 1 53.47956 1.972168
 14 4 5 1 53.46356 2.172852
 14 5 15 1 71.57904 2.172852
 15 5 6 1 71.55762 2.44043
 15 6 16 1 91.914 2.44043
 16 6 7 1 91.88641 2.785156
```

16 7 17 1 115.1196 2.785156  
 17 7 8 1 115.0858 3.208008  
 17 8 18 1 141.8732 3.208008  
 18 8 9 1 142.1298 0  
 19 10 20 1 7.187561 .5751953  
 20 10 11 1 7.18689 .5834961  
 20 11 21 1 21.78031 .5834961  
 21 11 12 1 21.77811 .6108399  
 21 12 22 1 37.05414 .6108399  
 22 12 13 1 37.05048 .6572266  
 22 13 23 1 53.48493 .6572266  
 23 13 14 1 53.47956 .7241211  
 23 14 24 1 71.58625 .7241211  
 24 14 15 1 71.57904 .8134766  
 24 15 25 1 91.92316 .8134766  
 25 15 16 1 91.914 .9287109  
 25 16 26 1 115.1306 .9287109  
 26 16 17 1 115.1196 1.067383  
 26 17 27 1 141.7878 1.067383  
 27 17 18 1 141.8732 0  
 1 28 2 2 7.184744E-04 2.299406  
 2 28 29 2 0 2.33533  
 2 29 3 2 2.177157E-03 2.33533  
 3 29 30 2 0 2.444188  
 3 30 4 2 3.703933E-03 2.444188  
 4 30 31 2 0 2.629384  
 4 31 5 2 5.346354E-03 2.629384  
 5 31 32 2 0 2.896702  
 5 32 6 2 7.155761E-03 2.896702  
 6 32 33 2 0 3.25449  
 6 33 7 2 9.188644E-03 3.25449  
 7 33 34 2 0 3.713922  
 7 34 8 2 1.150857E-02 3.713922  
 8 34 35 2 0 4.289351  
 8 35 9 2 1.421298E-02 4.289351  
 9 35 36 2 0 5

The following represents the graphical results of the plot program *P.BAS* applied to the above output file *OQ00*.



**APPENDIX D**  
**DATA FOR ANISOTROPIC CONDITIONS**



| ETA1   | ETA2   | ETA3   | ETA4    | FC    | CODE                         |
|--------|--------|--------|---------|-------|------------------------------|
| 0.3333 | 0.4119 | 3.0397 | 2.85369 | 0.904 | CASE:Q18/AR = .200/AF = .100 |
| 0.3333 | 0.2939 | 2.6464 | 2.38474 | 0.645 | CASE:Q18/AR = .200/AF = .020 |
| 0.3333 | 0.2354 | 2.4514 | 2.17727 | 0.517 | CASE:Q18/AR = .200/AF = .010 |
| 0.3333 | 0.1366 | 2.1218 | 1.83977 | 0.300 | CASE:Q18/AR = .200/AF = .001 |
| 0.5000 | 0.5987 | 3.6624 | 3.57208 | 0.931 | CASE:Q20/AR = .200/AF = .100 |
| 0.5000 | 0.4771 | 3.2570 | 3.12653 | 0.742 | CASE:Q20/AR = .200/AF = .020 |
| 0.5000 | 0.4113 | 3.0378 | 2.90350 | 0.639 | CASE:Q20/AR = .200/AF = .010 |
| 0.5000 | 0.2895 | 2.6318 | 2.50112 | 0.450 | CASE:Q20/AR = .200/AF = .001 |
| 0.8333 | 0.8877 | 4.6258 | 4.61001 | 0.980 | CASE:Q19/AR = .200/AF = .100 |
| 0.8333 | 0.8331 | 4.4438 | 4.42213 | 0.920 | CASE:Q19/AR = .020/AF = .020 |
| 0.8333 | 0.7980 | 4.3266 | 4.30695 | 0.881 | CASE:Q19/AR = .200/AF = .010 |
| 0.8333 | 0.7181 | 4.0603 | 4.04937 | 0.793 | CASE:Q19/AR = .200/AF = .001 |
| 0.3333 | 0.4559 | 3.1863 | 3.11397 | 0.992 | CASE:Q12/AR = .060/AF = .100 |
| 0.3333 | 0.4386 | 3.1286 | 2.99237 | 0.955 | CASE:Q12/AR = .060/AR = .020 |
| 0.3333 | 0.4165 | 3.0552 | 2.87568 | 0.916 | CASE:Q12/AR = .060/AF = .010 |
| 0.3333 | 0.2436 | 2.4786 | 2.20559 | 0.530 | CASE:Q12/AR = .060/AF = .001 |
| 0.5000 | 0.6438 | 3.8128 | 3.78567 | 0.994 | CASE:Q14/AR = .060/AF = .100 |
| 0.5000 | 0.6255 | 3.7517 | 3.68937 | 0.965 | CASE:Q14/AR = .060/AF = .020 |
| 0.5000 | 0.6034 | 3.6779 | 3.59126 | 0.931 | CASE:Q14/AR = .060/AF = .010 |
| 0.5000 | 0.4208 | 3.0695 | 2.93533 | 0.649 | CASE:Q14/AR = .060/AF = .001 |
| 0.8333 | 0.9059 | 4.6863 | 4.68372 | 0.998 | CASE:Q13/AR = .060/AF = .100 |
| 0.8333 | 0.8985 | 4.6617 | 4.65188 | 0.990 | CASE:Q13/AR = .060/AF = .020 |
| 0.8333 | 0.8896 | 4.6321 | 4.61714 | 0.980 | CASE:Q13/AR = .060/AF = .010 |
| 0.8333 | 0.8034 | 4.3446 | 4.32452 | 0.885 | CASE:Q13/AR = .060/AF = .001 |
| 0.3333 | 0.4594 | 3.1981 | 3.14737 | 0.999 | CASE:Q00/AR = .020/AF = .100 |
| 0.3333 | 0.4577 | 3.1932 | 3.13026 | 0.995 | CASE:Q00/AR = .020/AF = .020 |
| 0.3333 | 0.4554 | 3.1847 | 3.11004 | 0.990 | CASE:Q00/AR = .020/AF = .010 |
| 0.3333 | 0.4118 | 3.0394 | 2.85323 | 0.895 | CASE:Q00/AR = .020/AF = .001 |
| 0.5000 | 0.6479 | 1.9131 | 1.90541 | 0.999 | CASE:Q08/AR = .020/AF = .100 |
| 0.5000 | 0.6459 | 1.9098 | 1.89907 | 0.996 | CASE:Q08/AR = .020/AF = .020 |
| 0.5000 | 0.6433 | 1.9055 | 1.89132 | 0.992 | CASE:Q08/AR = .020/AF = .010 |
| 0.5000 | 0.5987 | 1.8312 | 1.78596 | 0.923 | CASE:Q08/AR = .020/AF = .001 |
| 0.8333 | 0.9075 | 4.6917 | 4.69162 | 1.000 | CASE:Q06/AR = .020/AF = .100 |
| 0.8333 | 0.9067 | 4.6890 | 4.68760 | 0.999 | CASE:Q06/AR = .020/AF = .020 |
| 0.8333 | 0.9057 | 4.6856 | 4.68287 | 0.998 | CASE:Q06/AR = .020/AF = .010 |
| 0.8333 | 0.8877 | 4.6258 | 4.61001 | 0.978 | CASE:Q06/AR = .020/AF = .001 |
| 0.3333 | 0.4599 | 3.1996 | 3.15200 | 0.999 | CASE:Q15/AR = .003/AF = .100 |
| 0.3333 | 0.4598 | 3.1993 | 3.15128 | 0.998 | CASE:Q15/AR = .003/AF = .020 |
| 0.3333 | 0.4597 | 3.1991 | 3.15056 | 0.998 | CASE:Q15/AR = .003/AF = .010 |
| 0.3333 | 0.4586 | 3.1955 | 3.13969 | 0.996 | CASE:Q15/AR = .003/AF = .001 |
| 0.5000 | 0.6487 | 3.8291 | 3.81528 | 1.007 | CASE:Q17/AR = .003/AF = .100 |
| 0.5000 | 0.6484 | 3.8279 | 3.81384 | 1.007 | CASE:Q17/AR = .003/AF = .020 |
| 0.5000 | 0.6483 | 3.8276 | 3.81333 | 1.007 | CASE:Q17/AR = .003/AF = .010 |
| 0.5000 | 0.6470 | 3.8233 | 3.80502 | 1.005 | CASE:Q17/AR = .003/AF = .001 |
| 0.8333 | 0.9077 | 4.6924 | 4.69251 | 1.011 | CASE:Q16/AR = .003/AF = .100 |
| 0.8333 | 0.9079 | 4.6929 | 4.69313 | 1.011 | CASE:Q16/AR = .003/AF = .020 |
| 0.8333 | 0.9077 | 4.6924 | 4.69251 | 1.011 | CASE:Q16/AR = .003/AF = .010 |
| 0.8333 | 0.9072 | 4.6905 | 4.68985 | 1.010 | CASE:Q16/AR = .003/AF = .001 |

**APPENDIX E**

**DATA FOR PARTIALLY PENETRATING DRAINS**

| ETA1   | ETA2   | ETA3   | ETA4   | FC    | CODE                         |
|--------|--------|--------|--------|-------|------------------------------|
| 0.3333 | 0.4319 | 3.1062 | 2.9310 | 0.948 | CASE:Q18/AR = .200/PF = .500 |
| 0.3333 | 0.3725 | 2.9085 | 2.5500 | 0.818 | CASE:Q18/AR = .200/PF = .250 |
| 0.3333 | 0.3301 | 2.7669 | 2.2746 | 0.725 | CASE:Q18/AR = .200/PF = .125 |
| 0.3333 | 0.2983 | 2.6612 | 2.0636 | 0.655 | CASE:Q18/AR = .200/PF = .062 |
| 0.5000 | 0.6230 | 3.7435 | 3.6521 | 0.968 | CASE:Q20/AR = .200/PF = .500 |
| 0.5000 | 0.5660 | 3.5533 | 3.3332 | 0.880 | CASE:Q20/AR = .200/PF = .250 |
| 0.5000 | 0.5216 | 3.4053 | 3.0823 | 0.811 | CASE:Q20/AR = .200/PF = .125 |
| 0.5000 | 0.4862 | 3.2873 | 2.8783 | 0.756 | CASE:Q20/AR = .200/PF = .062 |
| 0.8333 | 0.8986 | 4.6619 | 4.6432 | 0.992 | CASE:Q19/AR = .200/PF = .500 |
| 0.8333 | 0.8759 | 4.5862 | 4.5303 | 0.967 | CASE:Q19/AR = .200/PF = .250 |
| 0.8333 | 0.8558 | 4.5194 | 4.4299 | 0.945 | CASE:Q19/AR = .200/PF = .125 |
| 0.8333 | 0.8381 | 4.4604 | 4.3397 | 0.925 | CASE:Q19/AR = .200/PF = .062 |
| 0.3333 | 0.4521 | 3.1736 | 3.1028 | 0.984 | CASE:Q12/AR = .060/PF = .500 |
| 0.3333 | 0.4322 | 3.1075 | 2.9690 | 0.941 | CASE:Q12/AR = .060/PF = .250 |
| 0.3333 | 0.4167 | 3.0556 | 2.8641 | 0.907 | CASE:Q12/AR = .060/PF = .125 |
| 0.3333 | 0.4059 | 3.0197 | 2.7912 | 0.883 | CASE:Q12/AR = .060/PF = .062 |
| 0.5000 | 0.6420 | 3.8066 | 3.7804 | 0.991 | CASE:Q14/AR = .060/PF = .500 |
| 0.5000 | 0.6245 | 3.7482 | 3.6786 | 0.964 | CASE:Q14/AR = .060/PF = .250 |
| 0.5000 | 0.6103 | 3.7009 | 3.5963 | 0.942 | CASE:Q14/AR = .060/PF = .125 |
| 0.5000 | 0.6002 | 3.6675 | 3.5379 | 0.926 | CASE:Q14/AR = .060/PF = .062 |
| 0.8333 | 0.9056 | 4.6854 | 4.6830 | 0.998 | CASE:Q13/AR = .060/PF = .500 |
| 0.8333 | 0.8993 | 4.6645 | 4.6509 | 0.991 | CASE:Q13/AR = .060/PF = .250 |
| 0.8333 | 0.8941 | 4.6469 | 4.6241 | 0.985 | CASE:Q13/AR = .060/PF = .125 |
| 0.8333 | 0.8903 | 4.6342 | 4.6044 | 0.981 | CASE:Q13/AR = .060/PF = .062 |
| 0.3333 | 0.4575 | 3.1916 | 3.1436 | 0.995 | CASE:Q00/AR = .020/PF = .500 |
| 0.3333 | 0.4531 | 3.1769 | 3.1141 | 0.985 | CASE:Q00/AR = .020/PF = .250 |
| 0.3333 | 0.4500 | 3.1665 | 3.0925 | 0.978 | CASE:Q00/AR = .020/PF = .125 |
| 0.3333 | 0.4482 | 3.1606 | 3.0800 | 0.975 | CASE:Q00/AR = .020/PF = .062 |
| 0.5000 | 0.6467 | 1.9111 | 1.9050 | 0.998 | CASE:Q08/AR = .020/PF = .500 |
| 0.5000 | 0.6427 | 1.9045 | 1.8938 | 0.991 | CASE:Q08/AR = .020/PF = .250 |
| 0.5000 | 0.6401 | 1.9002 | 1.8859 | 0.987 | CASE:Q08/AR = .020/PF = .125 |
| 0.5000 | 0.6386 | 1.8977 | 1.8814 | 0.985 | CASE:Q08/AR = .020/PF = .062 |
| 0.8333 | 0.9073 | 4.6911 | 4.6921 | 0.999 | CASE:Q06/AR = .020/PF = .500 |
| 0.8333 | 0.9060 | 4.6867 | 4.6855 | 0.998 | CASE:Q06/AR = .020/PF = .250 |
| 0.8333 | 0.9051 | 4.6835 | 4.6805 | 0.997 | CASE:Q06/AR = .020/PF = .125 |
| 0.8333 | 0.9042 | 4.6808 | 4.6768 | 0.996 | CASE:Q06/AR = .020/PF = .062 |
| 0.3333 | 0.4591 | 3.1969 | 3.1539 | 0.997 | CASE:Q15/AR = .003/PF = .500 |
| 0.3333 | 0.4593 | 3.1978 | 3.1564 | 0.997 | CASE:Q15/AR = .003/PF = .250 |
| 0.3333 | 0.4572 | 3.1908 | 3.1454 | 0.993 | CASE:Q15/AR = .003/PF = .125 |
| 0.3333 | 0.4582 | 3.1939 | 3.1471 | 0.995 | CASE:Q15/AR = .003/PF = .062 |
| 0.5000 | 0.6479 | 3.8262 | 3.8173 | 1.006 | CASE:Q17/AR = .003/PF = .500 |
| 0.5000 | 0.6504 | 3.8346 | 3.8281 | 1.010 | CASE:Q17/AR = .003/PF = .250 |
| 0.5000 | 0.6429 | 3.8096 | 3.7965 | 0.998 | CASE:Q17/AR = .003/PF = .125 |
| 0.5000 | 0.6489 | 3.8295 | 3.8150 | 1.007 | CASE:Q17/AR = .003/PF = .062 |
| 0.8333 | 0.9052 | 4.6839 | 4.6852 | 1.008 | CASE:Q16/AR = .003/PF = .500 |
| 0.8333 | 0.9146 | 4.7152 | 4.7114 | 1.019 | CASE:Q16/AR = .003/PF = .250 |
| 0.8333 | 0.9013 | 4.6711 | 4.6727 | 1.004 | CASE:Q16/AR = .003/PF = .125 |
| 0.8333 | 0.9203 | 4.7345 | 4.7242 | 1.025 | CASE:Q17/AR = .003/PF = .062 |

**APPENDIX F**  
**OPTIMIZATION PROGRAM LISTING AND EXAMPLE**  
**OUTPUT**

OPTM.BAS Listing

```

0 '          OPTIMIZATION OF CAPSULE DESIGN
1 '
2 '          This program evaluates the relationships of Chapter 5
3 ' according to the methodology proposed therein. A predictor-
4 ' corrector procedure is used which iterates toward the solution
5 ' which satisfies all optimization relationships as well as the
6 ' characteristic relationships of the specific capsule design as
7 ' developed in Chapter 3 and the minimum contamination migration
8 ' criterion specified in Chapter 4.
9 '
100 REM Program Control
101 OPEN "OPTM.OUT" FOR OUTPUT AS #1
110 GOSUB 900:GOSUB 800'read formats, input data, and reflect coefficients
120 GOSUB 300'optimize
130 CLS:PRINT USING F0$;ITR,FC,FA,FP,H/L
131 PRINT #1,:PRINT #1,USING F0$;ITR,FC,FA,FP,H/L
140 GOSUB 400:GOSUB 500'compute and present results
150 PRINT'check ranges (see: Tables 2 and 12)
151 PI1=K1/K:IF PI1<150 OR PI1>10000 THEN PRINT"check PI1",
152 PI2=H/L :IF PI2<.0033 OR PI2>.2 THEN PRINT"check PI2",
153 PI3=T/H :IF PI3<.0625 OR PI3>.5 THEN PRINT"check PI3",
160 INPUT"Perspective";YN$:IF YN$="Y" THEN GOSUB 600
170 PRINT:INPUT"New values: FC,FP =";FC,FP
199 GOTO 120
300 REM Optimize
302 ITR=ITR+1:TEST=.001'IF ITR<3 THEN TEST=.1^ITR ELSE TEST=.001
304 PRINT USING"#.####";N1
306 N2=FC*(A*N1^2+B*N1+C):N2P=N2^2/(FC*(2*A*N1+B)*(1-N1)*N1)
310 DP=3*T^2/R/K*A1/GAMMA/(1/N2P+2+1/N2) 'Eq (5.28)
320 LAMBDA=R*K*DP/3/H:L=T*W*FP/LAMBDA*A3/GAMMA*N2P/2 'Eqs (5.9) & (5.17)
330 K1=(KA-KB)*GAMMA/A4*LAMBDA/T*1/N2P 'Eq (5.34)
332 IF K1<KB THEN K1=KB:PRINT "K1<KB: K1=KB set"
333 IF K1>KA THEN PRINT "K1>KB: check A4":STOP
334 N1C=1/(1+K/K1*L^2/H/T) 'Table 3
336 IF ABS(N1C-N1)>TEST THEN N1=N1+.4*(N1C-N1):GOTO 304
350 FH=(K1-KB)/(KA-KB) 'Eq (3.24)
352 FA=1/(FH^2+(KA/KB+KB/KA)*(1-FH)*FH+(1-FH)^2) 'Eq (3.25)
399 RETURN

```

```

400 REM Costs
410 N3=DP*(2+1/N2)/T/3:N4=N3:QS=N4*K/H
420 CA1=A1*T/H:CA2=A2:CA3=A3*W*FP/L:CA4=A4*FH:CA5=A5*QS*FQ:CA6=A6*QS
430 CB1=R*B1*QS*FQ:CB2=R*B2*QS:CB3=R*B3*QS*FQ:CB4=R*B4*QS:CB5=R*B5
440 CS=CA1+CA2+CA3+CA4+CA5+CA6+CB1+CB2+CB3+CB4+CB5
499 RETURN
500 REM summary
530 T1=20:PRINT:PRINT TAB(T1-2);F30$
531 PRINT TAB(T1):PRINT USING F31$;H , T
532 PRINT TAB(T1):PRINT USING F32$;W , DP
533 PRINT TAB(T1):PRINT USING F33$;KB, L
534 PRINT TAB(T1):PRINT USING F34$;KA, K1
535 PRINT TAB(T1):PRINT USING F35$;K , N1
536 PRINT TAB(T1):PRINT USING F36$;D , FH
540 PRINT #1, :PRINT #1, TAB(T1-2);F30$
541 PRINT #1, TAB(T1):PRINT #1, USING F31$;H , T
542 PRINT #1, TAB(T1):PRINT #1, USING F32$;W , DP
543 PRINT #1, TAB(T1):PRINT #1, USING F33$;KB, L
544 PRINT #1, TAB(T1):PRINT #1, USING F34$;KA, K1
545 PRINT #1, TAB(T1):PRINT #1, USING F35$;K , N1
546 PRINT #1, TAB(T1):PRINT #1, USING F36$;D , FH
550 T1=9:PRINT:PRINT TAB(T1);F50$
551 PRINT TAB(T1):PRINT USING F51$;CA1, CB1, CS
552 PRINT TAB(T1):PRINT USING F52$;CA2, CB2, 1/QS
553 PRINT TAB(T1):PRINT USING F53$;CA3, CB3
554 PRINT TAB(T1):PRINT USING F54$;CA4, CB4
555 PRINT TAB(T1):PRINT USING F55$;CA5, CB5
556 PRINT TAB(T1):PRINT USING F56$;CA6
560 PRINT #1, :PRINT #1, TAB(T1);F50$
561 PRINT #1, TAB(T1):PRINT #1, USING F51$;CA1, CB1, CS
562 PRINT #1, TAB(T1):PRINT #1, USING F52$;CA2, CB2, 1/QS
563 PRINT #1, TAB(T1):PRINT #1, USING F53$;CA3, CB3
564 PRINT #1, TAB(T1):PRINT #1, USING F54$;CA4, CB4
565 PRINT #1, TAB(T1):PRINT #1, USING F55$;CA5, CB5
566 PRINT #1, TAB(T1):PRINT #1, USING F56$;CA6
569 RETURN
600 REM perspective
605 SCREEN 2
610 SX=500/L/2:SY=.36*SX
612 TX=80:TY=100-T*SY
620 LINE (TX, TY)-(TX+SX*L*2, TY+SY*T), 3, BF
630 LINE (TX, TY)-(TX+SX*L*2, TY-SY*H*2), 3, B
640 LINE (TX, TY-SY*H*2)-(TX+SX*L*2, TY-SY*(H*2+T)), 3, BF
650 LOCATE 23, 1
699 RETURN

```

```

800 REM Input (Nomenclature by Inference)
810 'barrier design
811 READ K,D,MU3           :DATA .3, .12, 10
812   T=MU3*D
820 'cell design
821 READ H,W               :DATA 20, 1
822 READ KB,KA             :DATA 1E2, 1E4
830 'pump/treatment
831 READ FQ                :DATA 1
840 'cost coefficients
841 READ A1,A2,A3,A4,A5,A6 :DATA 3E-1, 1E-2, 1E+0, 5E-2, 3E-2, 7E-2
842 READ B1,B2,B3,B4,B5   :DATA 1E-3, 1E-2, 3E-4, 7E-4, 5E-4
843 READ I,J,N            :DATA .1, 0, 100
844   IF I=J THEN R=N/(1+I) ELSE R=(1-((1+J)/(1+I))^N)/(I-J)
845   GAMMA=(A5*FQ+A6)/R+B1*FQ+B2+B3*FQ+B4
850 'miscellaneous
851 READ A,B,C             :DATA -0.67, 1.69,-0.03
860 'seed values
861 READ FP,FC,N1         :DATA 1, 1, .2
870 'reflect cost coefficients
880 T1=10:PRINT #1,TAB(T1);F10$
881 PRINT #1,TAB(T1);:PRINT #1,USING F11$;A1,B1,I
882 PRINT #1,TAB(T1);:PRINT #1,USING F12$;A2,B2,J
883 PRINT #1,TAB(T1);:PRINT #1,USING F13$;A3,B3,N
884 PRINT #1,TAB(T1);:PRINT #1,USING F14$;A4,B4,R
885 PRINT #1,TAB(T1);:PRINT #1,USING F15$;A5,B5
886 PRINT #1,TAB(T1);:PRINT #1,USING F16$;A6
899 RETURN
900 REM formats
901 F0$="                ITR=##: FC=#.## (FA=#.#### FP=#.####) and AR=#.####"
910 F10$="                Cost Coefficients"
911 F11$="A1 = ##.##^####    B1 = ##.##^####    I = ##.##^####"
912 F12$="A2 = ##.##^####    B2 = ##.##^####    J = ##.##^####"
913 F13$="A3 = ##.##^####    B3 = ##.##^####    N = ##.##^####"
914 F14$="A4 = ##.##^####    B4 = ##.##^####    r = ##.##^####"
915 F15$="A5 = ##.##^####    B5 = ##.##^####"
916 F16$="A6 = ##.##^####"
920 F30$="Specified Variables Optimized Variables"
921 F31$="H = ##.##^####    T = ##.##^####"
922 F32$="W = ##.##^####    DP = ##.##^####"
923 F33$="KB = ##.##^####    L = ##.##^####"
924 F34$="KA = ##.##^####    K1 = ##.##^####"
925 F35$="K = ##.##^####    N1 = ##.##^####"
926 F36$="D = ##.##^####    FH = ##.##^####"
930 F50$="                Summary"
931 F51$="CA1 = ##.##^####    CB1 = ##.##^####    CS = ##.##^####"
932 F52$="CA2 = ##.##^####    CB2 = ##.##^####    1/QS = ##.##^####"
933 F53$="CA3 = ##.##^####    CB3 = ##.##^####"
934 F54$="CA4 = ##.##^####    CB4 = ##.##^####"
935 F55$="CA5 = ##.##^####    CB5 = ##.##^####"
936 F56$="CA6 = ##.##^####"
999 RETURN

```

Example Output

| Cost Coefficients |               |              |
|-------------------|---------------|--------------|
| A1 = 3.00E-01     | B1 = 1.00E-03 | I = 1.00E-01 |
| A2 = 1.00E-02     | B2 = 1.00E-02 | J = 0.00E+00 |
| A3 = 1.00E+00     | B3 = 3.00E-04 | N = 1.00E+02 |
| A4 = 5.00E-02     | B4 = 7.00E-04 | r = 1.00E+01 |
| A5 = 3.00E-02     | B5 = 5.00E-04 |              |
| A6 = 7.00E-02     |               |              |

ITR= 1: FC=1.00 (FA=0.2069 FP=1.0000) and AR=0.1018

| Specified Variables | Optimized Variables |
|---------------------|---------------------|
| H = 2.00E+01        | T = 1.20E+00        |
| W = 1.00E+00        | DP = 4.79E+00       |
| KB = 1.00E+02       | L = 1.97E+02        |
| KA = 1.00E+04       | K1 = 5.04E+02       |
| K = 3.00E-01        | N1 = 5.11E-01       |
| D = 1.20E-01        | FH = 4.08E-02       |

| Summary        |                |                 |
|----------------|----------------|-----------------|
| CA1 = 1.80E-02 | CB1 = 7.03E-04 | CS = 5.56E-02   |
| CA2 = 1.00E-02 | CB2 = 7.03E-03 | 1/QS = 1.42E+01 |
| CA3 = 5.09E-03 | CB3 = 2.11E-04 |                 |
| CA4 = 2.04E-03 | CB4 = 4.92E-04 |                 |
| CA5 = 2.11E-03 | CB5 = 5.00E-03 |                 |
| CA6 = 4.92E-03 |                |                 |

ITR= 8: FC=0.80 (FA=0.5422 FP=0.1250) and AR=0.3007

| Specified Variables | Optimized Variables |
|---------------------|---------------------|
| H = 2.00E+01        | T = 1.20E+00        |
| W = 1.00E+00        | DP = 5.43E+00       |
| KB = 1.00E+02       | L = 6.65E+01        |
| KA = 1.00E+04       | K1 = 1.86E+02       |
| K = 3.00E-01        | N1 = 7.72E-01       |
| D = 1.20E-01        | FH = 8.69E-03       |

| Summary        |                |                 |
|----------------|----------------|-----------------|
| CA1 = 1.80E-02 | CB1 = 7.75E-04 | CS = 5.24E-02   |
| CA2 = 1.00E-02 | CB2 = 7.75E-03 | 1/QS = 1.29E+01 |
| CA3 = 1.88E-03 | CB3 = 2.33E-04 |                 |
| CA4 = 4.35E-04 | CB4 = 5.43E-04 |                 |
| CA5 = 2.33E-03 | CB5 = 5.00E-03 |                 |
| CA6 = 5.43E-03 |                |                 |



## REFERENCES

1. Anderson, M.P., *Using Models to Simulate the Movement of Contaminants Through Groundwater Flow Systems*, **CRC Critical Reviews in Environmental Control**, Nov. 1979, vol.1, no.2, p.97.
2. Baer, J., **Hydraulics of Groundwater**, McGraw-Hill, Inc., New York, 1979.
3. Bouwer, Herman, **Groundwater Hydrology**, McGraw-Hill, Inc., New York, 1978.
4. Brebbia, C.A., and A.J. Ferrante, **Computational Hydraulics**, Butterworth, London, 1983.
5. Carnahan, B., H.A. Luther, J.O. Wilkes, **Applied Numerical Methods**, John Wiley and Sons, New York, 1969.
6. Desai, H.B., *Superfund: The Battle Continues*, **Civil Engineering**, ASCE, Feb. 1985, p.112.
7. DeWiest, R.J.M., Editor, **Flow Through Porous Media**, Academic Press, Inc., New York, 1969.
8. "EPA to propose stricter rules on toxic wastes", *Roanoke Times and World News*, Jan. 10, 1986.
9. Eurenium, J., A. Osihn, E. Strandell, *Uranium Mill Tailings Management - A Swedish Approach*, **Management of Wastes from Uranium Mining and Milling, Proc.**, Albuquerque, 1982, pp.679-692.
10. Fenner, R.T., **Computing For Engineers**, MacMillan Press, London, 1974.
11. Greenkorn, R.A., **Flow Phenomena in Porous Media**, Marcell Dekker, New York, 1983.

12. ...., *Groundwater Study Urges New System*, Coal News, Nov. 18, 1985, p.2.
13. Johnson, T.M., *Remedies at Existing Facilities, Virginia's Groundwater, Proc.*, WRRC, V.P.I. & S.U., Blacksburg, 1984, pp.21-33.
14. Kays, W.B., *Construction of Linings for Reservoirs, Tanks, and Pollution Control Facilities*, John Wiley and Sons, New York, 1977.
15. Langhaar, H.L., *Dimensional Analysis and Theory of Models*, 2nd Ed, Krieger Publ. Co., 1979.
16. Larsen, V.V., K. Brodersen, *Development Of A Waste-Containing Unit For Use In Shallow-Land Burial, Conditioning Of Radioactive Wastes For Storage And Disposal, Proc.*, Iaea, Vennia, Feb. 1983, pp.293-303
- 17 16. Linsley, R.K., Jr., M.A. Kohler, J.L.H. Paulhus, *Hydrology For Engineers, Second Edition*, McGraw-Hill, Kingsport, 1975.
- 18 17. Lush, D., J. Brown, R. Fletcher, J. Goode, T. Jurgens, *An Assessment of the Long Term Interaction of Uranium Tailings with the Natural Environment, Management, Stabilisation and Environmental Impact of Uranium Mill Tailings, Proc.*, Albuquerque, 1978, pp.373-398.
- 19 18. Marline Uranium Corporation and Union Carbide Corporation, *An Evaluation of Uranium Development in Pittsylvania County, Virginia*, vol.2, Oct. 1983.
- 20 19. Martin, J.B., H.J. Miller, *Generic Environment Impact Statement on U. S. Uranium Milling Industry, Management, Stabilisation and Environmental Impact of Uranium Mill Tailings, Proc.*, Albuquerque, 1978, pp.453-462.
- 21 20. Murry, R.L., "Radioactive Waste Storage and Disposal", *Proceedings of the IEEE*, vol.74, no.4, Apr. 1986, pp.552-579.
- 22 21. Neilsen, D.M., *Remedial Methods for Polluted Aquifers, Virginia's Groundwater, Proc.*, WRRC, V.P.I. & S.U., Blacksburg, 1984, pp.34-44.
- 23 22. ...., "New Technical Solutions To Hazardous Wastes", *Engineering Times*, vol.8, no.6, June 1986, p.4.
- 24 23. OECD Nuclear Energy Agency. *Disposal of Radioactive Waste, an Overview of the Principles Involved*, Paris, 1982.

- 25 24. Parker, J.C., M.T. van Genuchten, *Determining Transport Parameters form Laboratory and Field Tracer Experiments*, Virginia Agricultural Experiment Station, Bulletin 84-3, May, 1983.
- 26 25. Silka, L.R., *Understanding the Problem of Groundwater Contamination, Virginia's Groundwater*, Proc., WRRC, V.P.I. & S.U., Blacksburg, 1984, pp.5-20.
- 27 26. Steel, E.W., T.J. McGhee, *Water Supply and Sewarage, Fifth Ed.*, McGraw-Hill, New York, 1979.
- 28 27. ....., "Toxic Waste: Another Growing Debt", *Roanoke Times and World News*, March 18, 1985.
- 29 28. U.S. Environmental Protection Agency, *Construction Costs for Municipal Wastewater Treatment Plants: 1973 - 1977*, U.S. Printing Office, Washington, 1978.
- 30 29. U.S. Geological Survey, *A Galerkin Finite-Element Flow Model to Predict the Transient Response of a Radially Symmetric Aquifer*, U.S. Printing Office, Washington, 1984.
- 31 30. White, J.A., M.H. Agee, K.E. Case, *Principles of Engineering Economic Analysis*, John Wiley and Sons, New York, 1977.
- 32 31. Zienkiewicz, O., P. Mayer, Y.K. Cheung, *Solution of Anisotropic Seepage by Finite Elements*, *Journal of the Engineering Mechanics Division*, ASCE, February 1966, pp.111-120.

**The vita has been removed from  
the scanned document**